

Alma Mater Studiorum – Università di Bologna

DOTTORATO DI RICERCA IN
SCIENZE BIOTECNOLOGICHE, BIOCOMPUTAZIONALI,
FARMACEUTICHE E FARMACOLOGICHE

Ciclo 34

Settore Concorsuale: 05/G1 - FARMACOLOGIA, FARMACOLOGIA CLINICA E
FARMACOGNOSIA

Settore Scientifico Disciplinare: BIO/14 - FARMACOLOGIA

EPHB1 AND NOTCH4: TRANSMEMBRANE RECEPTORS AS NOVEL
PHARMACOLOGICAL TARGETS FOR GLIOBLASTOMA AND
THERAPEUTIC ANGIOGENESIS

Presentata da: Stefano Pezzini

Coordinatore Dottorato

Maria Laura Bolognesi

Supervisore

Santi Mario Spampinato

Esame finale anno 2022

Index

Abstract	4
Introduction	7
1. Ephrin ligands and Eph receptors	8
1.1 <i>Ephrin and Eph receptor structures</i>	8
1.2 <i>Eph/ephrin complex formation and activation</i>	9
1.3 <i>Bidirectional signalling: forward and reverse signalling</i>	10
1.4 <i>Signaling termination</i>	12
2. Cellular and molecular mechanisms of angiogenesis	13
2.1 <i>Vasculogenesis, angiogenesis and arteriogenesis</i>	13
2.2 <i>Cellular mechanisms of vascular growth: Sprouting and Intussusception</i> ..	14
2.3 <i>Vascular endothelial growth factors and receptors</i>	16
2.4 <i>Notch signaling pathway</i>	18
2.4.1 <i>Notch1</i>	20
2.4.2 <i>Notch4</i>	21
3. Eph receptors and ephrins in cancer and angiogenesis	21
3.1 <i>Eph/ephrin signalling in cancer</i>	21
3.1.1 <i>Dichotomous function of EphB1 receptor in malignant brain tumor</i>	24
3.1.1.1 <i>EphB1 in normal nerve tissue</i>	24
3.1.1.2 <i>Tumor-suppressing and –promoting roles of EphB1</i>	25
3.1.1.3 <i>EphB1 in glioma</i>	26
3.2 <i>EphrinB2-EphB4 in angiogenesis</i>	27
4. Tumor angiogenesis in glioblastoma	28
5. Innovative therapeutic approaches to target EphB1 receptor	28
5.1 <i>Eph receptor-binding peptides</i>	28
5.2 <i>Altered miRNAs in glioblastoma</i>	30
6. Therapeutic angiogenesis	31
6.1 <i>Therapeutic considerations for VEGF delivery: the importance of dose distribution control</i>	31
6.2 <i>Cell-based VEGF delivery</i>	34
6.3 <i>Recombinant factor engineering for matrix decoration</i>	36

Aim of the research.....	37
Materials and Methods.....	40
1. First part.....	41
<i>1.1 Reagents</i>	41
<i>1.2 Cell culture</i>	41
<i>1.3 Cell transfection and treatments</i>	42
<i>1.4 Wound healing assay</i>	42
<i>1.5 Cell proliferation assay</i>	42
<i>1.6 Quantitative real time PCR</i>	43
<i>1.7 Western blotting analysis</i>	44
<i>1.8 Statistical analysis</i>	44
2. Second part	46
<i>2.1 Fibrin matrix production and implantation into mice</i>	46
<i>2.2 Immunofluorescence tissue staining</i>	46
<i>2.3 Vessel measurements</i>	47
<i>2.4 Statistics</i>	47
Results	48
1. First part	49
<i>1.1 EphB1 is low expressed but functional in U87 cells and it is expressed in transfected U87 cells</i>	49
<i>1.2 EphB1 overexpression and/or activation decreases cell migration in native and transfected U87 cells</i>	50
<i>1.3 EphB1 overexpression and/or activation decreases cell proliferation in native and transfected U87 cells</i>	51
<i>1.4 EphB1 peptide antagonist increases cell migration in a concentration-dependent manner in native and transfected U87 cells</i>	52
<i>1.5 The addition of a beta-alanine to the N-terminus of the Hexapeptide increases cell migration in native and transfected U87 cells</i>	54
<i>1.6 The substitution to beta-alanine in the last position of the Hexapeptide decreases cell migration in native and transfected U87 cells</i>	58
<i>1.7 Discrepancy of EphB1 and Ephrin-B1 mRNA and protein levels between U87 and SH-SY5Y cells</i>	61

<i>1.8 The exposure to a proteasoma inhibitor does not influence EphB1 turnover in U87 cells</i>	61
<i>1.9 EphB1 expression could be regulated by post-transcriptional events involving miRNAs</i>	62
2. Second part	64
<i>2.1 High doses of VEGF induce aberrant angiogenesis in WT mice</i>	64
<i>2.2 Loss of Notch4 signaling pathway does not affect normal angiogenesis by moderate VEGF doses</i>	66
<i>2.3 Notch4 signaling is not required for normal intussusceptive angiogenesis by moderate doses of VEGF</i>	68
<i>2.4 Loss of Notch4 signaling prevents aberrant angiogenesis by high doses of VEGF</i>	72
<i>2.5 Notch 4 loss limits the degree of vascular enlargements by high VEGF levels</i>	75
Discussion	78
Conclusion	83
References	85

Abstract

The Eph receptor family of tyrosine kinases and its ligands, ephrins, are membrane-anchored molecules that regulate cell-cell interactions. They are expressed in most cells and tissue types. An increasing body of evidence is accumulating, showing that Eph/ephrin signalling regulates migration, proliferation, differentiation, adhesion, morphological changes and survival through cell-cell communication. Moreover, Eph/ephrin signaling is involved in tumorigenesis, metastasis and angiogenesis. Every member of this molecular system may act as tumor promoter or tumor suppressor, depending on the cellular context and type of cancer. EphB1 receptor expression is altered in different brain tumors. In glioblastoma EphB1 downregulation is correlated with aggressive cancer phenotypes, as this receptor may act as tumor suppressor. Starting from these evidences, we aimed at characterizing the role played by EphB1 receptor in glioblastoma by investigating its expression and modulation in U87 human glioblastoma cells.

The loss of EphB1 receptor expression and its subsequent reduced activity are relevant pro-tumoral events in glioblastoma cells. Consistently, treating U87 cells with the EphB1 receptor agonist or antagonist further reduces or increases cancer cell aggressiveness, respectively. Other different peptides, designed starting from the antagonist already available, affected U87 cell migration. Furthermore, the discordant levels of EphB1 mRNA and protein seem to indicate that the loss of EphB1 receptor expression in glioblastoma cells is due to some post-transcriptional events involving miRNAs.

The Eph/ephrin signaling pathway is also involved in angiogenesis. Cardio-vascular diseases, such as peripheral artery disease (PAD) and coronary artery disease (CAD), are the leading causes of death and disability in Western countries. Current procedures are insufficient to treat CAD and PAD patients. Therefore, therapeutic angiogenesis, which aims at inducing normal, stable and functional blood vessels by delivering growth factors to ischemic tissues, is an attractive strategy for these patients. VEGF is the master regulator of vascular growth both in development and postnatal life, and it represents the major molecular target for therapeutic angiogenesis. VEGF delivery appears to have a very limited therapeutic window in vivo, such that low doses are safe, but mostly inefficient, and higher doses become rapidly unsafe. However, previous studies in the host group show that the induction of normal or aberrant angiogenesis by VEGF depends strictly on the amount secreted in the microenvironment around each producing cell, and not on the total dose delivered. They recently found that stimulating

the EphrinB2/EphB4 pathway could prevent aberrant angiogenesis by excessive VEGF doses and convert it to normal. Preliminary data showed that targeting the endothelial-specific Notch4 pathway could induce a similar phenotype as activating EphB4. Therefore, here I investigated the Notch4 signaling pathway as a target for therapeutic angiogenesis. We found that Notch4 inhibition: 1) did not impair normal angiogenesis by low and safe levels of VEGF; 2) did not impair the initial formation of vascular enlargements; and 3) normalized aberrant angiogenesis by high VEGF levels of expression by limiting the degree of initial vascular enlargement induced by VEGF.

Introduction

1. Ephrin ligands and Eph receptors

Eph receptors, the largest family of receptor tyrosine kinases (RTKs), and their ephrin ligands are membrane-anchored molecules that regulate cell-cell interactions¹. They are expressed in a variety of cell and tissue types. Increasing evidences show that Eph/ephrin signalling regulates several cellular functions such as cell migration, proliferation, differentiation, adhesion, morphological changes and survival through cell-cell communication². Eph/ephrin-mediated effects are also involved in specialized processes such as synaptic plasticity, insulin secretion, bone remodeling and immune function¹. Eph receptors are classified on the basis of sequence homology and binding preferences: in the human genome there are 10 EphA receptors (EphA1–A10), which preferentially bind 6 glycosylphosphatidylinositol (GPI)-linked ephrin-A ligands (ephrins-A1–A6), and 6 EphB receptors (EphB1–B6), which preferentially bind 3 transmembrane ephrin-B ligands (ephrins-B1–B3)³. Furthermore, Ephs and ephrins interact promiscuously within each subclass, but cross-class interactions are known for EphA4, interacting with B-type ephrins⁴⁻⁵, and ephrin-A5, activating EphB2 as well as EphAs⁶.

1.1 Ephrin and Eph receptor structures

Eph-ephrin signalling relies on specific functional domains present in Ephs and ephrins (shown schematically on the left panel of Figure 1). On the extracellular side, Eph receptors are composed of a ligand-binding domain (LBD), which binds to the receptor-binding domain (RBD) of ephrins, followed by a Cys-rich domain (encompassing the sushi and epidermal growth factor (EGF)-like domain) and two fibronectin (FN) domains. The intracellular side of Eph receptors is composed of the transmembrane region (TM), the Tyr kinase domain (TK), the sterile alpha motif (SAM) and the PDZ domain. Ephrins, by contrast, are composed of a receptor-binding globular domain and a GPI link in the case of ephrin-A ligands, or a transmembrane domain and PDZ domains in the case of ephrin-B ligands².

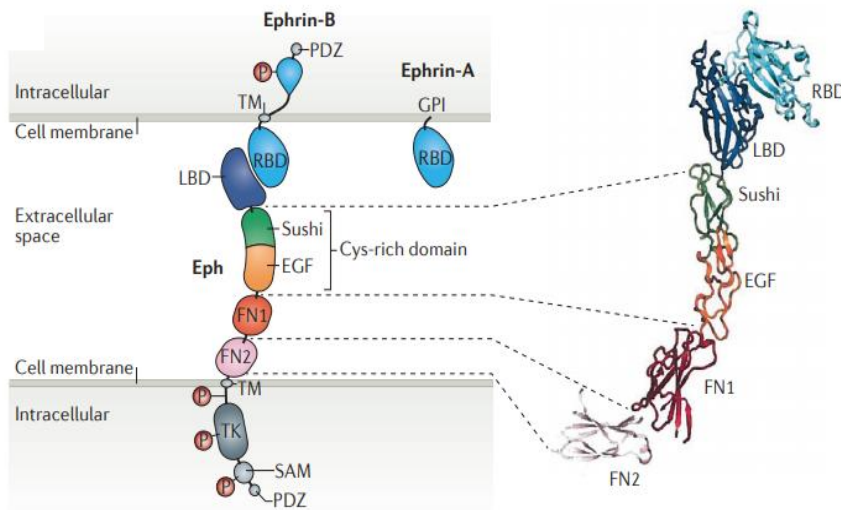


Figure 1: Structure of Eph receptors and ephrin ligands. PDZ: Post synaptic density 95-Discs large Zonula occludentes-1-protein, SAM: Sterile alpha motif, GPI: glycosylphosphatidylinositol.²

1.2 Eph/ephrin complex formation and activation

Eph receptors are not activated in a similar way as other RTK's, but require pre-clustered ligands to induce efficient downstream signaling⁷. Prior to activation, the Eph receptors are loosely distributed on the cell surface and display minimal kinase activity, unless receptor expression levels are considerably high^{1,8}. After activation, clusters of Eph receptors appear fairly rapidly at discrete spots on cell surface and ephrins localize to, and are concentrated in, membrane microdomains or rafts⁹. Thus, in contrast to other RTK's where receptor dimerization is enough to trigger biological activity, Eph receptors need high local density of ligands to induce downstream signaling. Moreover, the oligomerization state of the ligands seems to control not only the architecture of the receptor/ligand signaling assemblies, but also the precise downstream cellular responses¹⁰.

Biochemical and X-ray crystallographic investigations allowed to determine the high-resolution structures of the interaction domains of EphB2 and ephrin-B2 and of their complex^{11,12}. The EphB2–ephrin-B2 complex is a tetrameric, ring-like assembly in which two receptor and two ligand molecules interact via two distinct interfaces. One interface is very extensive and is responsible for high-affinity ligand-receptor dimerization, whereas the second interface is smaller and is responsible for the assembly of the EphB–ephrin-B dimers into the circular tetramer¹¹. The second, lower-affinity Eph-ephrin tetramerization interface shows a clear structural basis for subclass discrimination centered around an Eph surface loop (called the 'class-specificity' loop), whose length is invariant within each

subclass but differs by four residues between the two subclasses¹³. By contrast, the high-affinity dimerization interface, although showing structural features that could mediate subclass selectivity, does not provide a clear view into Eph class discrimination and suggests the possibility of cross-subclass Eph-ephrin interactions¹¹.

1.3 Bidirectional signalling: forward and reverse signalling

“Forward” signaling corresponds to the prototypical RTK mode of signaling, which is triggered by ligand binding and involves activation of the kinase domain. However, the activation mechanisms of Eph receptors have unique features as compared to other RTK families as described above.

Using soluble monomeric ephrin ligands, this interaction has been shown to occur through the insertion of the conserved hydrophobic loop (G–H loop) of the ephrin RBD into a hydrophobic cavity within the Eph receptor LBD^{12,14}. This ligand/receptor interaction induces conformational rearrangements in the receptor LBD, which further facilitates the formation of complementary Eph/Eph interaction interfaces and clustering¹⁵. Other domains, such as the CRD, SAM, and a portion of the FN-III domain within the receptor, favor additional Eph/Eph interactions thus stabilizing Eph/ephrin tetramers^{12,13,16}. The conformational changes upon the Eph/ephrin interaction are followed by the receptor autophosphorylation at two tyrosine residues within the juxtamembrane domain and one tyrosine residue within the activation segment of the kinase domain¹⁷. This disrupts the inhibitory interaction with the kinase domain, enhancing the kinase activity and transphosphorylation of additional tyrosine residues¹⁷. As typical for RTKs, the phosphorylated tyrosine residues serve as docking sites for Src Homology 2 (SH2) and phospho tyrosine binding (PTB) domain-containing adaptor proteins. These interactions can mediate signal transduction with variable duration and kinetics through multiple downstream signaling pathways, including phosphatidylinositol 3'-kinase (PI3K)-AKT, Janus kinase/Signal transducer and activator of transcription (JAK/STAT), Ras/mitogen-activated protein kinase (RAS/MAPK), as well as focal adhesion kinase (FAK) and Src kinase-mediated signals^{1,18-21} (Fig. 2). Through their PDZ-binding motif, Eph receptors associate with PDZ-domain-containing proteins such as AF6, Pick1, syntenin, and Grip1/2 to further regulate clustering, trafficking, and signaling²²⁻²⁴.

Eph/ephrin interactions trigger signaling events also in cells expressing the membrane-bound ligand, a mechanism referred to as “reverse signaling”. Intracellular signals

transduced by both ephrins A and ephrins B have been found to modify multiple responses at the cellular level. However, reverse signals through GPI anchored ephrinAs rely on lipid raft-mediated interaction with transmembrane protein complexes. Although ephrinAs lack an intracellular domain for phosphorylation-dependent recruitment of signaling molecules, clustered ephrinA5 has been found to recruit the Src family kinase Fyn to the same caveolae-like membrane domains, upon receptor binding (Figure 2). This promotes activation of β 1 integrin and ERK and increases cell–substrate adhesion^{25,26}. In contrast, EphB/ephrinB interaction triggers ephrinB phosphorylation on conserved tyrosine residues by Src family kinases, thus creating docking sites for SH2-domain-containing proteins such as Grb4²⁷ (Fig. 2). Like Eph receptors, ephrinBs also recruit PDZ-domain-containing proteins through their C-terminus, such as the protein tyrosine phosphatase PTP-BL, which in turn can dephosphorylate both ephrinBs and Src as a mechanism of reverse signaling attenuation²⁸. The reverse ephrinB signaling has been found to regulate cell invasion via, e.g., matrix metalloproteinase 8 (MMP8) secretion and Rac1 activation²⁹⁻³¹. Interaction of non-phosphorylated ephrinB1 with the PAR6 polarity protein instead regulates epithelial tight junction formation³². EphrinB2 can also exert cell–cell contact independent functions by stimulating actomyosin-dependent cell contraction through its PDZ-motif with a mechanism that does not require Eph receptor binding^{33,34}.

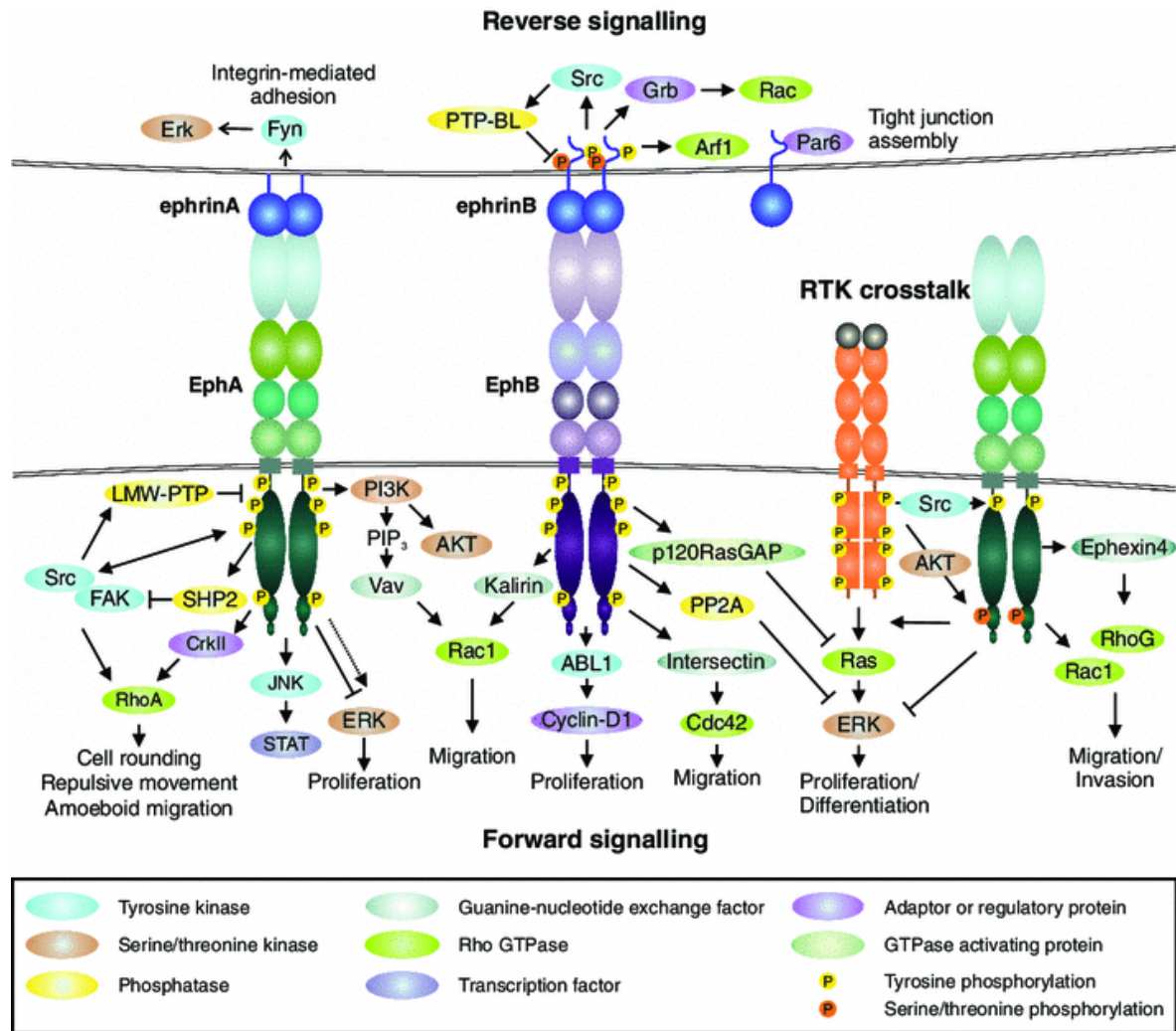


Figure 2: Eph/ephrin forward and reverse signaling³⁵.

1.4 Signaling termination

Following ligand-dependent activation, RTKs are typically internalized by endocytosis and can continue to signal from intracellular compartments until they are inactivated by dephosphorylation and degradation or trafficked back to the cell surface³⁶. For the Eph receptors, this process has unique features as a result of the plasma membrane association of the ephrins³⁷⁻³⁹. Eph receptor–ephrin complexes can be internalized into either the Eph receptor- or the ephrin-expressing cells through the formation of vesicles containing plasma membrane fragments derived from both cells. This Rac1-dependent process, which has been defined “trans-endocytosis”, is critical for removal of adhesive complexes from cell–cell contact sites to allow cell separation and repulsive effects. Another protein that contributes to Eph receptor internalization and degradation is the ubiquitin ligase Cbl, which can interact with several Eph receptors promoting their ubiquitination^{40,41}. Besides

trans-endocytosis, Eph receptor-ephrin complexes can convert adhesive interactions into cell repulsion by activating metalloproteases, such as ADAM family members.

2. Cellular and molecular mechanisms of angiogenesis

2.1 Vasculogenesis, angiogenesis and arteriogenesis

In vertebrate embryos, two distinct mechanisms, named respectively vasculogenesis and angiogenesis, fulfill the formation of the vascular network^{42,43}. Vasculogenesis is defined as the differentiation of endothelial precursor cells (angioblasts) into endothelial cells and the *de novo* formation of a primitive vascular network. Vasculogenesis starts with *in situ* differentiation of mesodermal cells into angioblasts or hemangioblasts, which in turn differentiate into endothelial cells and hematopoietic cells respectively. Endothelial cells coalesce to form aggregates named blood islands which fuse together and generate tube-like capillaries, which form *de facto* a primary capillary plexus in the yolk sac⁴⁴.

Vasculogenesis is largely governed by fixed genetic programs, even though environmental factors, such as hemodynamics and tissue oxygenation, can modify the vasculogenic program in the embryo⁴⁵. The molecular mechanisms underlying angioblast induction are mostly unknown. However, an important role is played by the secretion of Hedgehog proteins and vascular endothelial grow factor (VEGF) from the interacting mesoderm⁴⁶. Furthermore, other soluble factors and molecular pathways are involved in vascular morphogenesis, such as Transforming Growth Factor-beta (TGF- β), Angiopoietins/Tie, Wnt and Delta/Notch pathways⁴⁷.

In post-natal life, the main mechanism accounting for the formation of blood vessel is angiogenesis, even though vasculogenesis may still occurs⁴⁸. Angiogenesis is defined as the formation of new blood vessels starting from pre-existing ones, and occurs mainly in response to a low level of oxygen inside a tissue⁴⁹. Angiogenesis can occur by two different cellular processes, namely sprouting (or branching) angiogenesis and intussusception (also known as splitting angiogenesis). In the embryo, the vascularization of tissues and organs of non-mesodermal origin (e.g. the brain and the visceral organs) is mediated by sprouting⁵⁰, whereas the expansion of already formed microcapillary beds is gained by intussusception⁵¹. The newly generated vessels are immature, unstable and therefore prone to regression. The stabilization of newly induced vessels is achieved through a two-step maturation process. During the first step, ECs stop to proliferate and⁵² in response to VEGF, secrete Plated-Derived Growth Factor-BB (PDGF-BB). PDGF-BB is

responsible for the recruitment of mesenchymal cells, which will cover the newly induced vascular structure^{53,54}. Once coated, the endothelium produces and secretes transforming growth factor- β (TGF- β), which further inhibits EC division (stabilizing the vessel), and induces mesenchymal cell proliferation and differentiation into mature mural cells, named pericytes for small vessels (e.g. capillaries) and vascular smooth muscle cells (vSMC) for larger vessels (e.g. arteries and veins)⁵⁵. In the absence of perivascular cells, newly formed vessels start to regress after cessation of the angiogenic stimulus⁵⁶. The second step of the maturation process lead to the deposition of the endothelial basement membrane (BM) on the external surface of the vessel and the secretion of an extracellular matrix (ECM) rich in collagens, fibronectin, laminin and elastin⁵⁰. BM and ECM together provide mechanical support to the ECs, prevent large vessels from collapsing, reduce vascular leakage and avoid blood vessel regression. Also, ECM controls EC survival, migration and proliferation⁵⁷. Lastly, vascular networks undergo extensive vascular remodeling to form a functional and mature vasculature. This “trimming” includes distinct processes of vascular pruning, i.e. the regression of selected vascular branches⁵⁸.

A second mechanism involved in post-natal vascular growth is arteriogenesis⁵⁸. This process is characterized by the formation of mature functional arteries from pre-existing and poor-perfused interconnecting arterioles after an arterial occlusion, thereby bypassing the block and restoring blood flow to ischemic tissue downstream⁵⁹. This process is driven mostly by hemodynamic factors. The perception of these forces is allowed by several mechanosensory complexes located on the ECs membrane⁶⁰. The stimulation of these molecular sensors initiates an integrin-mediated pathway, which in turn activates a certain number of transcription factors such as early growth response protein 1 (Egr-1), activator protein 1 (AP-1) and Rho and induces consequently the expression of the arteriogenesis-related genes⁶¹.

2.2 Cellular mechanisms of vascular growth: Sprouting and Intussusception

After embryonic development, the main mechanism responsible for neovascularization is angiogenesis, i.e. the growth of new blood vessels from pre-existing ones. Angiogenesis is a multi-step process during which endothelial cell behavior has to be tightly controlled. Vascular endothelial growth factor (VEGF) is the master regulator of vascular growth both in development and disease and, upon expression as a single factor, is capable of initiating the cascade of events leading from endothelial activation to the generation of new

functional and stable vascular networks⁶². The best understood mode of vascular growth is sprouting, by which new vessels invade avascular areas of tissue guided by gradients of factors, e.g. during embryonic development. However, sprouting is not the only cellular process by which vessels can grow. In fact, several studies found that vascular growth can also take place through another complementary mechanism called intussusception, or splitting angiogenesis⁶³. Intussusception can be initiated very rapidly, e.g. by increased blood flow and shear stress even in the absence of growth factors⁶⁴. Recently it has been shown that over-expression of VEGF in skeletal muscle induces angiogenesis by intussusception rather than sprouting⁶⁵. It is still unclear what determines whether VEGF induces angiogenesis by sprouting or intussusception. However spatial and temporal distribution of VEGF in the microenvironment can play a crucial role. In fact, if a VEGF gradient is lacking, e.g. when the non-matrix-binding isoform VEGF₁₂₁ is expressed, endothelial cells proliferate without migrating and lead to vessel enlargement instead of vessel sprouts²²¹.

Sprouting angiogenesis relies on the functional specification of endothelial cells into either tip or stalk cells. Tip cells can sense VEGF gradients, and migrate towards the VEGF source, thereby guiding the nascent sprout. Stalk cells, which instead proliferate just behind the tip, form the body of the sprout and start the process of lumen formation (Figure 3A)⁶⁶. In contrast, the hallmark of intussusception is the formation of trans-luminal tissue pillars, which can occur either through a zone of contact between the endothelial cells of opposite capillary walls, with subsequent reorganization of the endothelial junctions and invasion of the pillar core by myofibroblasts, or through the extension and fusion of intraluminal protrusions made exclusively of endothelial cells (intraluminal sprouting). Subsequently, transluminal tissue pillars align along the length of the preexisting vessel, progressively fuse together and divide the affected vascular segment longitudinally into new, individual vascular structures (figure 3B)^{67,68}. The molecular regulation of intussusception remains poorly understood due to a paucity of appropriate models, and its elucidation will be key to providing a rational basis for the design of therapeutic angiogenesis strategies.

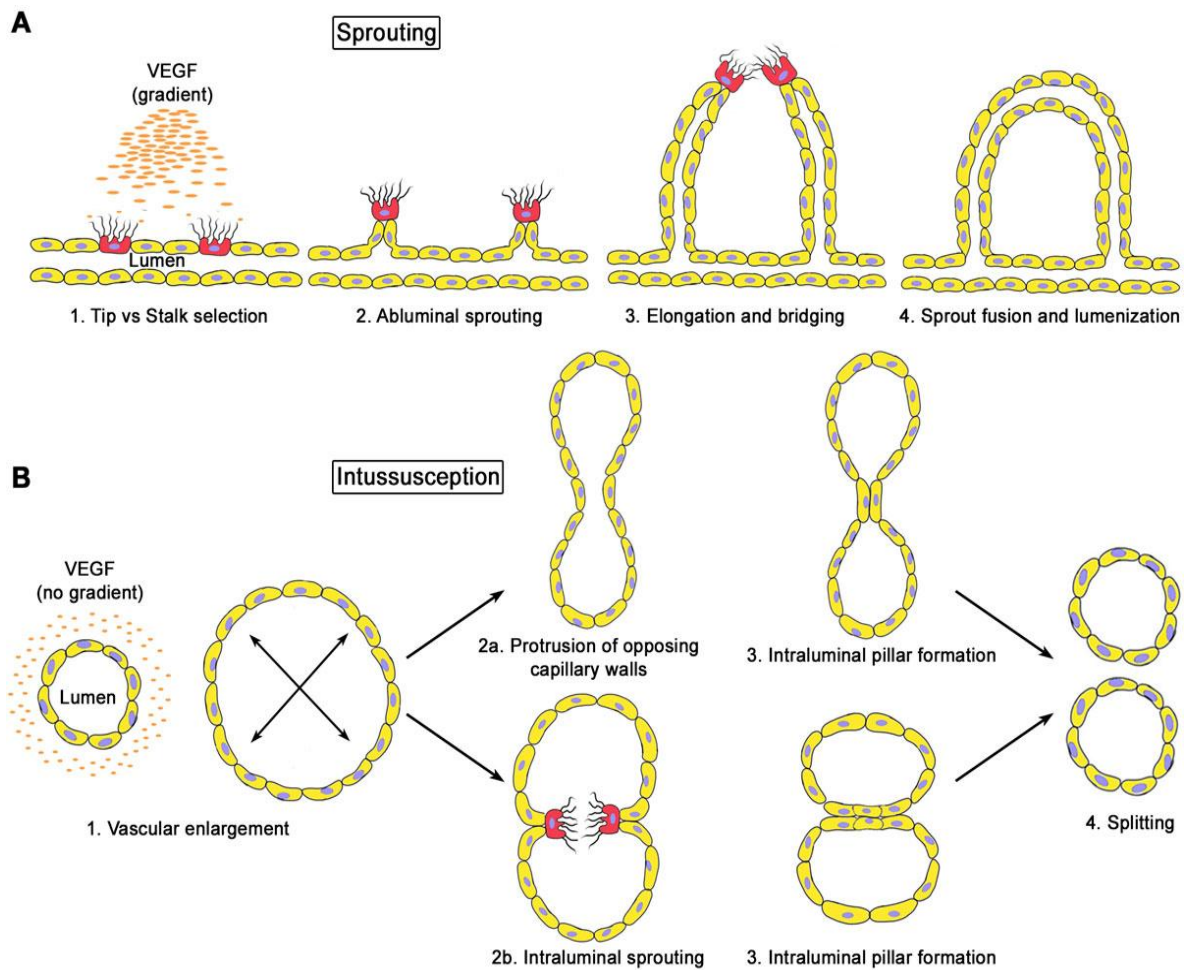


Figure 3: Mechanisms of angiogenesis: sprouting (A) vs intussusception, or splitting (B). (A) VEGF gradients in the extracellular matrix induce the functional specification of endothelial tip cells (in red), which migrate towards the gradient source, and stalk cells (in yellow), which proliferate behind the tip, forming abluminal sprouts that fuse together and generate new vessels. (B). In the absence of a gradient, all endothelial cells respond to VEGF by assuming a stalk phenotype without tip cells. The subsequent proliferation without migration leads to circumferential enlargement of vessels without sprouting followed by formation of intraluminal endothelial pillars which fuse together and cause longitudinal splitting into two new vessels²¹⁹.

2.3 Vascular endothelial growth factors and receptors

VEGF is a family of signaling proteins secreted by various cell populations such as T-cells, macrophages, keratinocytes and ECs, but also essentially every cell type in the body⁶⁹⁻⁷². The mammalian VEGF family consists of five structurally related members: VEGF-A, VEGF-B, VEGF-C, VEGF-D (also known as FIGF) and placental growth factor (PlGF), which can all occur in different splice variants and processed forms⁷³. Homologous polypeptides have been recently identified in non-mammalian organisms. They include Orf virus-encoded VEGF-E⁷⁴ and Eastern Cottonmouth snake's venom-isolated VEGF-F⁷⁵.

VEGFs fulfill their role by binding to three structurally related tyrosine kinase receptors (RTKs): Vascular Endothelial Growth Factor Receptor-1, -2 and -3 (VEGF-R1, VEGF-R2 and VEGF-R3, respectively). VEGFR-1 and VEGFR-2 are characterized by seven immunoglobulin (Ig)-like folds in the extracellular domain (ECD), a single-helix transmembrane region (TMD), and an intracellular domain (ICD), which, in turns, consists of a juxtamembrane domain (JMD), a split tyrosine kinase domain (TDK1 and TDK2) that is interrupted by a kinase insert domain (KID), and a carboxyl-terminal domain (CTD). Thanks to an alternative splicing process, they can also exist as soluble forms, called sVEGFR-1 and sVEGFR-2 respectively⁷⁶. VEGFR-3 has the same domain organization and molecular structure observed in the two other receptors. However, due to the substitution of two cysteine residues, it lacks a disulfide bridge in the fifth Ig-like domain⁷⁷. In addition to these receptors, VEGFs may also interact with co-receptors such as neuropilin-1 (NRP-1) and neuropilin-2 (NRP-2), macromolecules such as heparan sulfate (HS) and proteoglycans (i.e. syndecan and glypican) and also with non-VEGF binding auxiliary proteins, including vascular endothelial cadherin (VE-cadherin), integrins, ephrin-B2 and protein tyrosine phosphatase (PTP)⁷⁸.

VEGF-R1 can be bound with high affinity by VEGF-A, VEGF-B and PlGF. Nevertheless, it is characterized by a weak tyrosine autophosphorylation activity in response to the interaction with the growth factor⁷⁹. VEGF-R1 acts as negative regulator of angiogenesis by reducing the amount of VEGFs available to bind VEGF-R2⁸⁰. The same decoy activity was described for sVEGF-R1⁸¹.

VEGF-R2 is the main VEGF receptor expressed on ECs. It is able to bind VEGF-A and the processed forms of VEGF-C and VEGF-D. This receptor has a 10-folds lower affinity for VEGF-A when compared to VEGF-R1^{82,83}, still it is the main mediator of VEGF-A-induced stimulus on ECs differentiation, proliferation, and migration⁷⁶.

VEGFR-3 can bind VEGF-C and VEGF-D. It has an important role in early development during cardiac remodeling⁸⁴ and later to induce and to preserve the lymphatic ECs from apoptosis⁸⁵. sVEGF-R2, by interacting with the same VEGF isoforms bound by VEGF-R3, inhibits the proliferation of lymphatic ECs⁸⁶.

Finally, in vivo studies on transgenic NRP1^{-/-} and NRP2^{-/-} mice demonstrate that NRP1 is important during embryonic vascular system formation, whereas NRP2 is required for a correct formation of the lymphatic system⁸⁷.

The VEGF family members have a critical function in the differentiation of vascular and lymphatic ECs, and in blood vessel growth and maturation. In particular, VEGF-A is the major regulator of angiogenesis both in physiological and pathological conditions⁸⁸.

VEGF-A gene expression is mainly influenced by oxygen tension, as its transcription is heavily upregulated under hypoxic conditions, through to the stabilization of the hypoxia-inducible factor-1 (HIF-1)⁸⁹. HIF-1 is an oxygen-sensitive transcriptional activator composed by two subunits, HIF-1 α and HIF-1 β . Both these proteins are constitutively expressed, but HIF-1 α is rapidly degraded in normoxia conditions ($t_{1/2} \sim 5$ min). Conversely, under hypoxic conditions HIF-1 α becomes stable and translocates to the nucleus where it forms a complex with HIF-1 β , the resulting dimer binds the hypoxia response element (HRE) of VEGF-A thus inducing its transcription⁹⁰. Furthermore, nitric oxide (NO), a certain number of cytokines and oncogenic mutations can also up-regulate VEGF-A gene expression⁸⁰.

In addition to transcriptional regulation, VEGF-A activity is also controlled at the translational level thanks to two internal ribosome entry sites (IRES) located in its mRNA⁹¹ and the stability of this ribonucleic molecule can also be modulated⁹².

The human VEGF-A gene is located on chromosome 6 and is organized in eight exons, separated by seven introns⁹³. There are at least 12 subtypes of VEGF-A, generated through alternative splicing. This subtypes can be divided in two groups differing by their carboxyl-terminal six amino acids, termed respectively VEGF-A_{xxx} (pro-angiogenic) and VEGF-A_{xxx}b (anti-angiogenic), where xxx indicates the number of amino acids in the mature protein⁹⁴.

VEGF-B can bind VEGF-R1 and NRP-1 and is important for the protection of the brain from ischemic injury and for proper heart functionality during adult life^{95,96}.

Both VEGF-C and VEGF-D bind VEGF-R2, VEGF-R3 and NRP-2. VEGF-C is required for proper lymphangiogenesis⁷⁶ and VEGF-D promotes the metastatic spread of tumor cells via the lymphatic vessels⁹⁷. Lastly, PIGF seems to augment the ECs responsiveness to VEGF-A in a number of pathological conditions⁹⁸.

2.4 Notch signaling pathway

Notch signaling is an evolutionarily conserved pathway in multicellular organisms and impacts the fate of a variety of cell types during morphogenesis as it can affect differentiation, proliferation, and apoptosis⁹⁹. In particular, Notch can perform its

regulatory functions through two different signaling modalities: “lateral inhibition” and “boundary formation”¹⁰⁰. The Notch family in mammals comprises four receptors: Notch1, Notch2, Notch3 and Notch4 and five DSL (Delta/Serrate/Lag-2) ligands: Jagged1 (JAG1), Jagged2 (JAG2), Delta-like 1 (Dll1), Delta-like 3 (Dll3) and Delta-like 4 (Dll4). An interesting hallmark of the Notch signaling pathway is that Notch receptors have been found to be promiscuous with regard to ligand binding and no ligand specificity of Notch receptors has yet been fully characterized.

Notch receptors are type I single-pass trans-membrane proteins heterodimers. Namely, the extracellular domain of Notch receptors (NECD), composed of tandem epidermal growth factor (EGF)-like repeats, is responsible for the ligand binding, while the intracellular domain (NICD) constitutes the catalytic part of the molecule. Notch ligands are also type I single-pass trans-membrane proteins and therefore the activation of Notch signaling cascade requires close cell-to-cell interaction (juxtacrine signaling). When the interaction occurs, a series of proteolytic events take place. Initially a protease of the disintegrin and metalloprotease (ADAM) family cleaves Notch at site 2 (S2), creating an intermediate truncated version of Notch that is subsequently cleaved at site 3 (S3) and site 4 (S4) by the γ -secretase, an integral membrane protease complex. Consequently the NICD is released and can translocate into the nucleus where it interacts with the DNA-binding-protein CSL (CBF1/Suppressor of Hairless/LAG-1), forming a transcriptional complex. In turn, the newly formed complex can associate with the mammalian MAML (Mastermind/Lag-3), which displaces transcriptional co-repressors and recruits co-activators. This way, the up-regulation of downstream target genes, such as Hes (Hairy Enhancer of Split) 1, 5, and 6 is induced¹⁰⁰ (Figure 4).

In mammals, Notch1 and Notch4 receptors and Jag1, Dll1 and Dll4 ligands are mainly expressed by the vascular ECs¹⁰¹. Loss-of-function and gain-of-function studies¹⁰³⁻¹⁰⁵ showed that Notch signaling has an essential role in coordinating multiple aspects during vascular development, such as arteriovenous differentiation and regulation of sprouting and branching during sprouting angiogenesis¹⁰²

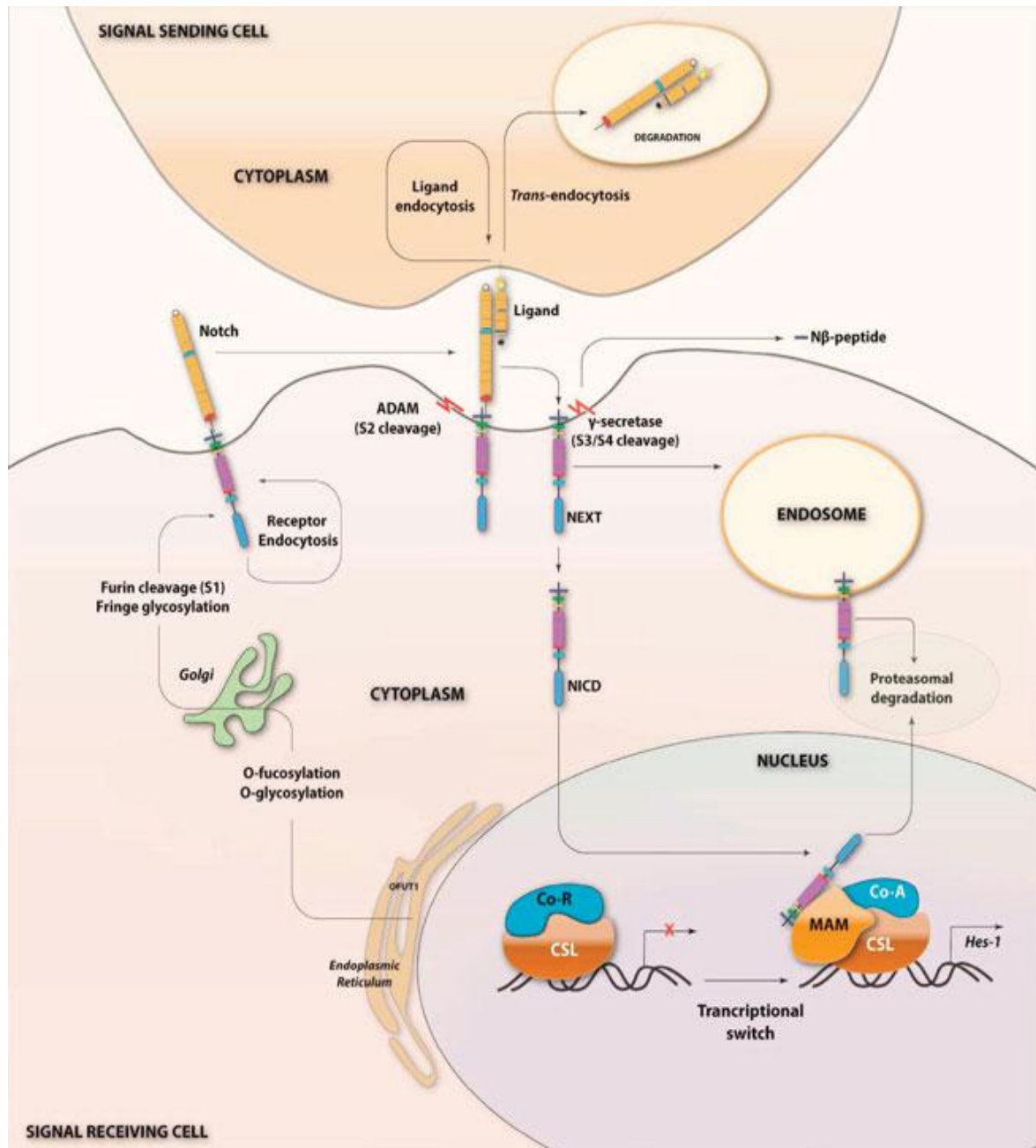


Figure 4: The Notch signaling pathway. NECD: NOTCH extracellular domain; NICD: NOTCH intracellular domain; NEXT: NOTCH extracellular truncated domain; CSL: CBF1/Suppressor of Hairless/LAG-1; MAM: Mastermind/Lag-3; Co-A: co-activators; Co-R: co-repressors; N β : short peptide released after cleavage at site 4¹⁰⁰.

2.4.1 Notch1

The Notch1 signaling pathway plays a fundamental role in sprouting angiogenesis. In particular, signaling between Notch1 and Dll4 has been shown to regulate the formation of appropriate numbers of tip cells by VEGF and to control vessel sprouting. In response to

VEGF, the first endothelial cells that increase their expression of VEGFR-2 and Dll4 acquire a tip cell phenotype. The up-regulated Dll4 on tip cells activates Notch signaling in neighboring cells and high Notch levels result in the inhibition of VEGFR-2 activity that makes these cells less responsive to VEGF and therefore excludes them from becoming tip cells (lateral inhibition) and induces them to acquire a stalk cell phenotype instead. Further studies showed that endothelial cells actively compete to acquire the leading tip cell position and this competition is driven by the fine-tuning of their VEGFR-1 and VEGFR-2 expression^{106,107}.

Jag1, a proangiogenic protein expressed by stalk cells, is also important in the process of tip cell selection. Jag1 competes with Dll4 for the binding of Notch1 receptor and functions by downregulating Notch1 signaling. This prevents Notch1 activation in adjacent tip cells and ensures the maintenance of VEGFR-2 expression and therefore the ability of these cells to detect VEGF¹⁰⁸. Furthermore, Jag1 can also counteract Dll4/Notch1 interactions between stalk cells, sustaining VEGF receptor expression in the newly formed, immature vascular plexus at the angiogenic front. The effect of Jag1 on Notch1 depends on the activity of the glucosaminyl-transferase Fringe. In fact, the different level of glycosylation can modify the receptor affinity binding for the different ligands and in particular a reduction of Notch1 activation upon Jag1 interaction¹⁰⁹.

2.4.2 Notch4

The Notch4 receptor is expressed in the endothelium and can be activated by Dll4 and Jag1 ligands. Notch4 constitutive activation can elicit abnormal vascular enlargement in mice¹¹⁰. In particular, the over-expression of a constitutively active form of Notch4 in an inducible transgenic murine model led to abnormal dilated vessels and the development of brain arteriovenous malformations (AVM), which originated from the enlargement of preexisting micro-vessels and displayed poor smooth muscle cell coverage¹¹¹. Recently it has also been shown that, by switching off the expression of the same constitutively active form of Notch4, the induced AV shunts are not permanent, but rather regress and revert to capillary-like microvessels¹¹².

3. Eph receptors and ephrins in cancer and angiogenesis

3.1 Eph receptors and ephrins in cancer

In the last two decades an increasing body of evidence has accumulated showing the involvement of Eph receptors and ephrins with different facets of tumorigenesis and cancer progression, such as tumor angiogenesis and vasculo-mimicry, tumor immunity and microenvironment, metastasis development and tumor stem cell propagation and maintenance. Overall, the emerging picture about this system in cancer appears often incongruous and, apparently, even paradoxical. In fact, every member of this complex communication cellular system was reported to have both negative and positive effects on tumorigenesis and tumor progression depending on cancer type; notably, even in the same tumor opposite outcomes are reported^{113,114}. This apparent paradox is related to the “phosphorylation status” and the fact that Eph receptors and ephrins can signaling dependently of each other through cross-talk with other signaling systems. For example, EphA2 has been found to enhance tumor cell proliferation and motility in cells overexpressing EGF receptors, an activity that likely contributes to tumorigenesis and metastatic progression in a mouse ErbB2 mammary adenocarcinoma model, promoting Erk and RhoA GTPase activity¹⁴. In glioblastoma and prostate cancer cell lines EphA2 was shown to promote oncogenic signals when it was overexpressed but not activated by ephrin ligands becoming a key substrate of the Akt-mTORC1 axis. Conversely, EphA2 was able to block Akt activation after ephrin-A1 stimulation in a tyrosine kinase-dependent manner^{115,116}. EphA2 is also expressed in mesenchymal and epithelial embryonic and adult tissues and is frequently overexpressed in melanoma, gliomas, breast, prostate, lung, colon, gastric, oesophageal, cervical, ovarian, bladder and renal cell carcinomas¹¹⁷⁻¹²¹. EphA2 forward signalling promotes tumour neovascularization¹²². In breast cancer, increased EphB2, EphB4 and EphA2 expression levels have been associated with poor prognosis^{123,124}. EphA2 is one of the four most highly phosphorylated proteins in basal breast carcinoma cells, and its overexpression facilitates anchorage-independent growth and tumorigenicity in non-transformed MCF10A mammary epithelial cells¹²⁵.

The roles of EphB2 and EphB4 during tumour progression are controversial. These receptors interact with ephrin B2, which is an important marker of normal and tumour vasculature, and increased expression of EphB2 and EphB4 causes the tumorigenic activation of angiogenic reverse signalling¹²⁶. In addition, EphB4 high levels are found to be prognostic for poor survival of patients with breast cancer¹²⁷. By contrast, the proliferation, viability and invasion of MDA-MB-231, MDA-MB-435 and MCF7 breast cancer cells are decreased by ephrin B2-activated EphB4 signalling¹²⁸, although a more

recent study suggests the opposite, underlining that EphB4 forward signalling triggers RAS–MAPK-dependent proliferation of MCF7 cancer cells¹²⁹. Likewise, although progressive loss of EphB2 or EphB4 expression during carcinoma progression seems to correlate with reduced survival rates¹³⁰, a recent survey of mRNA transcripts of paired stage I–IV colon cancer samples identified EphB2, EphB4 and EphA1 as the most significantly increased Ephs¹³¹. This dichotomous role of Eph receptors could be explained through detailed analysis of Eph-mediated prostate carcinoma cell migration, in which the lack of contact inhibition of metastatic PC3 cells was found to be due to adhesive ephrin B2–EphB3/EphB4 signalling overriding repulsive ephrin A5–EphA2/EphA4 signalling in the same cells. This would suggest that the sum of Eph signalling capacities in a tumour cell determine its invasive and metastatic properties¹³². In addition, some of these apparent disparities could be due to differences in the disease stages of the analyzed tumours and variability in methods, reagents and mRNA stability. EphA2 and EphA3 protein and mRNA overexpression correlate with poor patient prognosis in an aggressive mesenchymal subtype of glioblastoma, in which both Eph receptors seem to have kinase-independent roles in maintaining the glioma-initiating cell population in an undifferentiated, proliferative state^{133,134}. EphA3 has a role in the maintenance of leukaemic stem cells and it is significantly increased in a broad range of haematopoietic tumours but is undetectable in normal human lymphocytes and haematopoietic progenitors, making it an attractive therapeutic target for clinical development¹¹⁷.

EphA3 seems to have a protective role in small cell lung cancer (SCLC). Recently it was shown that this receptor was downregulated in SCLC patients and its expression positively correlated with overall survival. The clinical evidence was supported by both *in vitro* data, where EphA3 downregulation promoted cellular chemoresistance, and preclinical animal model, where its upregulation inhibited the growth of SCLC cell lines subcutaneously injected in BALB/C-nude mice¹³⁵.

EphA4 expression was positively correlated with patients survival in non-small cell lung cancer (NSCLC)¹³⁶ and this putative protective role was supported by *in vitro* evidence showing that EphA4 upregulation inhibited cellular migration and invasion in several lung cancer cell lines¹³⁷. Similarly to EphA4, both EphA5 and EphA7 were positively correlated with overall survival in NSCLC patients¹³⁶, but some reports showed opposite results. Indeed, EphA7 downregulation was able to inhibit proliferation and/or migration and invasion in different NSCLC cell lines. Regarding EphA5 instead, it mediated SCLC

radiation resistance in a kinase-dependent manner, thus suggesting the pharmacological inhibition of its activity as a promising therapeutic approach¹³⁸.

In NSCLC cell lines proliferation, cell migration and invasion was inhibited by ephrin-B3 downregulation¹³⁹. Regarding EphB2 instead, clinical data negatively correlated its expression with lung adenocarcinoma patients overall survival¹⁴⁰.

EphB6 seems to exert a protective role in colorectal cancer (CRC). Clinical evidence showed that mRNA and protein levels of EphB6 are significantly lower in CRC when compared to normal and adenoma tissues. Moreover, EphB6 expression positively correlated with the time of survival and negatively correlated with lymph node metastasis and depth of the local intestinal invasion¹⁴¹.

Likewise, recent clinical data addressed EphA5 and EphA1 as tumor suppressors. The loss of EphA5 protein positively correlated with lymph node metastasis, depth of intestinal wall invasion, poor tumor differentiation and TNM stage. Instead, EphA1 expression was reduced in patients with low survival and *in vitro* data demonstrated that EphA1 downregulation increased invasion of HRT18 human rectum adenocarcinoma cell line^{142,143}.

3.1.1 Dichotomous function of EphB1 receptor in malignant brain tumor

3.1.1.1 EphB1 in normal nerve tissue

It has been reported that both EphB receptors and ephrin-B ligands are expressed in different regions within the central nervous system, including the adult olfactory bulb, cerebellum and hippocampus¹⁴⁴. Increasing evidence has shown the involvement of Eph receptors and ephrin ligands in the regulation of synapse development and maturation, migration of neural progenitors, establishment of tissue patterns, topographic maps and plasticity in different areas of the developing brain¹⁴⁵.

It has been demonstrated that EphB1, EphB2 play the major roles in dendritic spine morphogenesis and synapse formation in the hippocampus¹⁴⁶. Moreover, Eph/ephrin system is also involved in contact-dependent neuron–astrocyte communication at synapses¹⁴⁷.

EphB1 is required for neurogenesis and migration of neural progenitors. For example, EphB1/ephrin-B3 signalling regulates the proliferation and migration of neural progenitors in the hippocampus. A lack of EphB1 significantly decreases the amount of neural progenitors and nestin-positive stem cells in the hippocampus, impairs organization and

migration of neural progenitors, and affects polarity, cell positioning and proliferation¹⁴⁸. EphB1 is also required for rerouting retinal ganglion cell projections ipsilaterally¹⁴⁹. EphB1 regulates the development of the neuronal system by increased expression of Nurr1, which promotes dopaminergic neuron differentiation, axonal growth arrest, synapse formation and neuronal survival¹⁵⁰. EphB1 receptor recruits Nck to stimulate the JNK pathway that promotes Nurr1 expression by binding to the AP1/c-jun binding site in the 5'-flanking region of the Nurr1 gene¹⁵¹. Moreover, EphB1 leads to the formation of membrane ion channels upregulating the expression of N-methyl-D-aspartate receptors¹⁵². Ion channels are permeable to Ca²⁺ that binds to the cAMP response element (CRE)-binding site on Nurr1 and stimulates its expression¹⁵³. The EphB1 receptor major ligands are ephrin-B1, ephrin-B2 and ephrin-B3. EphB1/ephrins reverse signaling has a distinctive effect on neurons produced at the same time and site. It can have a repulsive function, migrating cortical neurons or it can also inhibit the migration of striatal neurons. The difference in the downstream molecular machinery of neurons may contribute to the different physiological responses of the same ligand/receptor combination¹⁵⁴.

3.1.1.2 Tumor-suppressing and -promoting roles of EphB1

EphB1/ephrins signaling has perplexing dichotomous roles with tumor-suppressing and –promoting functions depending on the cellular context. The functions of EphB1/ephrins signaling in glioma are now beginning to be uncovered. Alterations in the expression of EphB1 have been involved in 1.49% of the cases of glioma¹⁵⁵. In glioblastoma multiforme (GBM) patients with higher EphB1 expression levels showed longer survival rates¹⁵⁶. Therefore, the overexpression and ligand-dependent EphB1 signaling can inhibit cell migration and invasion upon ephrin-B2 ligand stimulation which is considered as a negative regulator for glioma cell motility and invasion and a positive predictor for glioma patient survival¹⁵⁵.

A reduction in EphB1 expression level was detected in different tumors such as glioma, colorectal cancer, gastric cancer, renal cell carcinoma and ovary serous carcinoma. The mechanism that causes the decrease of EphB1 expression in these tumors remains unclear. One possible reason may be due to alternation of hypermethylation in CpG islands located in EphB1 promoter. The alternation of hypermethylation in promoter regions can influence gene expression levels in both normal and tumor cells¹⁵⁵. For example, hypermethylation

of the promoter regions of almost all Eph receptors and ephrin ligands, including EphB1 and ephrin-B2, has been found in acute lymphoblastic leukemia bone marrow samples and cell lines¹⁵⁷. The reduction of EphB1 expression in some tumors may be caused by different mechanisms of Eph/ephrin complex processing. The first mechanism involves protease-mediated degradation of Eph/ephrin complexes, where phosphatase with tensin homology (PTEN) impairs EphB1-dependent cell attachment and migration and releases tyrosine phosphatases and ubiquitin ligase Cbl to degrade EphB1¹⁵⁸. Another proposed mechanism involves endocytosis mediated by cell membrane-derived vesicles, which leads to the removal of Eph/ephrin complexes from the cell surface¹⁵⁹.

In addition to the tumor-suppressing roles of EphB1 in diverse tumor types, it controversially has tumor-promoting roles. This dichotomous function of EphB1 in tumors can be partially explained by the fact that Eph receptors are highly context-dependent and can vary across cancer types¹⁸. In addition to the tumor-suppressing role in glioma, EphB1 also promotes tumorigenesis in medulloblastoma¹⁶⁰ where EphB1 expression have an important role in radiation resistance and in cell migration. In Daoy cells the lack of EphB1 receptor reduces cell growth, viability and migration, as well as, the expression of important cell cycle regulators as cyclin E, besides increases the percentage of cells in G1 phase and enhancements radiation sensitivity. Moreover, EphB1 can interact with other tyrosine kinases receptors such as epidermal growth factor receptor (EGFR), contributing to the metastatic behavior of medulloblastoma cells as well as interacts with β 1-integrin producing cell migration and chemotaxis via stimulation of Src activity^{20,160,161}.

Forward signaling EphB1/ephrinB2 activates several adaptor proteins that promotes cell migration, such as Grb2, p52^{Shc} and Src whereby can activate MAPK/ERK regulating events involved in cell motility²⁰, as well as, can induce tyrosine phosphorylation of paxillin and form complex with Grb2, Grb7, integrins, Nck, paxillin, and FAK proteins in a c-Src-dependent manner¹⁵⁵.

3.1.1.3 EphB1 in glioma

Exploring the role of EphB1 receptor in glioblastoma is still in its infancy, and further studies are necessary to generate more comprehensive data. The action mechanism of EphB1/ephrins signaling appears to be complex in brain tumors. The function of EphB1 in regulating chemotactic migration and invasion of glioma cells has opposite effects depending on whether EphB1 is functioning ligand dependently or ligand independently. It

has been shown that in patients with malignant glioma, high EphB1 expression level is associated with longer survival and ligand-dependent EphB1 signaling significantly suppresses glioma invasion. These results support the role of EphB1 as a negative regulator of glioma cell invasion in a ligand-dependent mechanism; clinically, EphB1 expression serves as a favorable predictor for clinical outcome of glioma patients. In particular, EphB1 ligand-dependent signaling, but not ligand-independent signaling, reduced migration. This may be caused by distinct downstream signaling. EphB1 forward signaling reversed cytoskeletal changes provoked by ephrin-B2 and abrogated the effects of migration and invasion induced by ephrin-B2 signaling. It is unknown what molecules are involved in these phenotypic changes downstream of ephrin-B2 signaling in glioma cells. Furthermore, overexpression of EphB1 acts as a favorable prognosis predictor for glioma patients¹⁵⁶.

3.2 EphrinB2-EphB4 in angiogenesis

It was shown that the ephrinB2/EphB4 pathway, in particular ephrin-B2 reverse signaling involving PDZ interactions, regulates endothelial tip cell guidance to control angiogenic sprouting and branching in physiological and pathological angiogenesis. Furthermore, ephrin-B2 was found to localize on the *filopodia* of tip cells and to control both VEGFR2 and VEGFR3^{162,163} internalization and signaling, but it does not appear to affect endothelial proliferation during sprouting¹⁶². These studies provide evidence that ephrin-B2 functions as a general modulator of the VEGF pathway in all endothelial cell types during angiogenesis. On the other hand, the role of EphB4 remains to be elucidated. EphB4 is absent in tip cells and it is expressed on cells behind the growing front. It was also shown that EphB4 overexpression suppressed sprouting and switched vascular growth to circumferential enlargement, but independently of its kinase activity and rather through stimulation of ephrinB2 reverse signaling¹⁶⁴. On the contrary, it was recently shown that EphB4 forward signaling is crucial to regulate intussusceptive angiogenesis, which takes place essentially without migration and rather only through proliferation¹⁶⁵. Indeed, administration of monomeric sEphB4 not only inhibits activation of endogenous EphB4, but also interferes with ephrinB2 reverse signaling, by preventing interaction and productive multimerization of the two binding partners. From a therapeutic perspective, it is particularly important that EphB4 stimulation did not completely abolish VEGF-induced endothelial proliferation, but rather only reduced it by about 40%, thereby preventing

aberrant angiogenesis without interfering with normal vascular growth. These results identify EphB4 as a druggable target to modulate the outcome of VEGF gene delivery and support further investigation of its therapeutic potential¹⁶⁵.

4. Tumor angiogenesis in glioblastoma

Glioblastoma (GBM) tumors are highly vascularized tumors, and glioma growth depends on the formation of new blood vessels. Angiogenesis is a highly regulated process involving migration, proliferation and differentiation of vascular endothelial cells (ECs) under the stimulation of specific signals. It is controlled by the balance between its promoting and inhibiting factors¹⁶⁶. Angiogenesis is essential for tumor growth and progression. Tumors create abnormal and functionally immature blood vessels due to deregulated factors such as angiogenic growth factors, angiogenesis inhibitors, and other genetic factors by a process known as pathological angiogenesis¹⁶⁷. The disorderly grown tumor vasculature alters the tumor microenvironment and influences different aspects of tumor progression, allows penetration of the tumor cells and its ability to metastasize to distant sites¹⁶⁶. Brain tumor angiogenesis is mediated through the action of many angiogenic factors, such as VEGF, basic fibroblast growth factor (bFGF), hepatocyte growth factor (HGF), platelet-derived growth factor (PDGF), TGF- β , MMPs, and angiopoietins (Angs). These angiogenic factors are generally upregulated and impact tumor progression¹⁶⁸.

Due to the role played by angiogenesis in tumor growth, targeting tumor vasculature and inhibition of growth factors and signaling pathways required for endothelial cell growth and proliferation is one of the practical approaches for anti-angiogenic cancer therapy. Importantly, the use of angiogenesis inhibitory factors and drugs can inhibit glioma proliferation, inhibiting the formation of new tumor vessels¹⁶⁶. Several anti-angiogenic therapies have been evaluated in clinical trials as an alternative or complementary to conventional cancer treatments. Most of the anti-angiogenic agents currently in phase I/II trials for brain tumors target the VEGF pathway as VEGF family and its receptors function as the central signaling pathway of glioma angiogenesis¹⁶⁶.

5. Innovative therapeutic approaches to target EphB1 receptor

5.1 Eph receptor-binding peptides

The Eph/ephrin signaling response can be modulated by agonist and antagonist peptides with high selectivity and binding affinity towards the ligand-binding domain (LBD) of Eph receptors^{169,170}. As LBD is extracellular, these peptides do not need to cross the plasma membrane solving a major problem encountered in the use of therapeutics that bind to intracellular targets¹⁷¹.

These peptides present similarity sequence with 15 amino acid motifs found in the G-H loop of the ephrin-B ligands which is the region that mediates high-affinity interaction with the EphB receptors¹⁶⁹.

Peptides present several advantages and some disadvantages; they can bind with high affinity to protein interfaces even in the absence of the highly concave pockets and also present low toxicity¹⁷¹. But peptides have also potentially poor pharmacokinetic parameters and oral bioavailability. Furthermore, *in vivo*, peptides need high resistance to plasma proteases and persistence in the blood circulation; for that they have been bound with unnatural amino acids in process as cyclization, PEGylation or inclusion into nanoparticles, obtaining novel peptides with a reduced digestion, metabolic stability and prolonged peptide lifetime in the circulation¹⁷².

A series of dodecapeptides that can selectively target the ligand binding domains of several Eph receptors, or subset of receptors, were identified by phage display¹⁶⁹.

Additional evidence that some of the peptides bind to the ligand binding domain includes NMR chemical shift perturbations that suggest an interaction of the peptides with residues of the ligand binding domain^{173,174} and mutations of residues in the ligand binding domain that affected peptide binding¹⁷³. However, the most direct evidence comes from several X-ray crystal structures of peptide-Eph receptor complexes. To date, the crystal structures of 4 peptides in complex with the EphA4, EphB2 or EphB4 LBDs have been solved, revealing that peptides can bind to the ephrin-binding pocket in a variety of orientations¹⁷⁵⁻¹⁷⁷.

YSA, SWL and derivative peptides are agonists that can promote EphA2 tyrosine phosphorylation and downstream signaling as well as cause EphA2 degradation^{170,178}.

The KYL, VTM and APY peptides are antagonists that can inhibit ephrin-induced EphA4 activation in *in vitro* biochemical assays, in cultured cells, and in mouse hippocampal slices^{173,179,180}. Blockage of the EphA4 LBD complex by KYL can inhibit EphA4 activation by amyloid- β oligomero which are believed to play an important role in the synaptic dysfunction and cognitive impairment characteristic of Alzheimer's disease¹⁷².

Phage display screens identified SNEW as a dodecameric peptide that selectively binds to EphB2 with moderate affinity and inhibits EphB2/ephrin-B2 interaction in ELISAs with an IC50 value of 15 μM ^{169,176}.

Notably, 8 of the 13 peptides identified by panning on EphB2 also bound to EphB1, suggest a close similarity between the ephrin-binding pockets of the two receptors. EWLS antagonist peptide binds selectively to EphB1 inhibiting EphB1/ephrin-B2 interaction with an IC50 value of 10 μM and also competing for EphB1 binding with the other 4 peptides identified by panning on EphB1¹⁶⁹.

TNYL peptide was the best inhibitor of ephrin-B2 binding to EphB4, even though its potency was only 50-150 μM for the biotinylated and non-biotinylated versions, respectively. In addition, if RAW sequence in the C-terminal extension of TNYL formed TNYL-RAW, peptide increased potency compared to TNYL¹⁷².

Stability studies revealed that the TNYL-RAW peptide possesses very short half-life in cell culture medium and in plasma, suggesting high susceptibility to proteolytic degradation and clearance from blood circulation. Therefore, fusion to the Fc portion of an antibody, conjugation to 40 kDa branched polyethyleneglycol (PEG) polymer or nanoparticles and complexation of the biotinylated peptide with streptavidin have been used to inhibit peptide degradation and rapid blood clearance¹⁸¹.

It has been shown that SNEW and TNYL-RAW can block human umbilical vein endothelial (HUVEC) cell retraction caused by ephrin-induced EphB2 activation¹⁷² and ephrin-induced EphB4 activation respectively³³, indicating the ability of the peptides to counteract the cell shape changes and anti-migratory effects mediated by the EphB2 and EphB4 receptors. Finally, EphB2 and EphB4 can promote tumorigenesis by interacting with ephrin-B ligands¹⁸², opening the possibility of using antagonist peptides for cancer therapy.

5.2 Altered miRNAs in glioblastoma

Micro-RNAs (miRs) have a role in various biological and pathological processes, including the immune response, development, inflammation, and so on¹⁸³. More importantly, aberrant miRs also take part in the pathogenesis of malignant tumors, like lung cancer, breast cancer, prostate cancer, and GBM¹⁸⁴⁻¹⁸⁷. As a mode of epigenetic regulation, miRs bind to the 3' untranslated region of target mRNA to repress its expression. Some studies showed a significant low expression of some miRs and

overexpression of the other miRs in GBM^{188,189}. Aberrant miRs are involved in every aspect of the malignant biological hallmarks of GBM.

MiRs contribute to the eight malignant biological hallmarks of GBM. Aberrant miRs modulate RTK signaling networks, mainly the PI3K/ AKT and RAS/MAPK pathways, promoting proliferation in GBM cells, participate in the evasion of growth suppressor signaling by targeting genes relevant to the Rb and Tp53 pathways, regulate cell death by modulating the extrinsic and intrinsic pathways of apoptosis signaling, they are involved in maintaining the stemness of GSCs to promote the immortality of GBM cells, regulate the invasion and migration of GBM cells, induce angiogenesis in GBM, they are involved in modulating the immune microenvironment of GBM by post-transcriptional regulation, alter the metabolic mode of GBM cells by modulating the expression of oncogenes or tumor suppressor genes, such as glycolytic transporters and metabolic enzymes¹⁹⁰.

In our study we identified some interesting miRs, such as miR 129-5p, miR 182 and miR 128, that could be involved in EphB1 dysregulation.

MiR-129 is a miRNA family containing three members, miR-129-5p, miR-129-2-3p and miR-129-3p. Among them, miR-129-5p has been reported as a tumor suppressor in many types of carcinoma, including breast cancer¹⁹¹, hepatocellular malignancy¹⁹², lung adenocarcinoma¹⁹³ and is involved in glioma cell processes.

MiR-182-5p is emerging as an important regulator of various physiological and pathological processes. It's an oncogene in many types of cancers. In particular miR-182-5p promoted glioma cell growth, migration, invasion and its clinical relevance was confirmed in human GBM samples. Therefore, these results firmly established miR-182-5p as a functional mediator of glioma tumorigenesis^{194,195}.

Brain-enriched miR-128 has been shown to be downregulated in glioma tissues and cell lines¹⁹⁶ and it has also been shown to regulate cell death, survival and invasion by various types of cancer. miR-128 could target different genes in a certain tissue or cell lines and have different functions. In particular miR-128 can suppress glioma cell proliferation and reduce glioma self-renewal^{196,197}. miR-128 can also inhibit tumor growth and angiogenesis¹⁹⁶.

6. Therapeutic angiogenesis

6.1 Therapeutic considerations for VEGF delivery: the importance of dose distribution control

Many patients worldwide suffer from atherosclerotic cardiovascular diseases, including peripheral artery disease (PAD) and coronary artery disease (CAD). These diseases are caused by an artery occlusion that leads to an ischemic condition. Treatment of ischemic diseases is strongly based on prevention of disease progression, with lifestyle changes, i.e. avoid smoking, sedentary life and poor diet. Moreover, there are no effective pharmacological treatments to cure ischemic tissue and many patient are even not amenable to be treated with angioplasty or surgical bypass in order to revascularize their ischemic tissues. Therefore, therapeutic angiogenesis, which aims at restoring blood flow in ischemic tissues by delivering angiogenic growth factors, represents an attractive treatment strategy. VEGF is the most powerful and angiogenic growth factor and was widely used in pre-clinical and clinical studies. In particular, preclinical data showed a surprisingly narrow therapeutic window for VEGF gene delivery, i.e. low doses of VEGF have not sufficient angiogenic effects, and higher doses rapidly become unsafe, leading to the growth of vessels that often display abnormalities in muscle, heart and other tissues¹⁹⁷⁻²⁰⁰.

VEGF can tightly bind the ECM and therefore remains tightly localized at the *in vivo* implantation sites and does not diffuse through tissue²²². Starting from this observation, Banfi and co-workers demonstrated that VEGF does not have an intrinsically steep dose-response curve, but rather that the apparently tight therapeutic window is a consequence of delivery methods which do not permit control over the microenvironmental distribution of expression levels *in vivo*²¹⁸. They took advantage of a myoblast-based platform (see later, Chapter 6.2) to delivery VEGF *in vivo*. In particular, they produced a retrovirally transduced primary myoblast population in order to drive constitutive expression of exogenous VEGF in murine skeletal muscle. Retroviral vectors can integrate stably and randomly in the genome of each cell and therefore individual cells express different levels depending on the copy number and integration sites. However, the isolation of single cells and their expansion permits the generation of monoclonal populations, in which each cells produces the same amount of VEGF. A library of such monoclonal populations, each homogeneously secreting a different amount of VEGF over a wide range of levels, were isolated. On the other hand, VEGF expression by the polyclonal population represented uncontrolled and heterogeneous levels of VEGF. By implanting the polyclonal parental myoblast population and different monoclonal populations in skeletal muscle of mice, they

found that: 1) heterogeneous VEGF levels by polyclonal myoblast population always caused the growth of aberrant angioma-like vascular structures; 2) reducing the total VEGF dose by serially diluting the heterogeneous population could not avoid aberrant angiogenesis; and 3) delivering homogeneous levels of VEGF by the monoclonal populations instead induced the growth of only physiological microvascular networks over a wide range of microenvironmental VEGF doses, until a threshold level was reached, above which aberrant angiogenesis was initiated²⁰² (Figures 5 and 6).

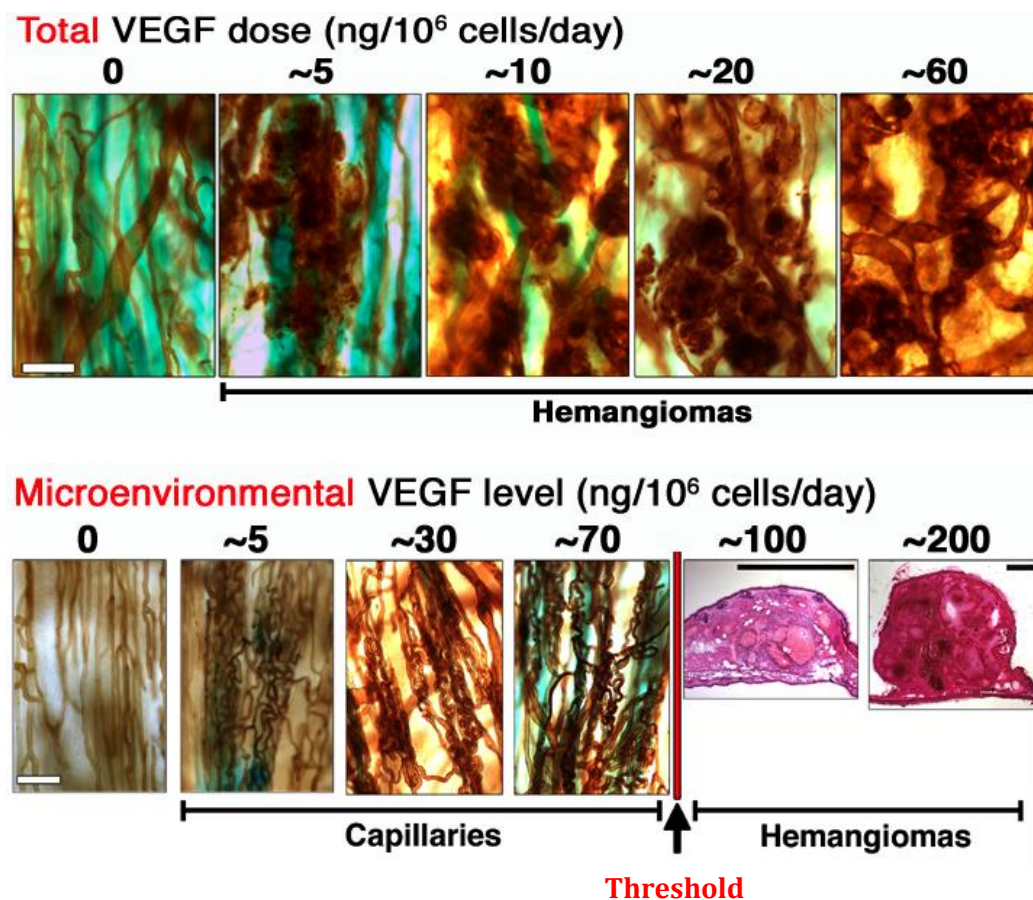


Figure 5. Total versus microenvironmental control over VEGF dose. Precise control over the VEGF delivered dose at a microenvironmental level allows to set apart normal angiogenesis from the aberrant one²⁰².

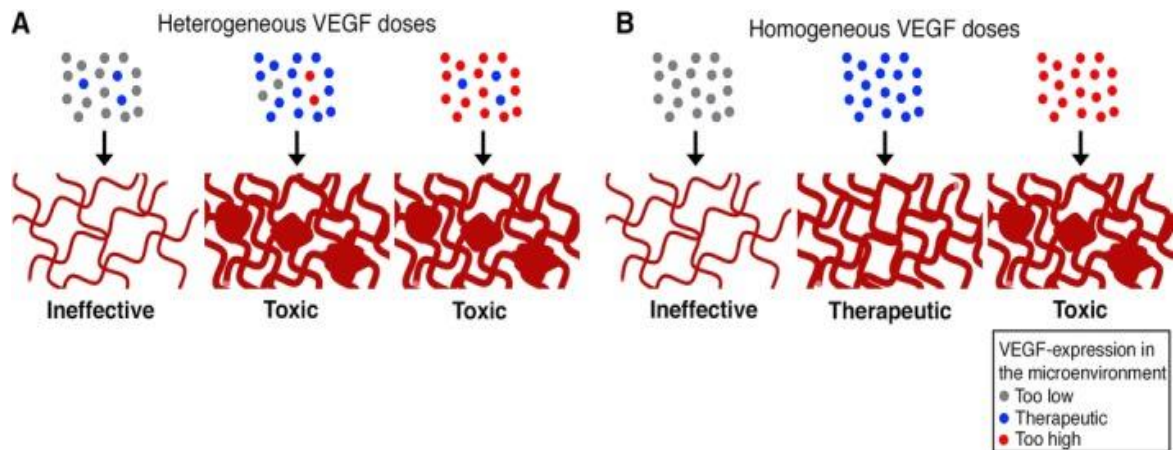


Figure 6: Functional outcomes of vascular endothelial growth factor (VEGF) dose distribution in tissue: (A) heterogeneous and (B) homogeneous VEGF dose distributions²¹⁸.

These results were corroborated also by similar findings by the controlled release *in vivo* of VEGF protein from *ad hoc* decorated fibrin hydrogels²⁰³. Remarkably, later studies showed the functional effects of different microenvironmental VEGF concentration in a mouse model of hindlimb ischemia and wound healing^{203,204}. The delivery of VEGF levels below the threshold in the ischemic tissues fully restored perfusion to non-ischemic levels, induced the growth of collateral arteries and reduced muscle damage, showing the functional benefits of optimized microenvironmental VEGF levels. When the same total dose was delivered, but expressed heterogeneously, only a moderate increase in blood flow was observed and aberrant vessel growth was always induced.

6.2 Cell-based VEGF delivery

Skeletal muscle is one of the target tissues of therapeutic angiogenesis strategies, as it is the organ affected by peripheral artery disease. Skeletal muscle consists of the fully differentiated, cylindrical, and polynucleated cellular syncytia called myofibers; and the unipotent, mononucleated myocytes precursors, named myoblasts. These latter are normally located between the sarcolemma and basement membrane of terminally-differentiated muscle fibers, representing a reserve population of precursor cells. They are able to proliferate and fuse in order to generate new myofibers and they can also join affected muscle fibers in response to damage, leading to muscle healing. Gene delivery to skeletal muscle can be achieved by two different strategies: the *in vivo* delivery, based on the use of vectors (either viral or nonviral), which are genetically engineered to pack the gene of interest and directly injected into the muscle tissue. Alternatively, in the *ex vivo*

delivery, cells are removed from the patient and expanded *in vitro*, where they are genetically engineered (e.g. with retroviral vectors) to carry the gene of interest and finally introduced back into the muscle, where they fuse into the pre-existing fibers. The myoblast-based approach is particularly suitable for *ex vivo* delivery strategies as they can be easily expanded *in vitro* from a small muscle biopsy without losing their potential to differentiate into myofibers, subsequently genetically engineered through a vector carrying the gene of interest and finally reinserted in the target area where, they fuse to the muscle fibers and start to produce the therapeutic transgene (Figure 7). Interestingly, after their implantation into the syngeneic host tissues, genetically engineered myoblasts have shown to be able to maintain high levels of gene expression for the entire life span of immunocompetent mice²⁰⁵. Moreover, the timing regulation of gene expression is achievable by using an inducible vector system, in which, for example, a tetracycline-inducible promoter is located upstream of the transcription unit. In this way, the production of the protein of interest occurs in response to systemic treatment with the antibiotic doxycycline. On the other hand, it is also possible to control both the level of gene expression and the distribution of the exogenous protein²⁰⁶.

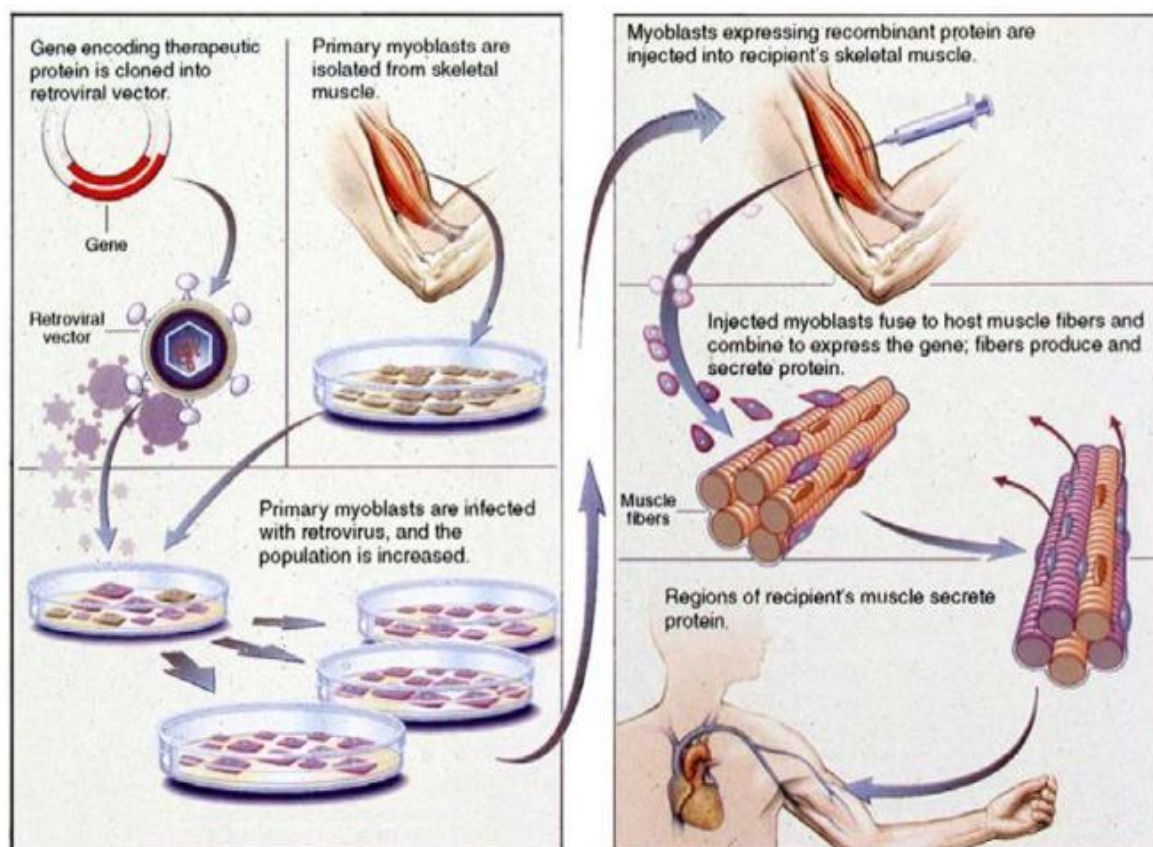


Figure 7: Myoblast-mediated gene therapy. Primary myoblasts are isolated from skeletal muscle, grown in culture and then transduced with a retroviral vector carrying the gene of interest. Later, myoblasts expressing the recombinant protein are reintroduced in the patient's skeletal muscle, where they fuse to host muscle fibers, produce and secrete the exogenous protein²⁰⁵.

6.3 Recombinant factor engineering for matrix decoration

It is desirable to independently control the dose and duration of angiogenic factor delivery in grafts. Many strategies have been developed to ensure sustained release of recombinant growth factors from natural and synthetic biomaterials. However, it has also been possible to create modified versions of growth factors by protein engineering, so that they can be used to decorate natural matrices and be presented to cells in their physiological context during tissue regeneration²⁰⁷. Tissue regeneration after damage starts in all cases with the deposition of a fibrin-based matrix rich in growth factors²⁰⁸, which provides ideal conditions for cell migration, vascular invasion and progenitor differentiation. Therefore, significant efforts have been directed at mimicking ECM decoration to ensure physiological presentation of morphogens. Growth factors have been incorporated into fibrin matrix exploiting the coagulation process itself. For example, murine VEGF₁₆₄ was fused to the octapeptide NQEQVSPL, which is the substrate of the transglutaminase coagulation factor XIIIa, allowing its covalent crosslinking into fibrin hydrogels and release only by enzymatic cleavage²⁰⁹. Further addition of the fibrinolysis inhibitor aprotinin, also engineered with the same technology, could finely tune the hydrogel degradation rate and therefore independently control the duration of factor release. Controlled VEGF delivery to skeletal muscle through this optimized platform was shown to yield exclusively normal, stable, and functional angiogenesis, over a wide range of easily control lable doses, and restored blood flow to ischemic tissues²¹⁰.

Aim of the research

Eph receptors and ephrin ligands are expressed in a wide variety of cell and tissue types. Eph/ephrin signalling regulates different cellular functions such as cell migration, proliferation, differentiation, adhesion, morphological changes and survival through cell–cell communication². Eph/ephrin signalling can occur in various modalities, depending on the direction of signal flow: forward signalling involves signal transduction from ephrins to Ephs; reverse signalling involves signalling from Ephs to ephrins; and bidirectional signalling involves the simultaneous activation of pathways downstream of ephrins and Ephs. Parallel signalling occurs when ephrins and Ephs on the same cell signal in response to Ephs and ephrins, respectively, present on a neighbouring cell. These different signalling modes can be elicited by either A or B class Ephs and ephrins. Anti-parallel signalling is a special case of simultaneously occurring forward signalling, whereby ephrin–Eph signals are propagated in both directions².

Furthermore, several studies support the role of Eph/ephrin signaling in tumorigenesis, metastasis, and angiogenesis. Every molecule of this system may act as tumor promoter or suppressor, dependent on cellular context and type of cancer. EphB1 receptor expression is altered in different brain tumors^{155,156}. Regarding glioblastoma, that is among the most aggressive brain tumors with an exceedingly poor prognosis²²¹ and lack of effective treatments, EphB1 downregulation may be correlated with aggressive cancer phenotypes, as this receptor may act as tumor suppressor¹⁵⁶.

Starting from these evidences, we aimed at characterizing the role played by EphB1 receptor in human glioblastoma by investigating its expression and modulation in U87 human glioblastoma cells.

First, we evaluated EphB1 expression in U87 cells that were either unmodified or transfected with p-CMV6-EphB1 plasmid and then we set up and characterized a glioblastoma *in vitro* model, expressing different levels of EphB1 receptor (low and high) and high levels of endogenous agonist EphrinB1. Subsequently, the migration assay in native and EphB1-overexpressing U87 cells has been used as a reliable *in vitro* research tool to screen compound libraries seeking for potential EphB1 agonists or antagonists.

Efforts aimed at elucidating the loss of EphB1 receptor expression or increasing its activation in glioblastoma cells may lead to the development of innovative pharmacological approaches to treat this aggressive malignant brain tumor.

Eph/ephrin system is also involved in angiogenesis, i.e. the growth of new blood vessels from pre-existing ones. Atherosclerotic cardiovascular diseases, such as peripheral artery

disease (PAD) and coronary artery disease (CAD), are the leading cause of death in the Western world. PAD patients with advanced ischemia often are not satisfactorily treated by current procedures and require limb amputations, with significant morbidity and mortality. In this context, therapeutic angiogenesis is an alternative and attractive strategy that aims at inducing the formation of new blood vessels to improve the perfusion of ischemic tissue by the delivery of growth factors that control vascular growth. VEGF is the master regulator of vascular growth and the key target of therapeutic angiogenesis approaches. However, first-generation clinical trials of VEGF gene therapy have been disappointing and clear clinical benefit has yet to be established²¹⁶. During the last two decades the Banfi group, that hosted me for 9 months, has studied the therapeutic implications of VEGF dose distribution in skeletal muscles. They found that VEGF expression can induce either normal or aberrant angiogenesis depending on its dose localized in the microenvironment around each producing cell *in vivo*. A search for the molecular mechanisms underlying the transition between normal and aberrant angiogenesis by different VEGF doses identified a role for the EphrinB2/EphB4 pathway, whereby EphB4 is a druggable target to modulate the outcome of VEGF gene delivery. Preliminary data by the host group further suggest a similar role for the endothelial-specific Notch4 signaling pathway. In fact, Notch4 inhibition could prevent aberrant angiogenesis by uncontrolled VEGF expression in skeletal muscle, similarly to the stimulation of EphB4 signaling. In agreement with these findings, others have previously shown that Notch4 constitutive activation leads to abnormal dilated vessels and the development of brain arteriovenous malformations (AVM)¹¹¹, whereas its inhibition leads to a regression of AV shunts and reversion to capillary-like microvessels¹¹².

During my period of research at the Department of Biomedicine, Basel, under the supervision of PD Dr. Banfi and Dr. Gianni-Barrera, I studied the role of Notch4 in the switch between normal and aberrant angiogenesis induced by specific doses of VEGF, through a loss of function approach and taking advantage of a state-of-the-art platform for the controlled and dose-dependent delivery of engineered growth factors.

Materials and Methods

1. First part

1.1 Reagents

p-CMV6-EphB1 plasmid was purchased from OriGene Technologies (Rockville, USA). Ephrin-B1 Fc (473-EB-200), was from R&D System (Minneapolis, MN). EWLSPN peptide was produced by the department of Chemistry Ciamician (University of Bologna) and dissolved in dimethylsulphoxide (DMSO). EWLSPN-derived peptides (A-EWLSPN, FITC-AEWLSPN, AAA-EWLSPN, FITC-AAAEWLSPN, EGP-EWLSPN, AWLSPN, EALSPN, EWASPN, EWLAPN, EWLSAN, EWLSPA) were designed and produced by the department of Chemistry Ciamician (University of Bologna) and dissolved in dimethylsulphoxide (DMSO). The final concentration of DMSO was less than 0.1% and did not cause any significant effect on the activities tested in this study. MG132 was purchased from Sigma (Steinheim, Germany) at a concentration of 10 mM.

Anti EphB1 (diluted 1:2000) and anti actin (diluted 1:5000) were from Cell Signaling Technologies (EuroClone, Pero, Italy). Anti phospho-EphB1 (diluted 1:2000) was from Sigma (Steinheim, Germany). Anti-rabbit or anti-mouse (diluted 1:8000) horse radish peroxidase-conjugated secondary antibodies were from Santa Cruz Biotechnology (Dallas, TX, USA).

1.2 Cell culture

Human glioblastoma U87 cells were purchased from American Type Culture Collection (Rockville, MD, USA). Cells were grown in Eagle's Minimal Essential Medium (EMEM) (Gibco, Thermo Fisher Scientific) supplemented with 1% L-Glutamine (Lonza Group Ltd, Basel, Switzerland), 1x non-essential aminoacids (Gibco, Thermo Fisher Scientific) and 1x antibiotic-antimycotic solution (Gibco by Life Technologies, Thermo Fisher Scientific) (defined cell culture medium), containing 10% fetal bovine serum (Lonza) and cultured at 37°C in a humidified atmosphere of 5% CO₂. Human neuroblastoma SH-SY5Y cells (European Collection of Cell Culture, Salisbury, UK) were grown in Dulbecco's Modified Eagle Medium (DMEM) (Gibco, Thermo Fisher Scientific) supplemented with 10% fetal bovine serum (Lonza), 1% L-Glutamine (Lonza), 1x non-essential aminoacids (Gibco), and 1x antibiotic-antimycotic solution (Gibco by Life Technologies) and cultured at 37°C in a humidified atmosphere of 5% CO₂.

1.3 Cell transfection and treatments

U87 cells were plated in cell culture dishes and at 70–80% confluence were transiently transfected with 5 ug/dish of p-CMV6-EphB1 plasmid using the Polyethylenimine branched Transfection Reagent (PEI) (Sigma, Steinheim, Germany), according to the manufacturer's protocol and treatments were started 24 h later. U87 native and transfected cells were treated with EphrinB1-Fc (1µg/ml; 24 h), or EWLSPN (20-200 nM; 18-24 h) or EWLSPN-derived peptides (20-200 nM; 18-24 h) or MG132 (5 µM; 24 h), or left untreated.

1.4 Wound healing assay

U87 cells were seeded in 60 mm-dishes until they reached 90% confluence. The cell monolayer was scraped in three straight lines to create “scratches” with a sterile 200-µL pipette tip. The debris and non-adherent cells were removed by washing the cells once with Eagle's Minimal Essential Medium (EMEM); the same serum-free cell culture medium with indicated treatments was added for 18 and 24 h. Images were acquired using an inverted phase-contrast microscope (Nikon; 5× objective) equipped with a Nikon digital camera. Six images per treatment were measured and analyzed by TScratch program²¹², a software tool for automated analysis of wound healing assays, comparing open area at 18 h or 24 h to that at 0 h. The migration rate, reflecting the change in the wound area over time, was expressed as percentage of cell migration calculated as follows: cell migration (%) = $[(A_{t\ 0h} - A_{t\ 18h\ or\ 24h})/A_{t\ 0h}] \times 100$, where, $A_{t\ 0h}$ is the area of wound measured immediately after scratching, and $A_{t\ 18h}$ or $A_{t\ 24h}$ are the areas of wound measured 18 h or 24 h after scratching.

1.5 Cell proliferation assay

U87 cells were plated on 12-well plated and transfected and/or treated for 24 h or maintained in cell culture medium containing 10% fetal bovine serum. Five hours before the end of the treatments, [methyl-³H] Thymidine (Perkin Elmer, Milan, Italy) (50 nM final concentration) was added to serum-free cell culture medium and the plate was incubated at 37 °C. Subsequently, medium was removed and cells were washed twice with PBS. 500 µl

of PBS was added to each well, the cells were scraped off and centrifuged at 13,000g for 3 min at 4 °C; supernatants were then discarded, pellets resuspended in 500 µl of cold trichloroacetic acid (10% w/v), incubated on ice for 20 min and centrifuged at 13,000g for 3 min at 4 °C. The obtained supernatant was then discarded, pellet suspended in 500 µl of cold methanol and centrifuged at 3 min for 13,000g at 4 °C. After that, the pellet was suspended in 200 µl of NaOH 1 N and heated at 55 °C for 10 min. Samples were then neutralized with 200 µl of HCl 1 N and 350 µl of the labeled DNA incubated in counting vials with 4 ml of Filter Count scintillation liquid (Perkin Elmer Italia). Vials were vortexed and incubated overnight at room temperature and the radioactivity was determined by liquid scintillation spectrometry.

1.6 Quantitative real time PCR

EphB1 mRNA levels were quantified in U87 native and transfected cells and in SH-SY5Y native cells by RT-PCR. Cells were transfected, then collected and centrifuged (500 g for 5 min) and rinsed with phosphate-buffered saline. Total cellular RNA was extracted with Tri-reagent® (Sigma-Aldrich) and digested with Rnase-free Dnase (Thermo Fisher Scientific) for 15 min at 25°C according to the manufacturer's instructions. For each sample, 2 µg of total RNA was converted into cDNA using High-Capacity cDNA Reverse Transcription Kits (Life Technologies, Italy), according to the manufacturer's instructions. Real-time PCR was performed for relative quantification of human EphB1 and Ephrin-B1 transcripts using the StepOne Instrument (Life Technologies) and the GoTaq® qPCR master mix (Promega, Madison, Wisconsin, USA). To amplify EphB1 cDNA, a sense primer (5'-GACTGACGATGATTACAAGTCAGAGC-3') and an antisense primer (5'-AGATGGCCACCAAGGACACA-3') were used at 0,25 µM final concentration for producing 101-bp fragment (1953-2053bp; GenBankAccession no. NM_004441.4). To amplify the Ephrin-B1 cDNA, a sense primer (5'-TTGGCCAAGAACCTGGAG-3') and an antisense primer (5'-GCCCTTCCCCTTAGGAACT-3') were used at 0,25 µM final concentration. As a control, a 169-bp fragment of the human L19 ribosomal protein gene (62–230 bp; GenBank Accession BC062709) was amplified with a sense primer (5'-CTAGTGTCCCTCCGCTGTGG-3') and an antisense primer (5'-AAGGTGTTTTTCCGGCATC-3') at 0,25 µM final concentration. The three amplifications follow the same protocol consisting of: 95°C for 10 min followed by 40 cycles of 95°C for 15 s and 60°C for 60 s. After that, the temperature was lowered to 60°C

for 30 s and the specificity of the reaction was verified by analysis of the melting curve once the appropriate double-stranded DNA melting temperature had been reached. For data analysis, relative expression of RT-PCR products was determined using the $\Delta\Delta C_T$ method²¹³; where C_t is the threshold cycle, i.e. the cycle number at which the sample's relative fluorescence rises above the background fluorescence and $\Delta\Delta C_t = [C_t \text{ gene of interest (unknown sample)} - C_t \text{ L19 (unknown sample)}] - [C_t \text{ gene of interest (calibrator sample)} - C_t \text{ L19 (calibrator sample)}]$. One of the control samples was chosen as the calibrator sample and used in each PCR. Each sample was run in triplicate and the mean C_t was used in the $\Delta\Delta C_t$ equation. L19 was chosen for normalization because this gene showed consistent expression relative to other housekeeping genes among the treatment groups in our experiments.

1.7 Western blotting analysis

To detect EphB1, pEphB1 and β -actin, U87 native or transfected, treated or non-treated cells, derived from 60-mm dishes used for wound healing assay, were scraped off and pelleted after 48 h of transfection and 24 h of exposure to different treatments. Proteins (30 μ g to assay EphB1 and pEphB1 or 20 μ g to assay β -actin) were separated by SDS-PAGE on 10% (w/v) acrylamide/bisacrylamide gels and electrotransferred onto nitrocellulose membranes. Membranes were incubated in TBS-T (20 mmol/L Tris-HCl, pH 7.5, 137 mmol/L NaCl, 0.05% (v/v) Tween 20) containing 5% (w/v) bovine serum albumin for 1 h at room temperature. Membranes were then incubated for 12 h at 4°C with the appropriate primary antibody, rinsed with TBS-T, and incubated with peroxidase-conjugated anti-rabbit or anti-mouse secondary antibodies (Santa Cruz Biotechnology, Dallas, Texas, USA) at room temperature for 1.5 h and the blots were developed with Clarity™ Western ECL substrate (Bio-Rad Laboratories, Segrate, Milan, Italy). Blot images were digitally acquired by LAS3000 Imager (Fujifilm Corporation, Stamford, CT, USA) and protein expression semi-quantitatively analyzed using AIDA software (Raytest Isotopenmessgeraete GmbH, Mannheim, Germany). The same protocols were performed to determine changes in protein levels of EphB1 receptor (30 μ g) and β -actin (20 μ g) in SH-SY5Y native cells.

1.8 Statistical analysis

All data are expressed as mean \pm SEM for the number of experiments indicated. Statistical analyses were performed via GraphPad Prism (version 5.0; GraphPad Software, Inc., La Jolla, CA, USA) using one-way ANOVA followed by Newman-Keuls post-test or using standard Student t test. P values < 0.05 were considered significant.

2. Second part

2.1 Fibrin matrix production and implantation into mice

Fibrin matrices were prepared by mixing a solution containing 25 mg/mL of human fibrinogen (plasminogen-, von Willebrand Factor-, and fibronectin-depleted; Enzymes Research Laboratories, Swansea, UK), 2.0 U/mL thrombin (Sigma Aldrich, St Louis, Buchs, Switzerland), 2.0 U/mL factor XIIIa (CSL Behring, Switzerland), combined with 2.5 mM Ca²⁺ (Sigma Aldrich, St Louis, Buchs, Switzerland) in 4-(2-hydroxyethyl)-1-piperzineethanesulfonic acid (HEPES; Lonza, Basel, Switzerland). Matrices containing aprotinin and VEGF₁₆₄ were obtained by adding the engineered proteins to the cross-linking enzymes solution before mixing with fibrinogen. The covalent cross-linking of recombinant VEGF and aprotinin into fibrin hydrogels and its release by enzymatic cleavage was allowed by using the α_2 -Plasmin Inhibitor-derived octapeptide NQEQVSPL (α_2 -PI₁₋₈), which is a substrate for the transglutaminase coagulation factor XIIIa, and fusing it onto the N-terminus of murine VEGF₁₆₄ or aprotinin by a protein engineering approach previously developed by J.A. Hubbell at EPFL, Lausanne, Switzerland^{214,215}. The mix with α_2 -PI₁₋₈-VEGF₁₆₄ and the cross-linking solution had a final concentrations of 25 μ g/mL (intermediate VEGF dose), or 100 μ g/mL (high VEGF dose). Control gels contained all the reagents except α_2 -PI₁₋₈-VEGF. The fibrinogen solution was placed into a cloning well of a plastic mini-tray placed on ice, the cross-linking enzymes were added and mixed three times. The resulting mix was rapidly aspirated with a 0.3 ml insulin syringe with integrated 30 G needle (Micro-Fine, Becton Dickinson, Allschwill, Switzerland) and immediately injected into gastrocnemius (GC) and vastus intermedius (VI) muscles of mice, to allow *in situ* polymerization. A total volume of 50 μ l was injected each time in the following immunocompetent murine strains: 1) Notch-4-deficient mice (N4^{D1}) (010544 B6;129S1-Notch4^{tm1Grid}/J, The Jackson Laboratory supplied by Charles River Laboratories, Sulzfeld, Germany), 2) Notch-4 knockout (N4^{-/-}) and littermate wild-type mice (N4^{+/+}) (C57BL/6N-NOTCH4^{tm1(KOMP)Vlcr}, Australian Phenomics Facility). After injection of fibrin hydrogels, *in situ* polymerization was allowed for 20 seconds before slowly extracting the needle.

2.2 Immunofluorescence tissue staining

All the studies were performed on frozen tissue sections. Mice were anesthetized and sacrificed by vascular perfusion of 1% paraformaldehyde (PFA) in PBS pH 7.4 for 3 min

under 120 mm/Hg of pressure. Vastus intermedius (VI) and gastrocnemius (GC) muscles were harvested, post-fixed in 0.5% PFA for 2 hours, cryoprotected in 30% sucrose in PBS overnight at 4°C, embedded in OCT compound (CellPath, Newtown, Powys, UK), frozen in freezing isopentane and cryosectioned. 14- μ m tissue sections were then immunostained. The following primary antibodies and dilutions were used: rat monoclonal anti-mouse endomucin (clone V.7C7, Santa Cruz Biotechnologies, Santa Cruz, CA, USA) at 1:100; goat polyclonal anti-mouse podocalyxin (R&D Systems) at 1:100; rabbit polyclonal anti-laminin (Abcam) at 1:200. Fluorescently labeled secondary antibodies (Invitrogen, Basel, Switzerland) were all used at 1:200. Images were acquired with 40x objective on a Carl Zeiss LSM710 3-laser scanning confocal microscope (Carl Zeiss, Feldbach, Switzerland) and analyzed with ImageJ software.

2.3 Vessel measurements

Vessel length density (VLD) and diameters were measured in 14 μ m-thick cryosections as previously described^{202,204}. Vessel length density (VLD) was quantified in fluorescently immunostained cryosections as described²⁰². Briefly, 10 fields per muscle were analyzed by tracing the total length of vessels in the acquired field and dividing it by the area of the fields. Vessels diameters were analyzed in 10 randomly acquired fields in each area of effect per sample measuring a total of 1,000 to 5,000 individual vessel diameters per condition. Fluorescence images were acquired as Z-Stack with 40x objective on a Carl Zeiss LSM710 3-laser scanning confocal microscope (Carl Zeiss, Feldbach, Switzerland) and analyzed with ImageJ software.

2.4 Statistics

Data are presented as means \pm standard error. The significance of differences was assessed with the GraphPad Prism 8 software, using analysis of variance (ANOVA) followed by the Bonferroni test (for multiple comparisons). $P < 0.05$ was considered statistically significant.

Results

1. First part

The experiments reported in this section were mainly carried out in the human glioblastoma cell line U87-MG (now on called U87), that is frequently employed in brain cancer research. In this case U87 cells express low levels of our target receptor EphB1 and we wanted to study the possible consequences of this low expression in human glioblastoma cells. We also employed the human neuroblastoma cell line SH-SY5Y, because it expresses several human-specific protein and protein isoforms, like some tyrosine kinase receptors. Indeed, we previously identified that SH-SY5Y cells express EphB1 endogenously. We employed this cell line to compare the expression of EphB1 in U87 cells with cells that endogenously express the receptor.

1.1 EphB1 is low expressed but functional in U87 cells and it is expressed in transfected U87 cells

To evaluate EphB1 mRNA and protein levels in U87 cells we performed Real-time PCR and western blot respectively. We analyzed EphB1 mRNA and protein levels in native U87 cells and after transfection with pCMV6-EphB1 plasmid. EphB1 mRNA and protein levels were low in native U87 cells. EphB1 mRNA (Fig. 1A) and protein (Fig. 1B and 1C) were increased in transfected U87 cells after 48h. In this way we set up and characterized a glioblastoma *in vitro* cell model, expressing different levels of EphB1 receptor (low and high). For the EphB1 receptor low levels model we utilized native U87 cells and for EphB1 high levels model we used transfected U87 cells.

To investigate if EphB1 receptors were functional in U87 cells, they were exposed to soluble agonist EphrinB1-Fc for 24h. Cell lysates were analyzed by immunoblotting using anti-P-EphB1 and anti-EphB1. EphrinB1-Fc significantly increased EphB1 phosphorylation after 24h (Fig. 1D and 1E).

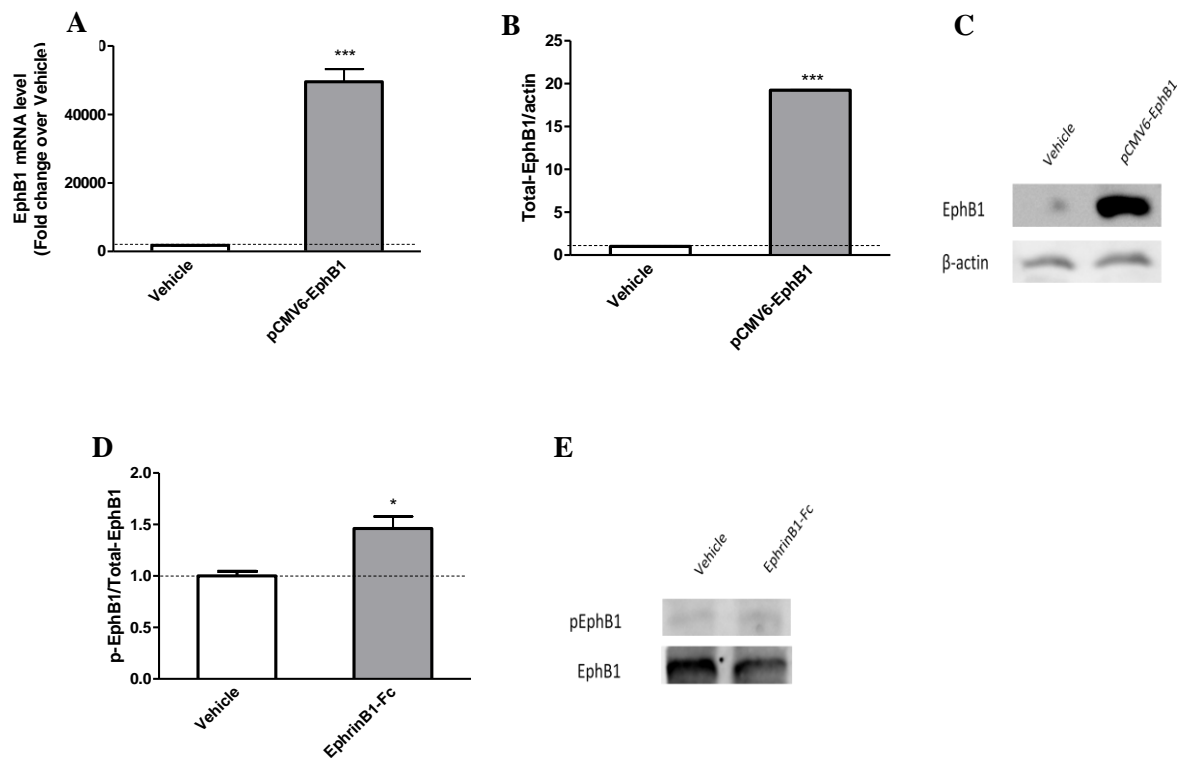


Fig. 1. (A) Real-time PCR of EphB1 receptor and Ephrin-B1 mRNA levels in U87 cells after transfection with pCMV6-EphB1 plasmid or exposure to vehicle. Data are presented as the mean \pm SEM of $n=6$. *** = $p<0,001$ vs vehicle (Unpaired t test with Welch's correction). (B) Quantification of Total EPHB1 receptor levels in U87 cells after transfection with pCMV6-EphB1 plasmid or exposure to vehicle (C) and representative blots of U87 cells after transfection with pCMV6-EphB1 plasmid or exposure to vehicle. Data are presented as the mean \pm SEM of $n=10$. *** = $p<0,001$ vs vehicle (Unpaired t test with Welch's correction). (D) Quantification of P-EPHB1 levels in U87 cells exposed to 1 μ g/mL EphrinB1-Fc or vehicle at 24h (E) and representative blots of U87 cells exposed to 1 μ g/mL EphrinB1-Fc or vehicle at 24h. Data are presented as the mean \pm SEM of $n=5$. * = $p<0,05$ vs vehicle (Unpaired t test with Welch's correction).

1.2 EphB1 overexpression and/or activation decreases cell migration in native and transfected U87 cells

To evaluate cell migration in U87 cells, we used a wound-healing assay and six images per treatment/ per each experiment were acquired and analyzed by TScratch program. We observed that the transfection with pCMV6-EphB1 plasmid decreased migration to nearly half at 18h (Fig. 2A and 2B) and 24h (Fig. 2C and 2D), as compared to vehicle-treated cells. The administration of EphB1 soluble agonist EphrinB1-Fc (1 μ g/mL) further reduced cell migration in native and transfected U87 cells at 18h and 24h.

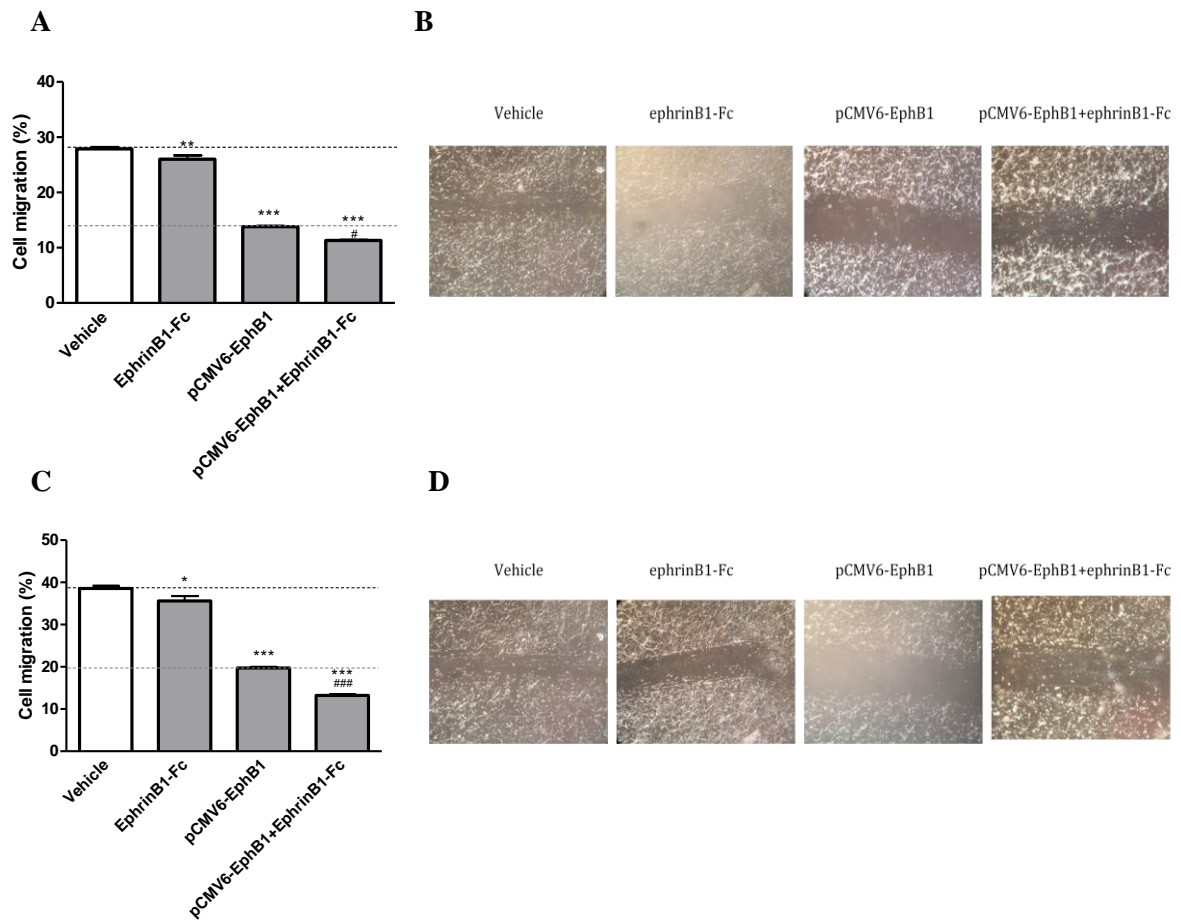


Fig. 2. Transfection with pCMV6-EphB1 plasmid decreases cell migration in U87 cells. The effect of the transfection and/or treatment with 1 $\mu\text{g}/\text{mL}$ EphrinB1-Fc on U87 cell migration evaluated by wound closure in a scratch assay; images were acquired after 18h and 24h. (A) Quantification of cell migration after maintenance of cells in serum-free medium (vehicle); transfection with pCMV6-EphB1 plasmid and/or treatment with 1 $\mu\text{g}/\text{mL}$ EphrinB1-Fc at 18h and (B) representative images of U87 cell migration after transfection with pCMV6-EphB1 plasmid and/or treatment with 1 $\mu\text{g}/\text{mL}$ EphrinB1-Fc at 18h. Data are presented as the mean \pm SEM of $n=6$. *** = $p<0,001$ vs vehicle; ** = $p<0,01$ vs vehicle; # = $p<0,05$ vs pCMV6-EphB1 (Newman-Keuls test after ANOVA). (C) Quantification of cell migration at 24h in the same conditions described above and (D) representative images of U87 cell migration at 24h. Data are presented as the mean \pm SEM of $n=6$. *** = $p<0,001$ vs vehicle; * = $p<0,05$ vs vehicle; ### = $p<0,001$ vs pCMV6-EphB1 (Newman-Keuls test after ANOVA).

1.3 EphB1 overexpression and/or activation decreases cell proliferation in native and transfected U87 cells

To evaluate cell proliferation in U87 cells, we employed a cell proliferation assay, incorporating [methyl- ^3H] Thymidine and determining radioactivity by liquid scintillation spectrometry. In line with the previous data, EphB1 overexpression determined a

remarkable decrease in U87 cell proliferation at 24h. The exposure to EphB1 soluble agonist EphrinB1-Fc (1 $\mu\text{g}/\text{mL}$) did not influence cell proliferation in native and transfected U87 cells (Fig 3).

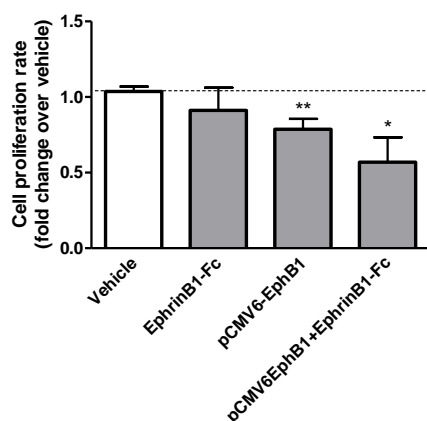
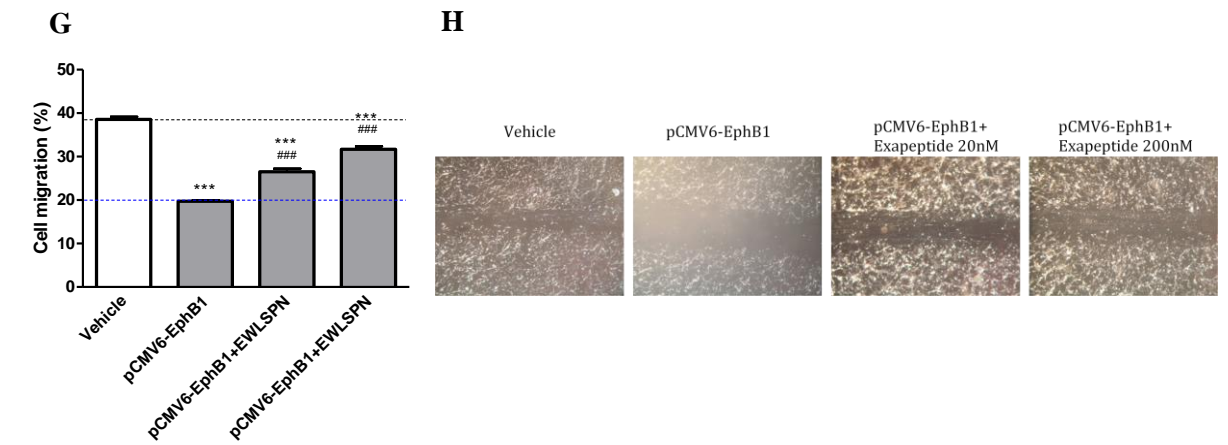
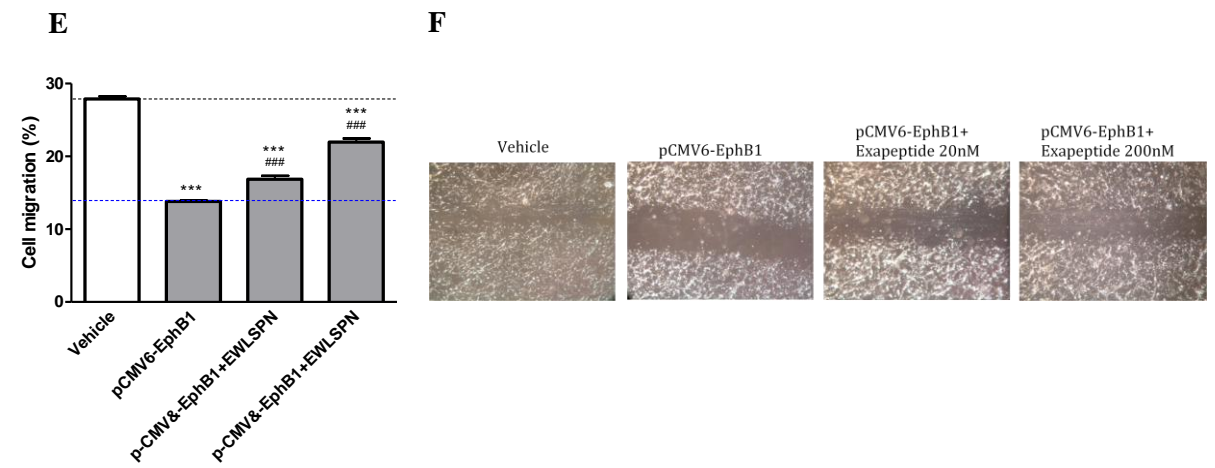
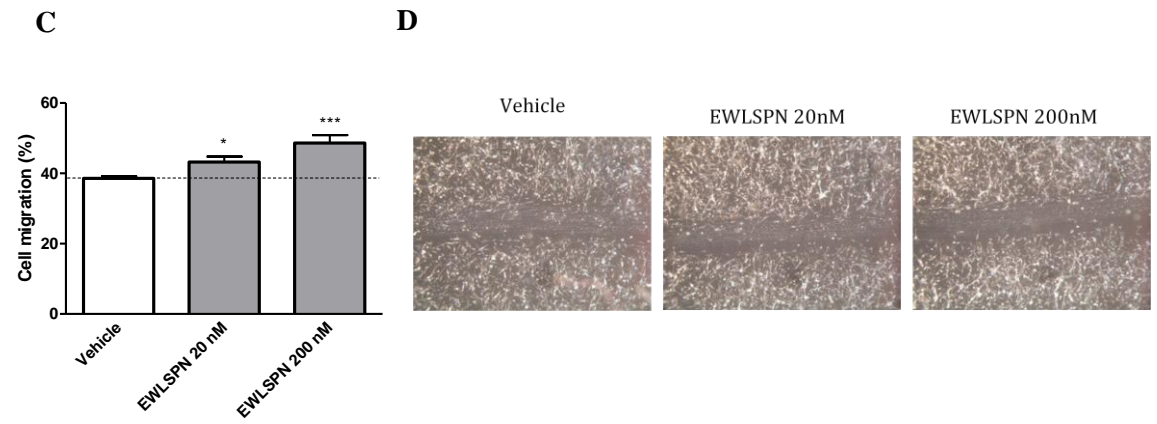
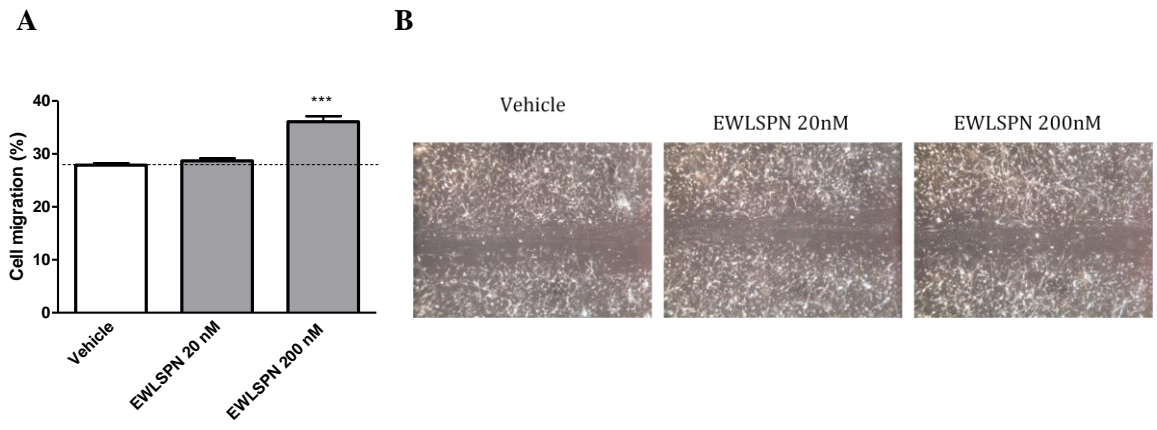


Fig. 3. Transfection with pCMV6-EphB1 plasmid decreases cell proliferation in U87 cells. The effect of the transfection and treatment with 1 $\mu\text{g}/\text{mL}$ EphrinB1-Fc on U87 cell proliferation evaluated by the radioactivity of the cells; the proliferation assay was performed at 24h. Quantification of cell proliferation after transfection with pCMV6-EphB1 plasmid and/or treatment with 1 $\mu\text{g}/\text{mL}$ EphrinB1-Fc at 24h. Data are presented as the mean \pm SEM of $n=7$. ** = $p<0,01$ vs vehicle; * = $p<0,05$ vs vehicle (Newman-Keuls test after ANOVA).

1.4 EphB1 peptide antagonist increases cell migration in a concentration-dependent manner in native and transfected U87 cells

In previous studies it has been demonstrated that Hexapeptide (EWLSPN) inhibits p42/44 MAPK phosphorylation EphrinB1-Fc-mediated at higher concentration in EphB1-expressing HEK293. Indeed, Hexapeptide can counteract EphrinB1-Fc-mediated activation of p42/44 phosphorylation with IC_{50} 1,21 μM . In this experiment we investigated the role of Hexapeptide on cell migration in U87 cells. We administered 20-200 nM Hexapeptide to native or transfected U87 cells. In line with previous data, has been noted that Hexapeptide worked as an EphB1 novel peptide antagonist, because its administration to native or transfected U87 cells caused a concentration-dependent increase in cell migration at 18h and 24h (Fig 4A-H).

To investigate if Hexapeptide influenced the activation of EphB1 receptors, antagonizing them, western blottings were performed. Western blot analysis ascertained that EphB1 phosphorylation was significantly reduced in U87 cells transfected with pCMV6-EphB1 plasmid and treated with Hexapeptide at 20 nM and 200 nM (Fig. 4I, J).



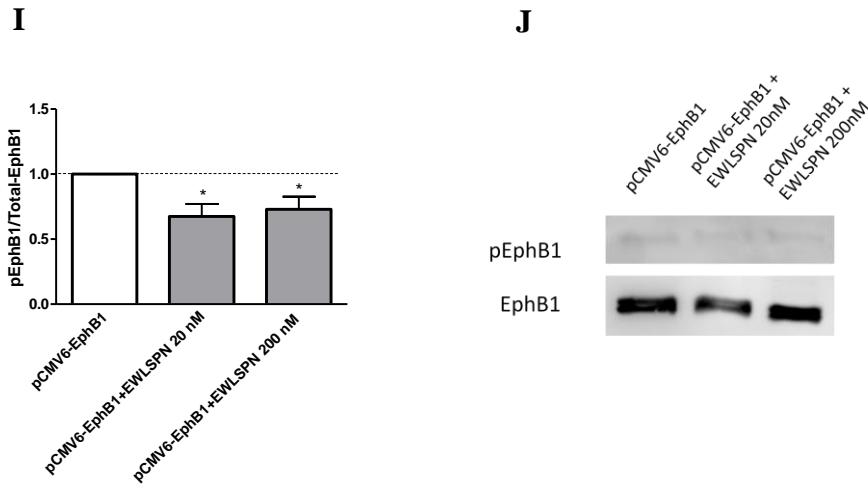


Fig. 4. The Hexapeptide increased cell migration in native and transfected U87 cells and decreased EphB1 receptor phosphorylation in transfected U87 cells. (A-H) The effect of the transfection and/or treatment with 20-200 nM Hexapeptide on U87 cell migration evaluated by wound closure in a scratch assay; images were acquired after 18h and 24h. (A) Quantification of cell migration at 18h after maintenance of cells in serum-free medium (vehicle) or administration of 20-200 nM Hexapeptide and (B) representative images of U87 cell migration at 18h after administration of 20-200 nM Hexapeptide. Data are presented as the mean \pm SEM of $n=12$. *** = $p<0,001$ vs vehicle (Newman-Keuls test after ANOVA). (C) Quantification of cell migration at 24h in the same conditions described above and (D) representative images of U87 cell migration at 24h. Data are presented as the mean \pm SEM of $n=12$. *** = $p<0,001$ vs vehicle; * = $p<0,05$ vs vehicle; (Newman-Keuls test after ANOVA). (E) Quantification of cell migration after transfection with pCMV6-EphB1 plasmid and/or administration of 20-200 nM Hexapeptide and (F) representative images of U87 cell migration after transfection with pCMV6-EphB1 plasmid and/or administration of 20-200 nM Hexapeptide at 18h. Data are presented as the mean \pm SEM of $n=12$. *** = $p<0,001$ vs vehicle; ### = $p<0,001$ vs pCMV6-EphB1 (Newman-Keuls test after ANOVA). (G) Quantification of cell migration after transfection with pCMV6-EphB1 plasmid and/or administration of 20-200 nM Hexapeptide at 24h and (H) representative images of U87 cell migration after transfection with pCMV6-EphB1 plasmid and/or administration of 20-200 nM Hexapeptide at 24h. Data are presented as the mean \pm SEM of $n=12$. *** = $p<0,001$ vs vehicle; ### = $p<0,001$ vs pCMV6-EphB1 (Newman-Keuls test after ANOVA). (I) Quantification of P-EphB1 levels in U87 cells after transfection with pCMV6-EphB1 plasmid and exposure to 20-200 nM Hexapeptide or vehicle and (J) representative blot of U87 cells after transfection with pCMV6-EphB1 plasmid and exposure to 20-200 nM Hexapeptide or vehicle. Data are presented as the mean \pm SEM of $n=4$. * = $p<0,05$ vs pCMV6-EphB1 (Newman-Keuls test after ANOVA).

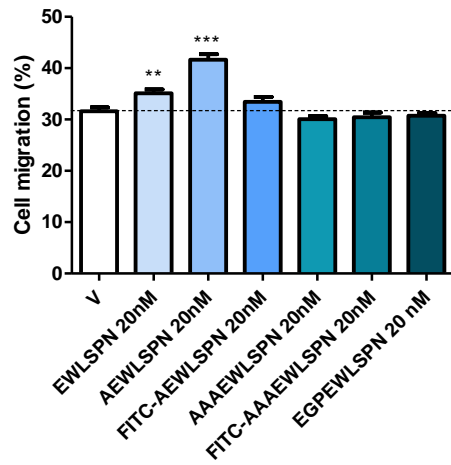
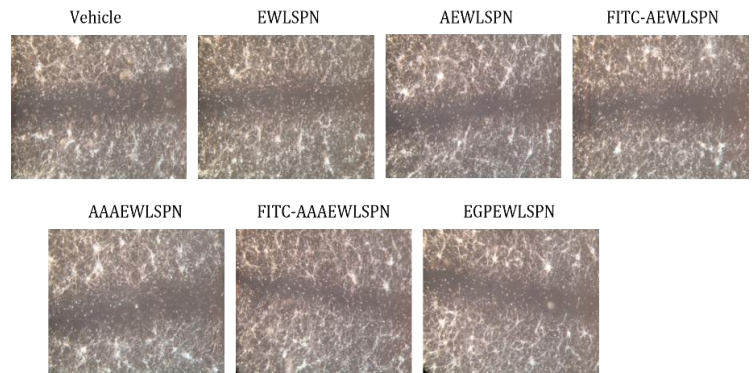
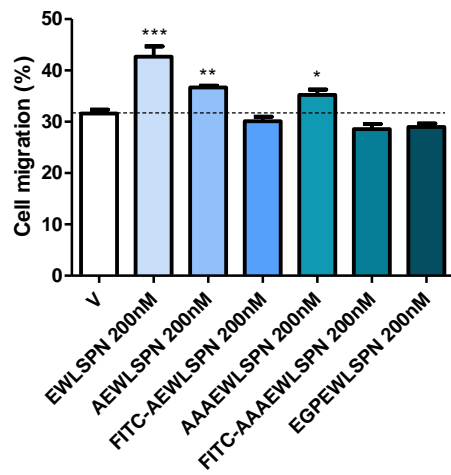
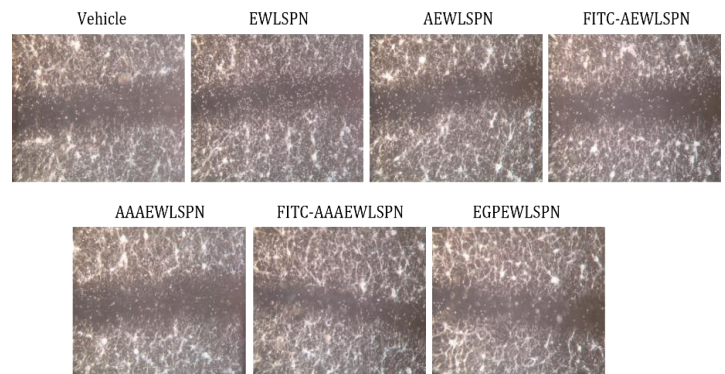
1.5 The addition of a beta-alanine to the N-terminus of the Hexapeptide increases cell migration in native and transfected U87 cells

Starting from the Hexapeptide, that we observed to display an antagonist effect, the research group directed by Proff. Alessandra Tolomelli and Walter Cabri at Department of Chemistry (G. Ciamician) designed novel peptides with modifications at the N-terminus of the Hexapeptide or an alanine scanning library in order to evaluate if a modification in the

n-terminus of the Hexapeptide changed its activity or which aminoacid residues were important for the antagonist activity of the Hexapeptide.

We evaluated the cell migration in native U87 cells exposed to these novel peptides at 24h (20 nM or 200 nM). Consistently with previous results, we have observed the increase of cell migration after exposure to the Hexapeptide at 20 nM and 200 nM. The administration of the Hexapeptide added of a beta-alanine, further increased cell migration especially at 20 nM. The addition of the FITC group, three alanine or another tripeptide to the N-terminus of the Hexapeptide likely altered the capability of the peptides to bind EphB1 as their administration to U87 cells did not affect the migration, except for AAAEWLSPN that increased cell migration at 200 nM (Fig.5A-D).

EphB1 overexpression determined a remarkable decrease in cell migration at 24h. The administration of 20-200 nM Hexapeptide to the transfected cells increased cell migration. The administration of the Hexapeptide added of a beta-alanine, further increased cell migration especially at 20 nM. The addition of a FITC group to AEWLSPN impaired cell migration increase induced by the addition of a beta-alanine at 20-200 nM. The addition of triple beta-alanine at 20 nM likely altered the capability of the peptides to bind EphB1 as their administration to U87 cells did not affect the migration. The addition of triple beta-alanine at 200 nM increased cell migration as compared to the cells overexpressing EphB1 receptor. The addition of a FITC group to AAAEWLSPN impaired the cell migration increase induced by the addition of triple beta-alanine at 20-200 nM. The Hexapeptide with the EGP sequence added to its N-terminus increased cell migration in U87 cells overexpressing EphB1 as compared to the cells overexpressing EphB1 receptor at 20-200 nM; this effect was not observed in native U87 cells expressing EphB1 receptor at low levels; thus, suggesting that the EGP sequence added to the Hexapeptide N-terminus may affect peptide affinity to EphB1 receptor (Fig.5E-H).

A**B****C****D**

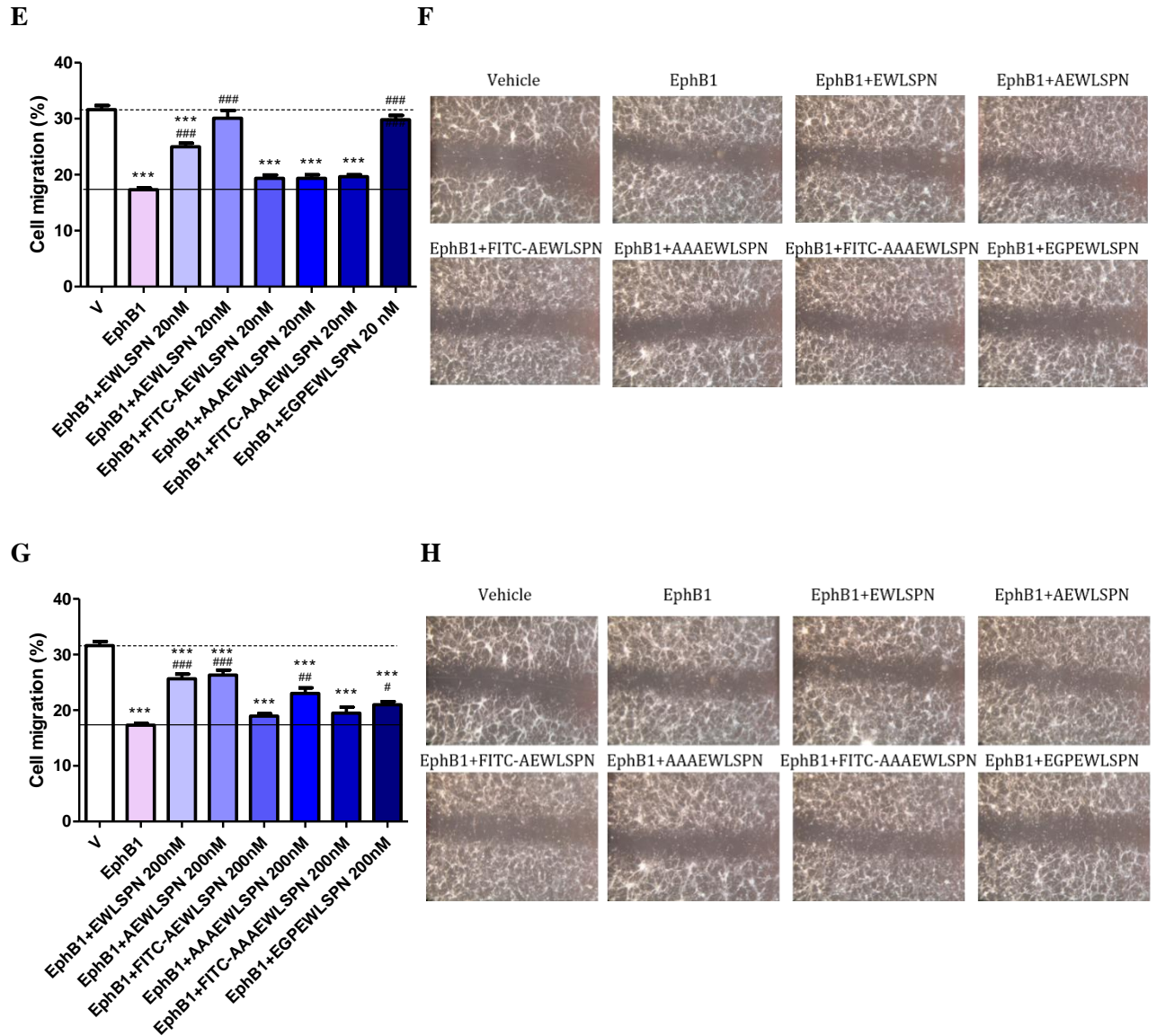


Fig. 5. The role of novel EWLSPN-derived peptides on cell migration in native and transfected U87 cells. The effect of the transfection and/or treatment with 20-200 nM EWLSPN-derived peptides on U87 cell migration evaluated by wound closure in a scratch assay; images were acquired after 24h. (A) Quantification of cell migration at 24h after maintenance of cells in serum-free medium (vehicle) or administration of 20 nM EWLSPN-derived peptides and (B) representative images of U87 cell migration at 24h after administration of 20 nM EWLSPN-derived peptides. (C) Quantification of cell migration at 24h after maintenance of cells in serum-free medium (vehicle) or administration of 200 nM EWLSPN-derived peptides and (D) representative images of U87 cell migration at 24h after administration of 200 nM EWLSPN-derived peptides. Data are presented as the mean \pm SEM of $n=12$. *** = $p<0,001$ vs vehicle; ** = $p<0,01$ vs vehicle, * = $p<0,05$ vs vehicle (Newman-Keuls test after ANOVA). (E) Quantification of cell migration after transfection with pCMV6-EphB1 plasmid and administration of 20 nM EWLSPN-derived peptides and (F) representative images of U87 cell migration after transfection with pCMV6-EphB1 plasmid and administration of 20 nM EWLSPN-derived peptides at 24h. (G) Quantification of cell migration after transfection with pCMV6-EphB1 plasmid and administration of 200 nM EWLSPN-derived peptides and (H) representative images of

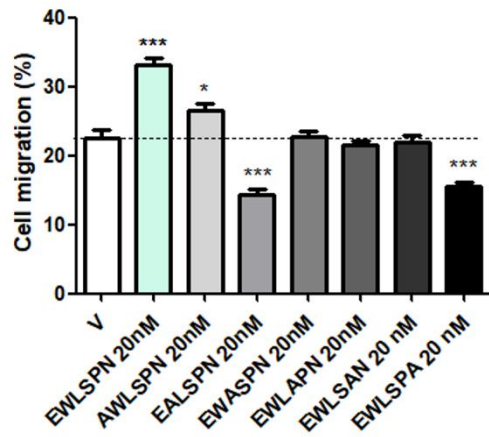
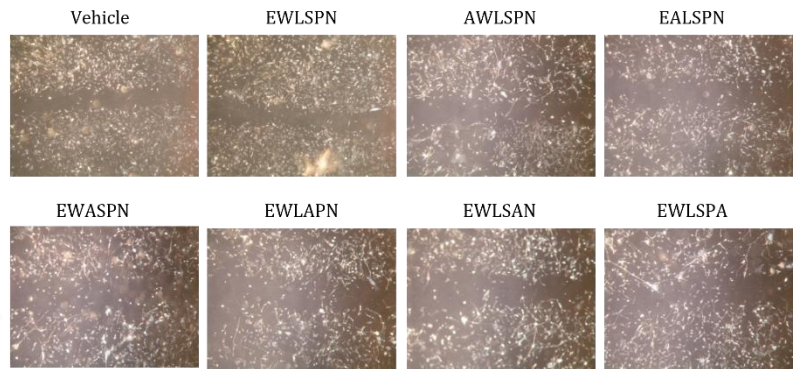
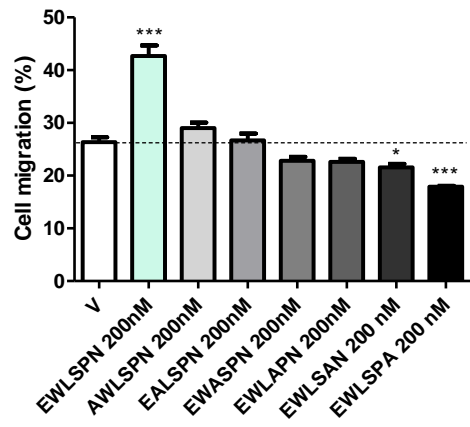
U87 cell migration after transfection with pCMV6-EphB1 plasmid and administration of 200 nM EWLSPN-derived peptides at 24h. Data are presented as the mean \pm SEM of n=6. *** = p<0,001 vs vehicle; ### = p<0,001 vs pCMV6-EphB1, ## = p<0,01 vs pCMV6-EphB1, # = p<0,05 vs pCMV6-EphB1 (Newman-Keuls test after ANOVA).

1.6 The substitution to beta-alanine in the last position of the Hexapeptide decreases cell migration in native and transfected U87 cells

An alanine scanning library was designed so that single substitution to alanine was obtained per each of the six position in the Hexapeptide sequence; this, aiming at characterizing which residues are crucial to EWLSPN antagonist activity and which modification may lead to identify a novel EphB1 receptor agonist.

We administered the alanine scanning library at 20 nM in native U87 cells and EWASPN, EWLAPN and EWLSAN did not alter cell migration at 24h. The administration of AWLSPN increased cell migration, displaying a lower antagonist effect compared to Hexapeptide. The administration of EALSPN and EWLSPA decreased cell migration, displaying a potential agonist activity (Fig. 6A and 6B). We administered the alanine scanning library at 200 nM in native U87 cells and AWLSPN, EALSPN, EWASPN and EWLAPN did not alter cell migration at 24h. The administration of EWLSAN and EWLSPA decreased cell migration, displaying a potential agonist activity (Fig. 6C and 6D).

Alanine scanning library was tested also in U87 cells overexpressing EphB1 receptor. As we have observed before, EphB1 overexpression reduced cell migration. The Hexapeptide increased cell migration, as compared to the cells overexpressing EphB1 receptor. The administration of AWLSPN at 20 nM did not change cell migration at 24h, as compared to the cells overexpressing EphB1 receptor. The other peptides at 20 nM reduced cell migration at 24h, showing a potential agonist activity (Fig. 6E and 6F). At 200 nM only EWLSPA decreased cell migration in transfected U87 cells as compared to the cells overexpressing EphB1 receptor, displaying an agonist effect (Fig. 6G and 6H).

A**B****C****D**

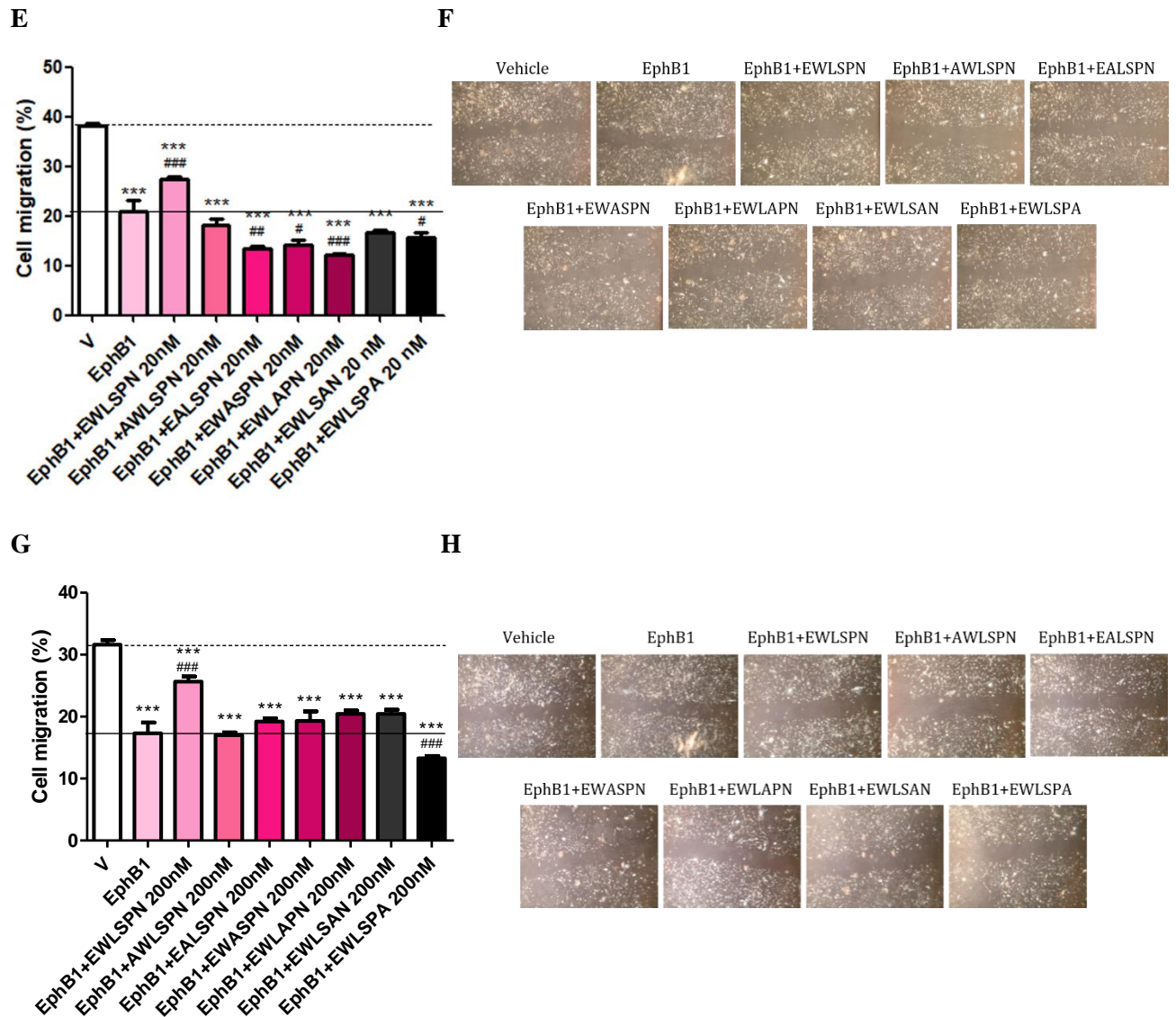


Fig. 6. The role of alanine scanning library on cell migration in native and transfected U87 cells. The effect of the transfection and/or treatment with 20-200 nM alanine scanning library on U87 cell migration evaluated by wound closure in a scratch assay; images were acquired after 24h. (A) Quantification of cell migration at 24h after maintenance of cells in serum-free medium (vehicle) or administration of 20 nM alanine scanning library and (B) representative images of U87 cell migration at 24h after administration of 20 nM alanine scanning library. (C) Quantification of cell migration at 24h after maintenance of cells in serum-free medium (vehicle) or administration of 200 nM alanine scanning library and (D) representative images of U87 cell migration at 24h after administration of 200 nM alanine scanning library. Data are presented as the mean \pm SEM of $n=6$. *** = $p < 0,001$ vs vehicle; * = $p < 0,05$ vs vehicle (Newman-Keuls test after ANOVA). (E) Quantification of cell migration after transfection with pCMV6-EphB1 plasmid and administration of 20 nM alanine scanning library and (F) representative images of U87 cell migration after transfection with pCMV6-EphB1 plasmid and administration of 20 nM alanine scanning library at 24h. (G) Quantification of cell migration after transfection with pCMV6-EphB1 plasmid and administration of 200 nM alanine scanning library and (H) representative images of U87 cell migration after transfection with pCMV6-EphB1 plasmid and administration of 200 nM alanine scanning library at 24h. Data are presented as the mean \pm SEM of $n=6$.

*** = $p < 0,001$ vs vehicle; ### = $p < 0,001$ vs pCMV6-EphB1; ## = $p < 0,01$ vs pCMV6-EphB1; # = $p < 0,05$ vs pCMV6-EphB1 (Newman-Keuls test after ANOVA).

1.7 Discrepancy of EphB1 and Ephrin-B1 mRNA and protein levels between U87 and SH-SY5Y cells

To investigate EphB1 mRNA and Ephrin-B1 mRNA levels in U87 and SH-SY5Y cells we used Real-time PCR, amplifying a cDNA sequence of EphB1 and Ephrin-B1 mRNA, as previously described. The protein content of EphB1 was then analyzed by western blot. Similar levels of EphB1 mRNA were observed in U87 and SH-SY5Y cells. As regards Ephrin-B1 mRNA, we found significantly higher levels of this mRNA in the SH-SY5Y cell line than in U87 cells (Fig. 7A).

On the other hand, U87 cells displayed much lower EphB1 protein levels compared to SH-SY5Y cells, that express high EphB1 protein levels (Fig.7B and 7C).

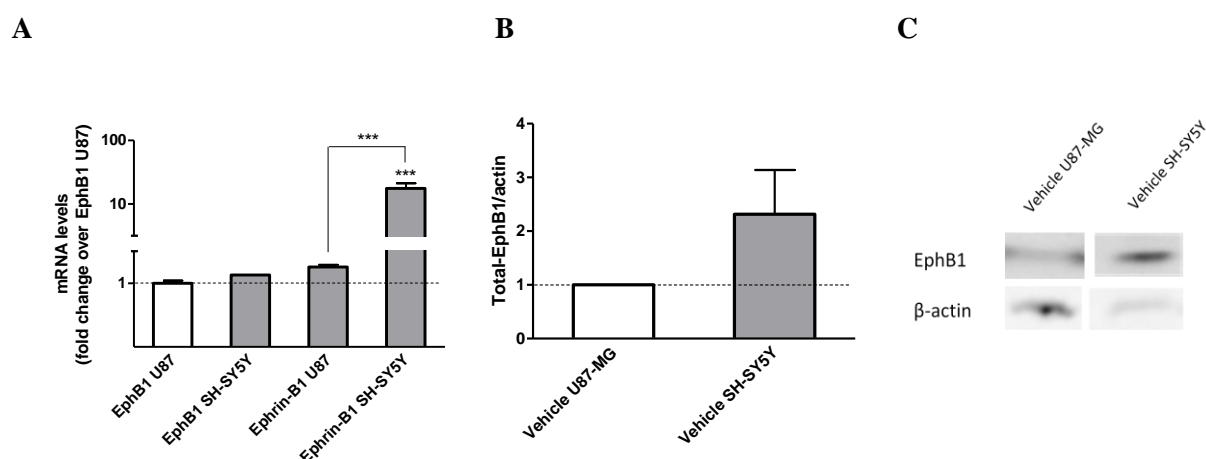


Fig. 7. (A) Real-time PCR of EphB1 and Ephrin-B1 mRNA levels in U87 human glioblastoma cells and SH-SY5Y human neuroblastoma cells. Data are presented as the mean \pm SEM of $n=6$. *** = $p < 0,001$ vs EphB1 U87 and Ephrin-B1 U87 (Newman-Keuls test after ANOVA). (B) Quantification of Total EPHB1 receptor levels in U87 and SH-SY5Y cells exposed to vehicle (C) and representative blots of U87 and SH-SY5Y cells exposed to vehicle. Data are presented as the mean \pm SEM of $n=4$.

1.8 The exposure to a proteasome inhibitor does not influence EphB1 turnover in U87 cells

We wondered if EphB1 low protein levels were due to a fast protein turnover in U87 cell line. We exposed U87 cells to a proteasome inhibitor, MG132 at 5 μ M, that is the usual concentration employed in this context. EphB1 protein levels, detected by western blot, did

not change after the exposure to MG132 at 24h as compared to the vehicle, in which we administered the same solution used for the proteasome inhibitor, without it (Fig. 8).

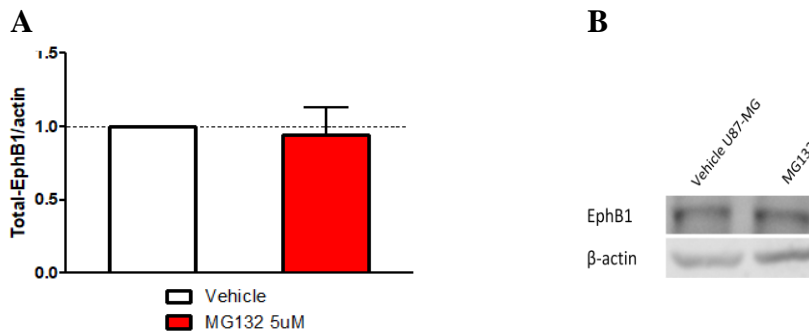


Fig. 8. (A) Quantification of EPHB1 protein levels in U87 cells exposed to 5 μ M MG132 or vehicle at 24h (B) and representative blots of U87 cells exposed to 5 μ M MG132 or vehicle at 24h. Data are presented as the mean \pm SEM of n=5.

1.9 EphB1 expression could be regulated by post-transcriptional events involving miRNAs

Considering that we showed that EphB1 receptor downregulation in glioblastoma cells, event that is tightly related to the severe aggressiveness and malignancy of such tumor, is related to post-transcriptional mechanisms modulating its expression, we started digging into potential miRNAs involved in such dysregulation.

Through prediction softwares and comparing the data with results present in literature, we selected the most predicted miRNAs: miR128-3p, miR129-5p, miR182-5p, miR4428. These miRNAs have the best score for affinity and efficacy on EphB1 3' UTR.

We found the binding sites of this miRNAs (Fig. 9). At the beginning we will analyze miR182-5p and miR129-5p, because miR182-5p is an oncomir in glioblastoma and is significantly expressed in U87 cells⁸, miR129-5p is an oncosuppressor in glioma and downregulates EphB1 in other cancers⁹.

Studies about EphB1 3' UTR and miRNAs are ongoing.

3301 agtcagtcaccaacggcaatggcattgagaactcttgtttcttggggaaggagaggagggga
miR128-3p
 3361 aaaggaccaggggtcaagggggaccagaggttgaccactgtggaatgtactggagagactg
 3421 gcttctcagctgaggaatgcatttccatcagtgagaagaatcaaccggacctgttgctagca
 3481 ggcaatctccatttctcagtgacagaagcatgtttgagatgccgtgggaaaccaaata
 3541 taataataaaaatataaaaaggtgatgttcaacagaagtgaagacaaaacaatatgcatc
 3601 aggagaacaagagtaaacccagctcccatttctcagtgggctgcagttgccaaccacagg
 3661 aagaaaggaaggaggtagaggaagaacagaagcagtgttccatttcttctcctcacca
miR4428
 3721 atgacattcttttcttttctccttctcctcctgagagtgccctccttctccca
 3781 cactcgtttccctttgctcatgactcctgtagggaagtcttcaaacaaaaccagctc
miR182-5p
 3841 ctgagtctccagatgttggtctgtcagttgccaaggactttgctgaccactgcatgggg
 3901 atccaaccaattcaattaatgtcttcatattgaagaagagatgtacctcaattgaaaac
miR129-5p
 3961 ctcgtttttcttttgtttgcatttctgcaaaaaggaaaaagaaaccacaaattggggaa
 4021 aaaaaaagaagaaaaacctgtttccgtgtgcaaaagcacacatatgtatgtctgtgttat
miR128-3p
 4081 aaaatgactgtgcttgttcgtaacagatgcaacaagaaagaagaactgggaagtctttg
 4141 tccctaggaaatccaaagggctggaatatggtgttggtttggctttctggttggcccaa
 4201 tcggcctattggctcaatgggaagagaggagaggagaaaaataaaatgaaaggaaaaaa
 4261 aaaagtttgcaaattcagacaggaaacaggtgagtggtttgaattggatgcagtggtggc
 4321 catcctggaatgatactgactgattaattattcctgataacatctcaagaaaaggagaag
 4381 gaaagtgtttctggagaatgttctttcacatcactggaatctgcaattcaagaagtgaca
 4441 agggagaattcttgctttacctatggactggcttaagccgtgtggcatccgaggaatgtt
 4501 tcaaatgtgtctgtgtttctctttacattccttgttgacctcattgttcaattcacttt
miR4428 miR4428
 4561 tgtaaattccacctaacatttaattattttaaatctctcctttaccttaattctccttgc
 4621 taattttatctgtctaattaaaaagagcagaagcatgtctgggtttacgtaaaa

Fig. 9. TargetScan, miRanda, DIANA Tools were the prediction softwares that we used to select the most predicted miRNAs and their relative binding sites.

2. Second part

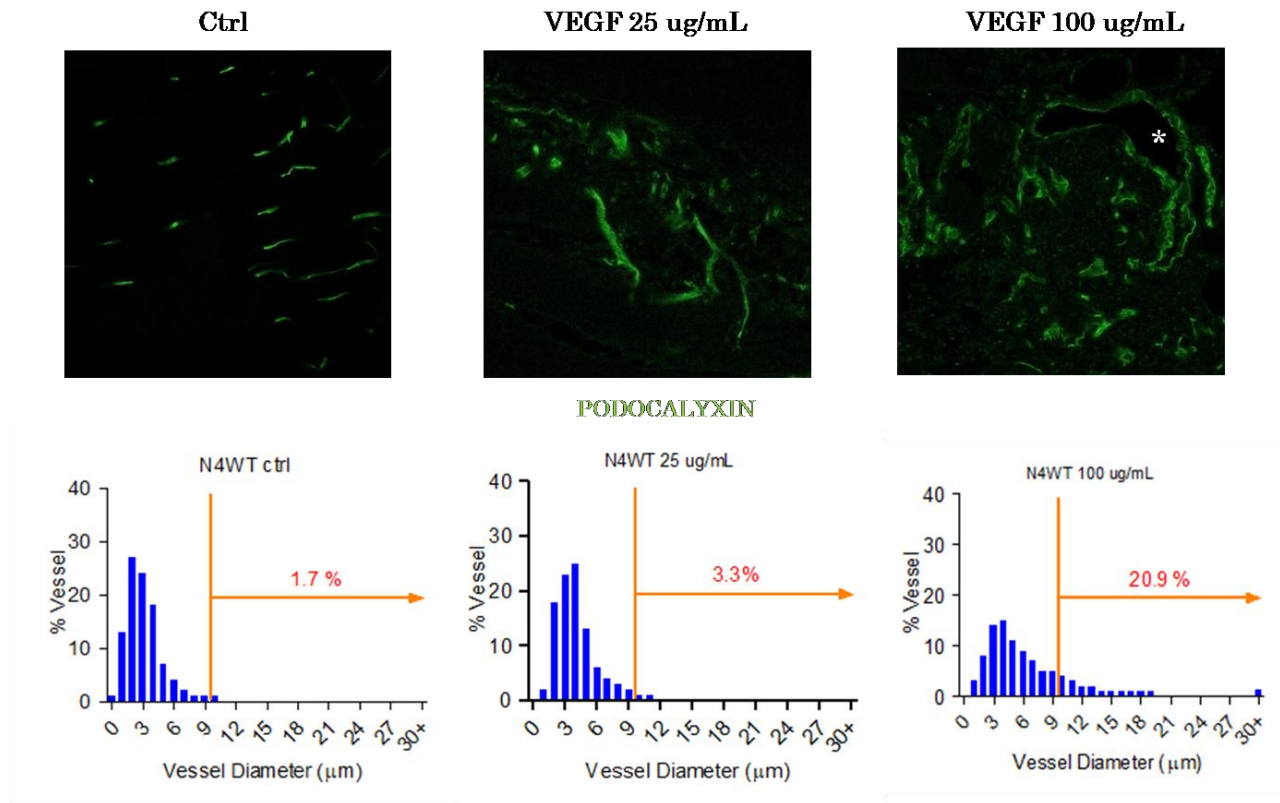
2.1 High doses of VEGF induce aberrant angiogenesis in WT mice

A clinically-relevant fibrin-based platform has been developed by the host group for sustained and customizable release of angiogenic factors as recombinant proteins, as described above in the introduction section (Chapter 6.3). Taking advantage of this platform, we established a fibrin-based delivery tool for VEGF dose-dependent angiogenesis. Results showed that delivery of recombinant engineered VEGF proteins in skeletal muscle of immune-deficient SCID mice induced normal or aberrant angiogenesis depending on its microenvironmental levels²¹⁰. Therefore, we first sought to verify whether different VEGF doses can induce normal and aberrant vascular growth in immune-competent wild type mice (WT). Fibrin gels were prepared with 2 different VEGF concentrations, previously shown to induced normal and aberrant angiogenesis in skeletal muscle ($V_{25} = 25 \mu\text{g/mL}$ and $V_{100} = 100\mu\text{g/mL}$, respectively)²¹⁰ and injected into hindlimb muscles of WT mice. Empty fibrin gels (ctrl) were used as negative control.

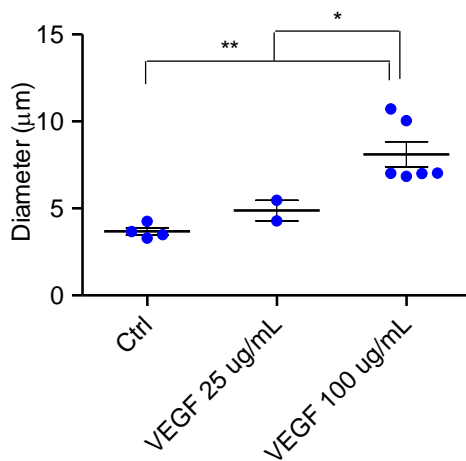
The V_{25} dose induced the growth of morphologically normal capillaries, which were similar to those found with control empty gels, whereas V_{100} induced aberrant vascular structures, as expected (Fig. 1A). Quantification of vessel diameters, analyzed either as size distributions (Fig. 1A) or average \pm SEM (Fig. 1B), showed that ctrl gels and V_{25} induced normal capillaries with homogeneous sizes that were uniformly distributed around a median diameter of $3.31\pm 0.20 \mu\text{m}$ and $4.40\pm 0.62 \mu\text{m}$ and with a 90th percentile value of 5.96 ± 0.51 and $7.17\pm 1.14 \mu\text{m}$, respectively.

In contrast, the aberrant structures induced by V_{100} were markedly enlarged (average diameters: ctrl = $3.68\pm 0.21 \mu\text{m}$, $V_{100} = 5.11\pm 0.72 \mu\text{m}$ $p < 0.01$) with 20.9% of vessels larger than $10 \mu\text{m}$ (Fig. 1A-B). The induced angiogenesis was quantified by measuring the vessel length density (VLD), calculated as the total length of vessels in the acquired field divided by the area of the field, independently of their diameter. Both V_{100} and V_{25} induced robust angiogenesis compared to control gels and the vascular density was actually higher with V_{100} (Fig. 1C).

A



B



C

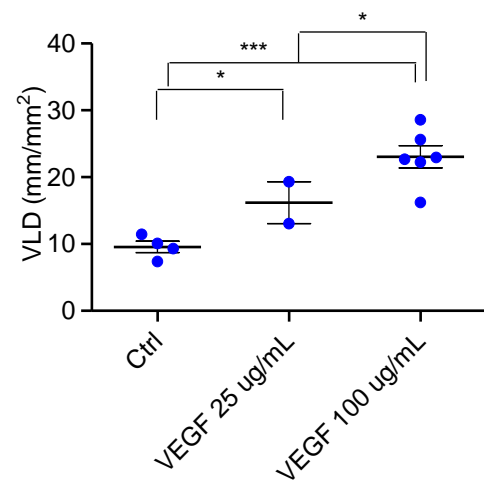


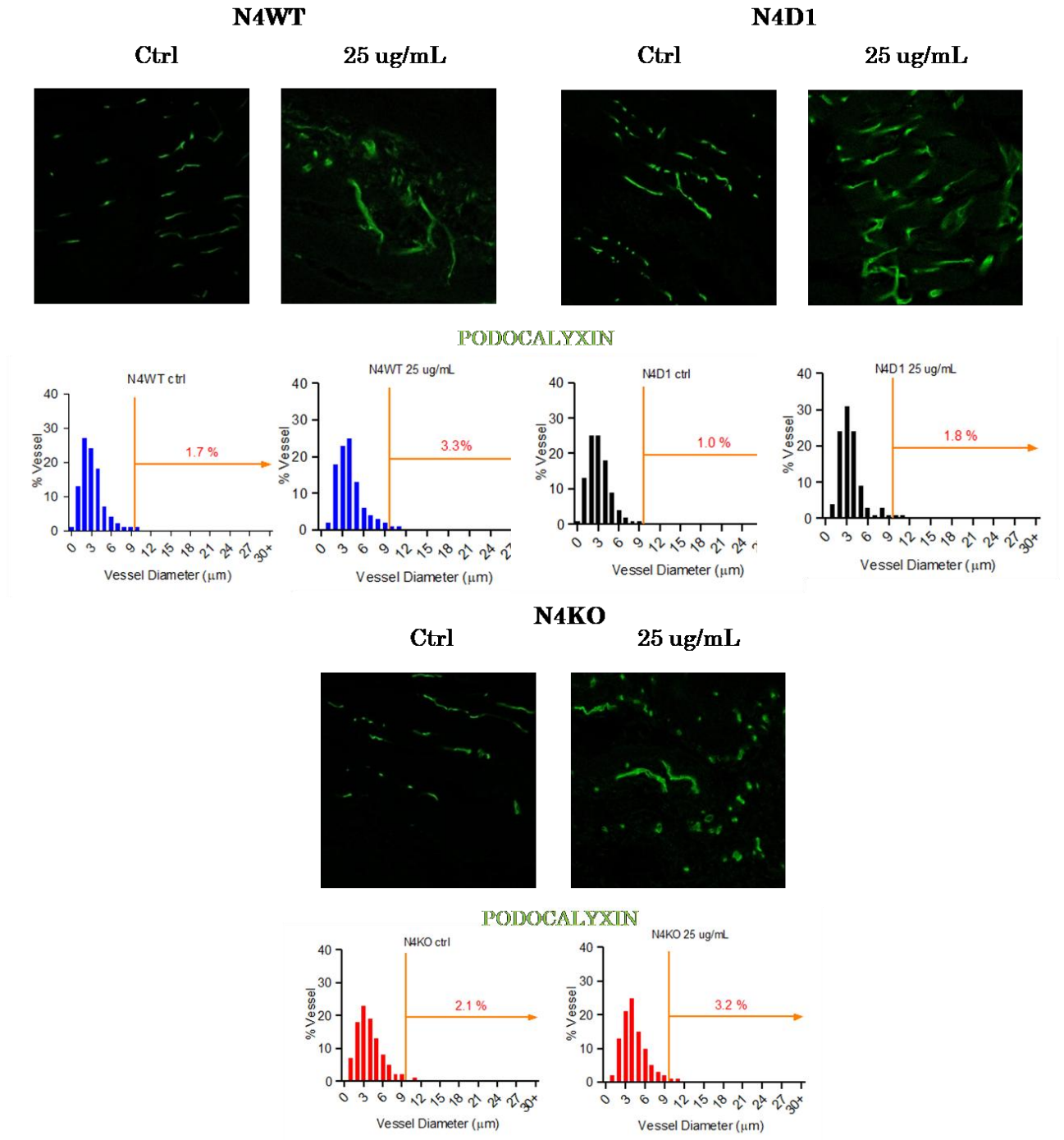
Fig. 1. High doses of VEGF induce aberrant angiogenesis in WT mice. Mouse WT hindlimb muscles were injected with fibrin hydrogen I containing V₁₀₀, V₂₅ or Ctrl and harvested at 7 days post implantation. A) Cryosections were immunostained for endothelium (podocalyxin, green). Quantification of vessel diameter distribution; *lumen of aberrant structures. B) Quantification of vessel diameters. Values represent means of individual measurements in each sample ± SEM. n=2-6 independent samples/group; * = p<0.05 and ** = p<0.01 (Newman-Keuls test after ANOVA). C) Quantification of the vessel length density (VLD): i.e., the total vessel length in the area of each measured field; *** = p<0.001 and * = p<0.05 (Newman-Keuls test after ANOVA).

2.2 Loss of Notch4 signaling pathway does not affect normal angiogenesis by moderate VEGF doses

To determine whether Notch4 was required for VEGF-induced normal angiogenesis by V_{25} we adopted a loss of function approach by taking advantage of two different transgenic murine models: (a) a Notch4 full knock-out mouse (N4KO), in which the whole sequence of the Notch4 gene is replaced with LacZ and Neo expression cassettes²²⁰; and (b) a Notch4-deficient murine model (N4D1), expressing a truncated Notch4 gene lacking the intracellular domain of Notch4 receptor (NICD4) and in which, therefore, Notch4 activation is prevented, but the extracellular domain of the protein is still present¹⁰³. C57/B6 wild-type mice (WT) were used as control.

All 3 strains were injected with V_{25} or Ctrl fibrin hydrogels and tissues were harvested at day 7. In all mice, V_{25} induced networks of only morphologically normal capillaries, similar in size to vessels found in control samples (WT average diameters: ctrl = 3.68 ± 0.21 μm , V_{25} = 4.48 ± 0.59 ; p=n.s.; median diameter: ctrl = 3.31 ± 0.20 μm , V_{25} = 4.40 ± 0.62 μm ; and 90th percentile: ctrl = 5.96 ± 0.51 μm , V_{25} = 7.17 ± 1.14 μm ; N4D1 average diameters: ctrl = 3.83 ± 0.30 μm , V_{25} = 4.03 ± 0.15 ; p=n.s.; median diameter: ctrl = 3.50 ± 0.33 μm , V_{25} = 3.68 ± 0.25 μm ; and 90th percentile: ctrl = 5.77 ± 0.28 μm , V_{25} = 5.66 ± 0.11 μm ; N4KO average diameters: ctrl = 4.30 ± 0.28 μm , V_{25} = 4.97 ± 0.16 ; p=n.s.; median diameter: ctrl = 3.83 ± 0.36 μm , V_{25} = 4.53 ± 0.08 μm ; and 90th percentile: ctrl = 6.81 ± 0.27 μm , V_{25} = 7.62 ± 0.38 μm ; Fig. 2A-B). Also, V_{25} alone caused in all murine strains similar vascular growth, which was significantly increased in VLD compared to fibrin-only controls (N4WT: ctrl = 9.56 ± 0.85 μm , V_{25} = 16.18 ± 3.12 ; p<0.05; N4D1: ctrl = 8.81 ± 0.76 μm , V_{25} = 20.78 ± 6.43 ; p<0.01; N4KO: ctrl = 6.95 ± 1.35 μm , V_{25} = 17.89 ± 1.51 ; p<0.05; Fig.2C).

A



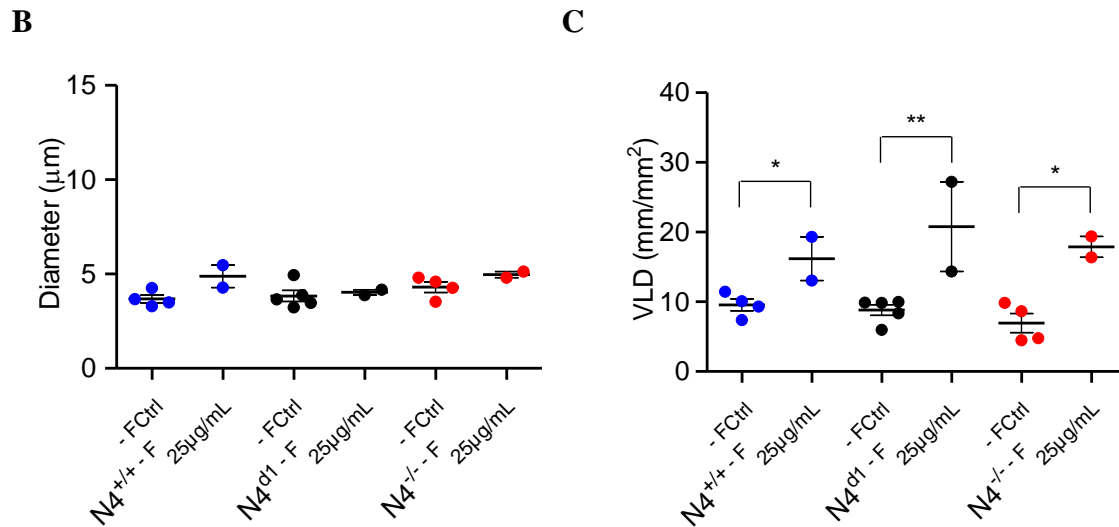


Fig. 2. Loss of Notch4 signaling does not prevent normal angiogenesis by V₂₅. WT/N4D1/N4KO hindlimb muscles were injected with fibrin hydrogel decorated with V₂₅ or ctrl fibrin gels. Mice were sacrificed by 7 days. A) Immunostaining of frozen sections stained for endothelium (podocalyxin, green) and quantification of vessel diameter distribution. B) Quantification of vessel diameters. Values represent means of individual measurements in each sample ± SEM. n=2-5 independent samples/group. C) Quantification of the vessel length density (VLD): i.e., the total vessel length in the area of each measured field; ** = p<0,01 and * = p<0,05 (Newman-Keuls test after ANOVA).

2.3 Notch4 signaling is not required for normal intussusceptive angiogenesis by moderate doses of VEGF

We have recently found that VEGF over-expression in skeletal muscle at therapeutic doses induces physiological angiogenesis by the cellular mechanism of intussusception rather than sprouting⁶⁵. Here we asked whether Notch4 signaling was necessary for the process of intussusceptive angiogenesis induced by moderate VEGF doses (V₂₅). To address this point, we injected hindlimb muscle of WT, N4KO and N4D1 mice with V₂₅ fibrin hydrogel and ctrl fibrin gels. Animals were sacrificed at 3- and 4-day time points, i.e. at the stage when VEGF causes pre-existing vessels to enlarge and intussusceptive pillar formation is starting.

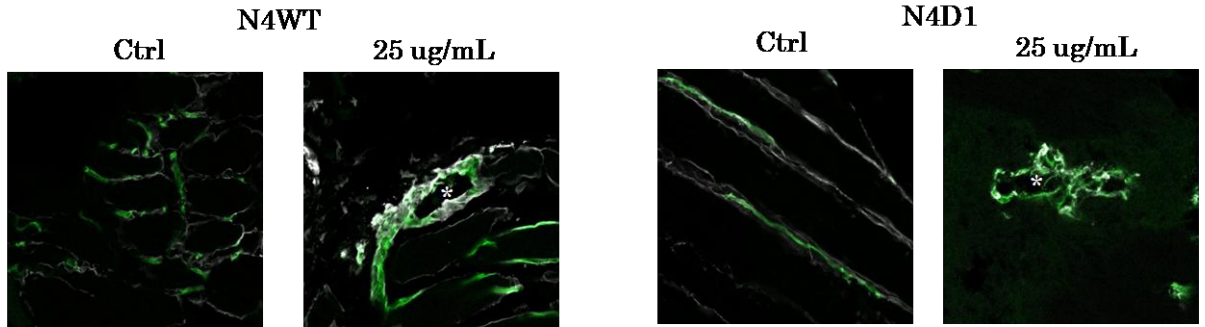
Quantification of vessel diameter distributions and mean values showed that V₂₅ caused vascular enlargements in all murine strains. In fact, vessels in areas implanted with control gels were uniformly distributed whereas V₂₅ gels induced heterogeneous vascular enlargements, both at 3 days (WT = average diameters: ctrl = 3.85±0.31 µm, V₂₅ =

8.00±1.57; p<0.01; median diameter: ctrl = 3.54±0.25 µm, V₂₅ =5.72±0.82 µm; and 90th percentile: ctrl = 5.60±0.57 µm, V₂₅ =15.97±3.74 µm; N4D1 = average diameters: ctrl = 2.84±0.09 µm, V₂₅ = 6.25±0.82; p<0.01; median diameter: ctrl = 2.57±0.09 µm, V₂₅ =6.25±0.82 µm; and 90th percentile: ctrl = 4.30±0.11 µm, V₂₅ =19.66±2.73 µm; N4KO = average diameters: ctrl = 3.15±0.41 µm, V₂₅ =15.39 µm; median diameter: ctrl = 2.86±0.40 µm, V₂₅ =11.54 µm; and 90th percentile: ctrl = 4.80±0.62 µm, V₂₅ =34.09 µm; figure 3A and D) and at 4 days (WT = average diameters: ctrl = 4.01±0.26 µm, V₂₅ = 10.20±1.24; p<0.01; median diameter: ctrl = 3.72±0.28 µm, V₂₅ =6.92±0.86 µm; and 90th percentile: ctrl = 6.03±0.65 µm, V₂₅ =21.59±2.33 µm; N4D1 = average diameters: ctrl = 4.94±0.66 µm, V₂₅ = 9.91±1.62; p<0.01; median diameter: ctrl = 4.02±0.44 µm, V₂₅ =7.84±1.54 µm; and 90th percentile: ctrl = 8.78±1.87 µm, V₂₅ =19.21±2.45 µm; N4KO = average diameters: ctrl = 3.89±0.50 µm, V₂₅ = 9.81±1.50; p<0.01; median diameter:ctrl = 3.54±0.43 µm, V₂₅ =7.57±1.16 µm; and 90th percentile: ctrl = 5.67±0.71 µm, V₂₅ =17.96±3.33 µm; figure 3B and E).

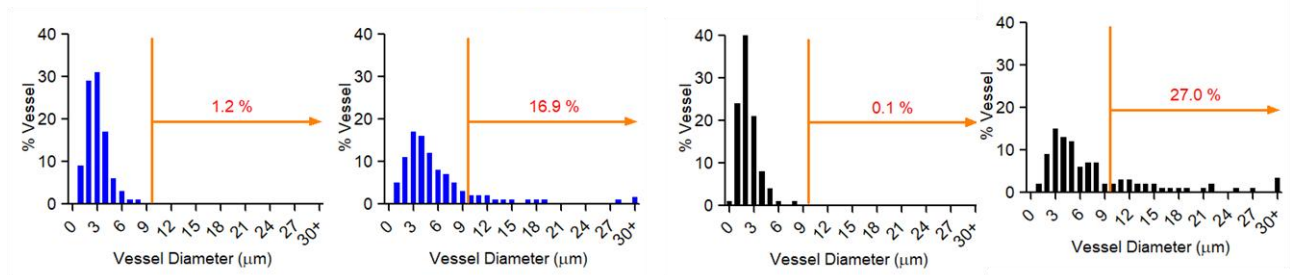
Further, the samples were stained for two different markers i.e. podocalyxin, which marks specifically the luminal side of polarized endothelial cells, and laminin, which marks the basal lamina and therefore defines the external boundary of vessels. As shown in figure 3 A-C, at both time-points, the podocalyxin-positive cells of enlarged vascular structures were completely contained within the respective basal lamina and no endothelial extensions could be seen protruding outside of it, thereby confirming the lack of signs of sprouting. Remarkably, in the enlarged vascular structures it was possible to observe the hallmark of active intussusceptive angiogenesis, i.e. the formation of pillars as intraluminal endothelial-only protrusions (arrows in Figure 3C)

A

3 days



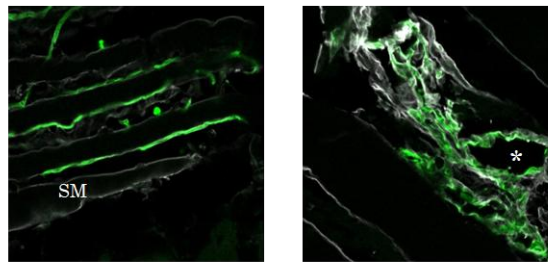
PODOCALYXIN LAMININ



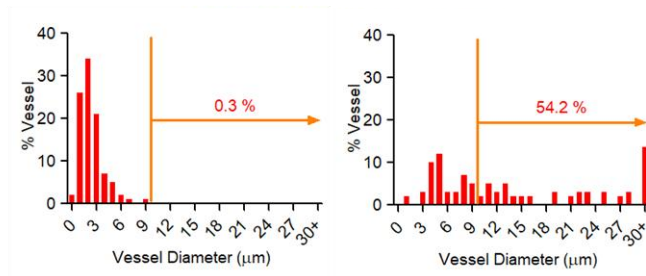
N4KO

Ctrl

25 ug/mL

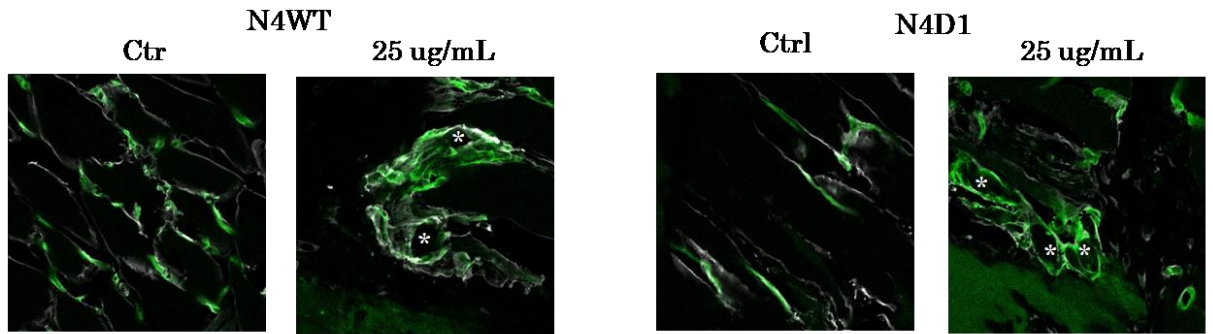


PODOCALYXIN LAMININ

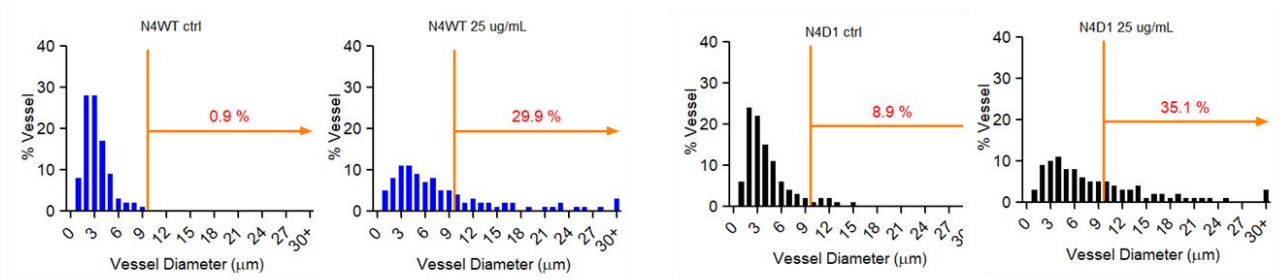


B

4 days

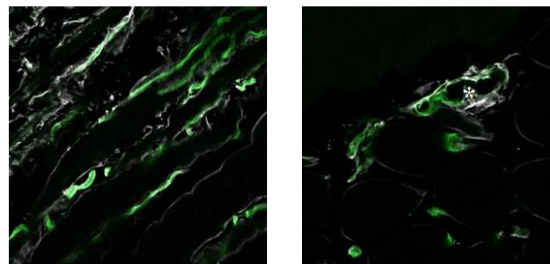


PODOCALYXIN LAMININ

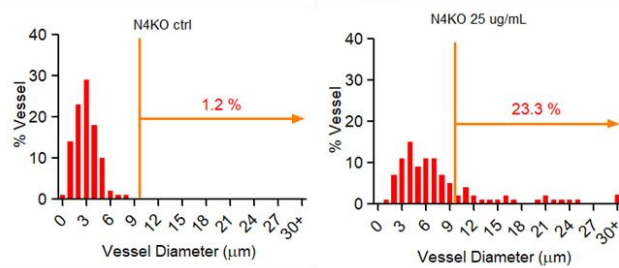


N4KO

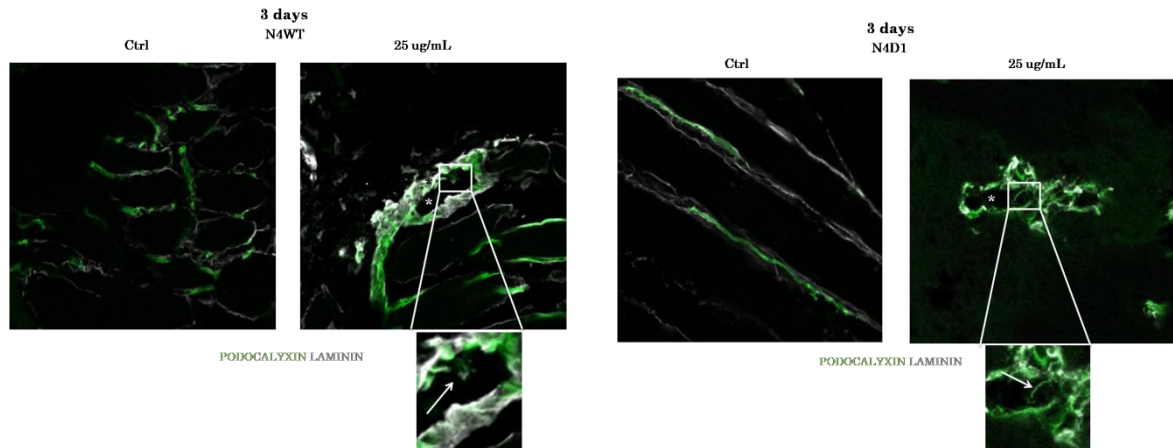
Ctrl 25 ug/mL



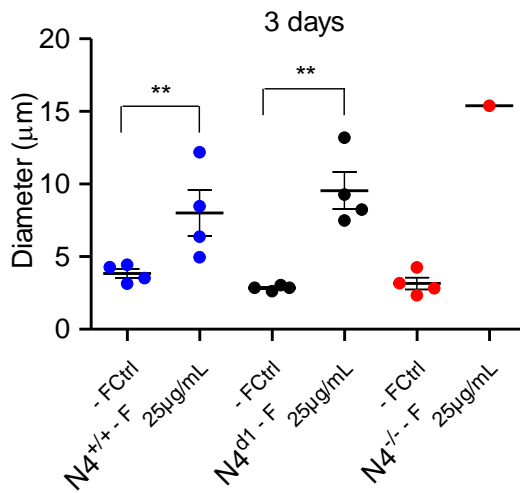
PODOCALYXIN LAMININ



C



D



E

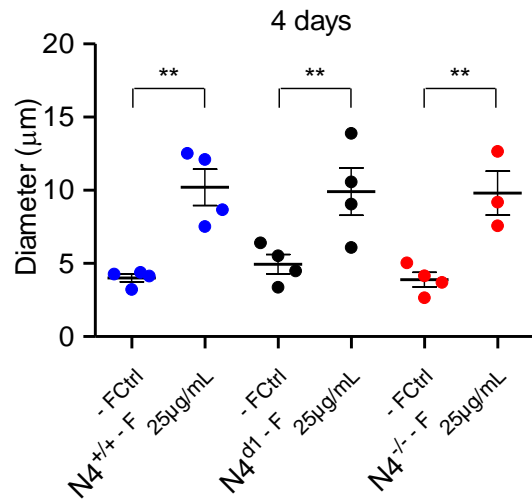


Fig. 3. V₂₅ induced angiogenesis by intussusception. Mouse N4WT/N4D1/N4KO hindlimb muscles were injected with fibrin hydrogel decorated with V₂₅ or empty fibrin gels. Mice were sacrificed by 3 and 4 days. A-B) Immunostaining of frozen sections stained for vessel lumen (podocalyxin, green) and basal lamina (laminin, grey) and quantification of vessel diameter distribution by 3 and 4 days. *lumen of vascular structures; SM: skeletal muscle. C) High magnification of vascular lumen displaying signs of intraluminal endothelial protrusions. D-E) Quantification of vessel diameters at 3 and 4 days post fibrin implantation. Values represent means of individual measurements in each sample \pm SEM. n=1-4 independent samples/group; ** = $p < 0,01$ (Newman-Keuls test after ANOVA).

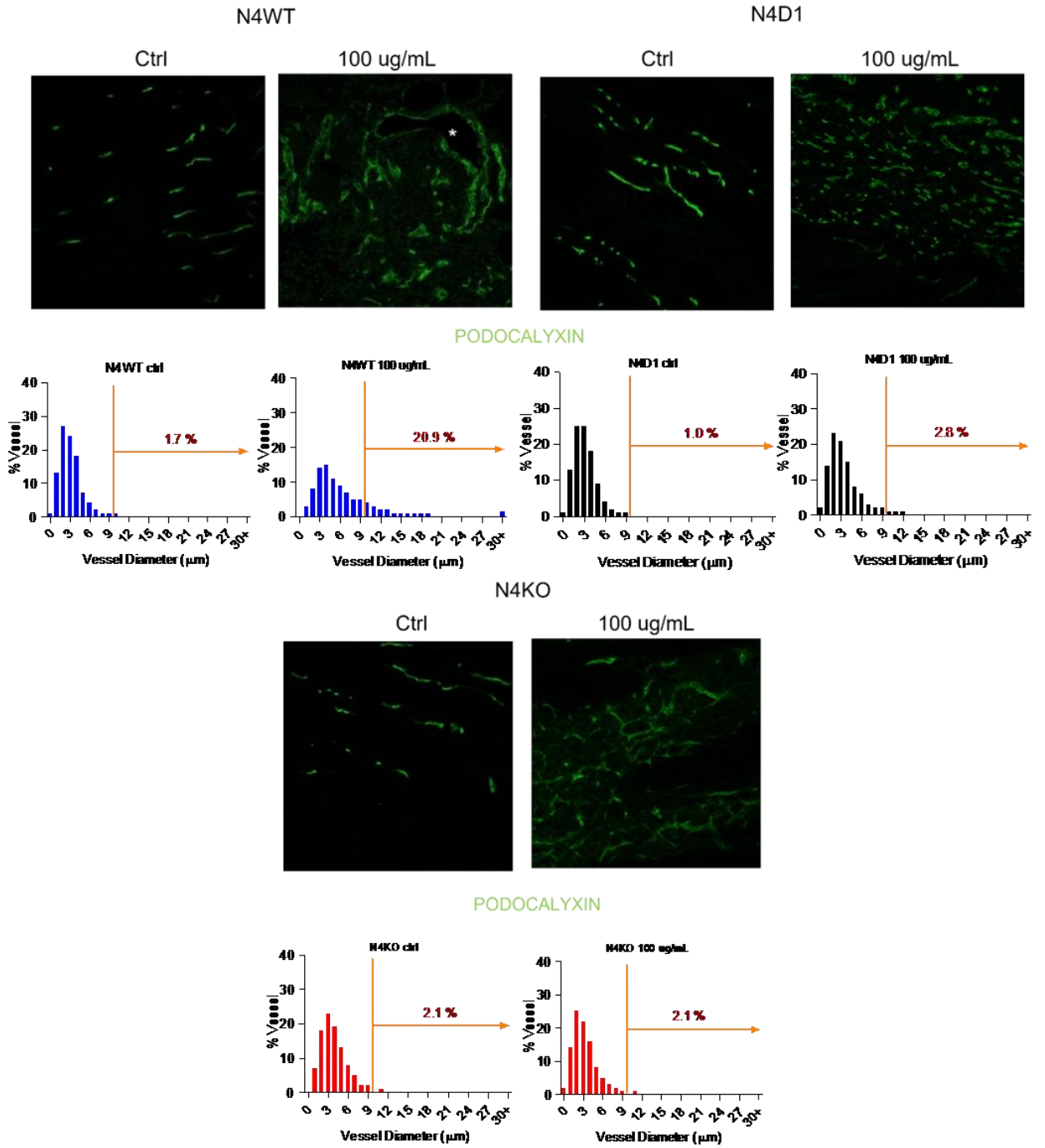
2.4 Loss of Notch4 signaling prevents aberrant angiogenesis by high doses of VEGF

As it has been shown in figure 1, high levels of VEGF caused aberrant vascular structures in wild type mice. Therefore, here we asked whether Notch4 is required for the induction

of aberrant structures by high levels of VEGF. To test this hypothesis, fibrin hydrogels decorated with V_{100} or empty fibrin gels were injected into hindlimb muscles of N4KO and N4D1 mice, and of WT as positive control.

Seven days after implantation, control gels without any factor did not alter the pre-existing vasculature, which consisted of morphologically normal capillaries, and quantification of vessel diameters showed that capillaries were uniformly distributed, with a 90th percentile value of 5.96 ± 0.51 , 5.77 ± 0.28 and $6.81 \pm 0.27 \mu\text{m}$ in WT, N4D1 and N4KO, respectively (Fig. 4A-B). As expected, V_{100} induced aberrant vascular structures which were significantly enlarged compared to control vessels in wild type mice (average diameters: ctrl = $3.68 \pm 0.21 \mu\text{m}$, $V_{100} = 8.11 \pm 0.72$, $p < 0.01$, Figure 4A). In contrast, Notch4 signaling impairment was sufficient to avoid the appearance of aberrant vascular structures. In fact, high levels of VEGF induced the growth of exclusively normal capillaries, which were similar to the capillaries found in control samples, in both N4D1 and N4KO mice (average diameters: N4D1: ctrl = $3.83 \pm 0.30 \mu\text{m}$, $V_{100} = 4.05 \pm 0.37$, $p = \text{n.s.}$; N4KO: ctrl = $4.30 \pm 0.28 \mu\text{m}$, $V_{100} = 3.87 \pm 0.31$, $p = \text{n.s.}$, Fig. 4A-B). Also, the quantification of the amount of induced angiogenesis (measured as VLD) showed that V_{100} caused a significant increase in VLD in the presence of Notch4 inhibition compared to control samples, as aberrant vascular structures were substituted by networks of normal capillaries (VLD: WT: ctrl = $9.56 \pm 0.85 \text{ mm/mm}^2$, $V_{100} = 23.05 \pm 0.85 \text{ mm/mm}^2$, $p < 0.001$; N4D1: ctrl = $8.81 \pm 0.76 \text{ mm/mm}^2$, $V_{100} = 32.29 \pm 1.49$, $p < 0.001$; N4KO: ctrl = $6.95 \pm 1.35 \mu\text{m}$, $V_{100} = 26.63 \pm 1.95$, $p < 0.001$; figure 4C).

A



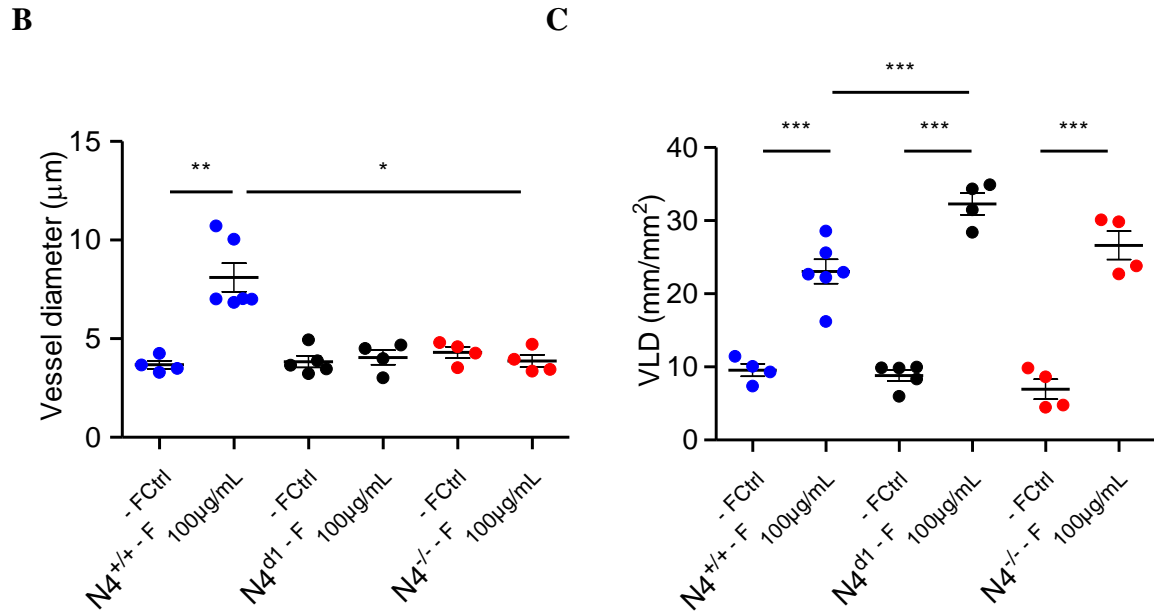


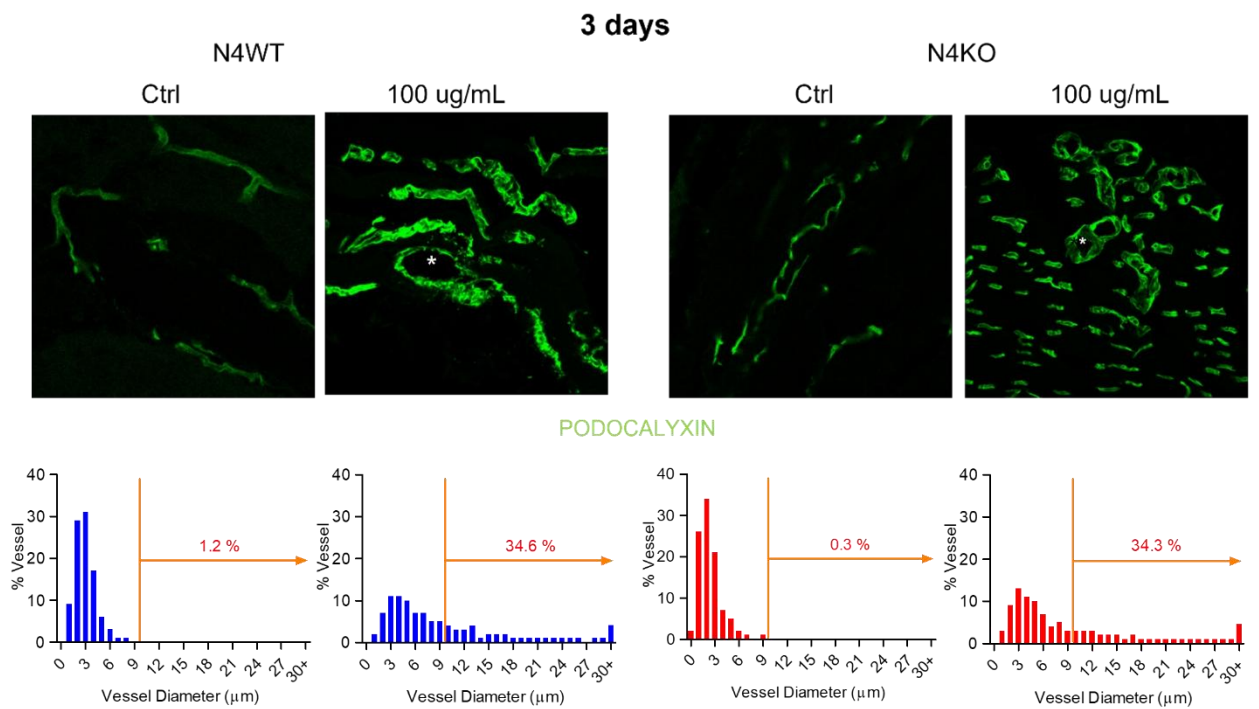
Fig. 4. Aberrant angiogenesis by high doses of VEGF is prevented by the loss of Notch4. Mouse N4WT/N4KO/N4D1 hindlimb muscles were injected with fibrin hydrogel decorated with V₁₀₀ or control hydrogels. Mice were sacrificed at 7 days. A) Immunostaining of frozen sections stained for endothelium (podocalyxin, green) and quantification of vessel diameter distribution. *lumen of aberrant structures. B) Quantification of vessel diameters after 7 days. Values represent means of individual measurements in each sample \pm SEM. n=4-6 independent samples/group; * = p<0,05 and ** = p<0,01 (Dunn's multiple comparisons test after Kruskal-Wallis test). C) Quantification of the vessel length density (VLD): i.e., the total vessel length in the area of each measured field; *** = p<0,001 (Sidak's multiple comparisons test after ANOVA).

2.5 Notch4 loss limits the degree of vascular enlargements by high VEGF levels

We previously found that the switch between normal and aberrant angiogenesis correlates with the size of initial vascular enlargements⁶⁵. Therefore, here we determined whether the loss of Notch4 prevents VEGF-induced aberrant angiogenesis by modulating the initial morphogenic events of VEGF-induced vascular enlargement and splitting. To test this hypothesis, fibrin hydrogels decorated with V₁₀₀ or empty fibrin gels were injected into hindlimb muscles of N4WT and N4KO mice and muscles were harvested at 3 and 4 days after gel implantation. Normal capillaries in areas implanted with ctrl gels had a very homogeneous size (3-day time-point: WT ctrl: median = 3.54 \pm 0.25, 90th percentile = 5.60 \pm 0.57; N4KO ctrl: median = 2.86 \pm 0.40, 90th percentile = 4.80 \pm 0.62; 4-day time-point: WT ctrl: median = 3.72 \pm 0.28, 90th percentile = 6.03 \pm 0.65; N4KO ctrl: median = 3.54 \pm 0.43, 90th percentile = 5.57 \pm 0.71); V₁₀₀ caused a similar enlargement of the pre-

existing capillaries at 3 days in both WT and N4KO murine strains (WT V_{100} : median = 9.39 ± 1.81 , 90th percentile = 27.14 ± 3.80 ; N4KO V_{100} : median = 7.10 ± 0.97 , 90th percentile = 17.90 ± 2.43 ; Figure 5A and 5C). However, some of these vessels continued to grow at 4-day time-point in WT mice, as evidenced both by the further increase in average diameter by 3 and 4 days (mean diameter day 3 = 10.71 ± 1.23 μm ; day 4 = 13.22 ± 2.10 μm , figure 5C and 5D), as well as in the amount of vessels with a diameter ≥ 10 μm (40.7% at 4 days from 34.3% at 3 days; figure 5A-B). On the other hand, the enlarged vessels found at 3 days did not undergo any further increase in growth in N4KO murine strain (mean diameter day 3 = 10.57 ± 1.35 μm , day 4 = 8.90 ± 1.00 μm , $p < 0.05$; Figure 5C-D) and quantification of diameter distribution showed a decrease in the amount of vessels with a diameter ≥ 10 μm at 4 days compared to 3 days.

A



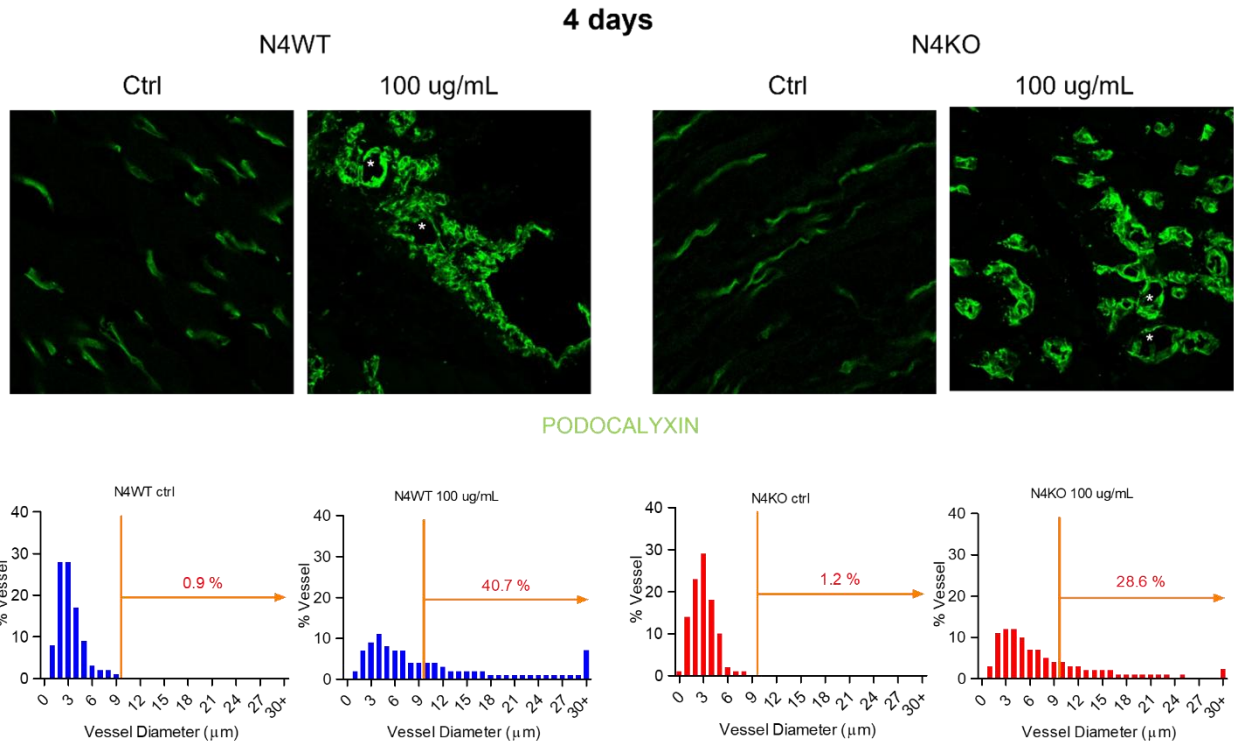
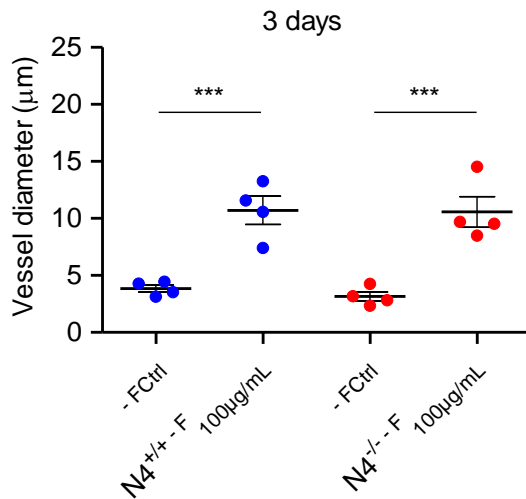
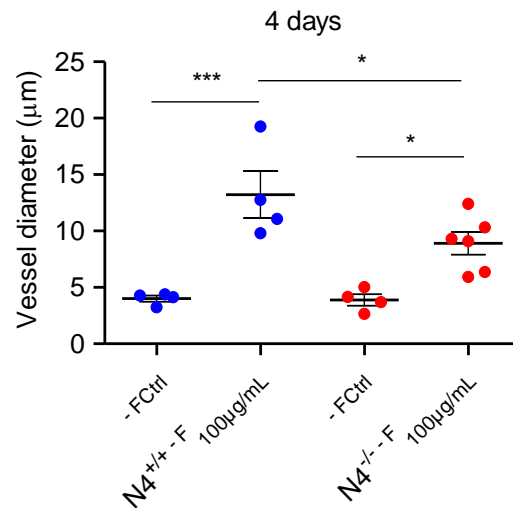
B**C****D**

Fig. 5. Notch 4 loss limits the degree of vascular enlargements caused by high levels of VEGF. Mouse N4WT/N4KO hindlimb muscles were injected with fibrin hydrogel containing V₁₀₀ or control fibrin gels. Mice were sacrificed at 3 and 4 days post injection. A-B) Immunostaining of frozen sections stained for endothelium (podocalyxin, green) and quantification of vessel diameter distribution at 3 and 4 days. C-D) Quantification of vessel diameters at 3 and 4 days. Values represent means of individual measurements in each sample ± SEM. n=4-6 independent samples/group; * = p<0,05 and *** = p<0,001 (Dunn's multiple comparisons test after Kruskal-Wallis test).

Discussion

First part

Increasing evidences support the role of Eph/ephrin signaling in tumorigenesis, metastasis, and angiogenesis. Every member of this molecular system may play perplexing dichotomous roles with tumor suppressing or promoting functions depending on the cellular context and type of cancer. Altered expression of EphB1 receptor was detected in different brain tumors^{155,156}. As regards glioblastoma, that is among the most aggressive brain tumors with an exceedingly poor prognosis²¹¹ and lack of effective treatments, it was shown that EphB1 is downregulated, may act as a tumor suppressor and the loss of its expression may be correlated with aggressive cancer phenotypes¹⁵⁶.

Moving from these considerations, we aimed at characterizing the role played by EphB1 receptor in human glioblastoma by investigating its expression and modulation in U87 human glioblastoma cells.

Results presented here demonstrate that the loss of EphB1 receptor expression and its subsequent reduced activity are relevant pro-tumoral events in glioblastoma cells. Consistently, EphB1 overexpression significantly reduces cell migration and proliferation. Moreover, treating U87 cells with the EphB1 receptor agonist (ephrinB1-Fc) further reduces cancer cell aggressiveness, increasing EphB1 activation, and reducing cell migration in native and transfected U87 cells. To corroborate these data, the treatment with an EphB1 peptide antagonist (Hexapeptide) increases cancer cell aggressiveness, augmenting cell migration in a concentration-dependent manner in native and transfected U87 cells, and decreasing EphB1 activation in transfected U87 cells.

Starting from these considerations, different novel peptides were designed starting from the Hexapeptide, and the migration assay in native versus EphB1 overexpressing U87 cells was developed within this project as a reliable *in vitro* research tool to screen compound libraries seeking for potential EphB1 agonists or antagonists. In particular, the addition of a beta-alanine improves the antagonist effect of the native Hexapeptide, mostly in native and transfected U87 cells at 20 nM. The addition of a FITC group seems to prevent the peptides from binding to EphB1 receptor, spurring us to think about changing FITC position or finding another labeled probe in order to get to an effective EphB1 receptor labeled ligand. FITC is indeed a quite large molecule; therefore it is not surprising that its addition to the N terminus of candidate ephrinic peptides may hamper their ability to interact with their target receptors (as it has been shown, at least for binding to EphB1, that the N-terminal EWL sequence plays a relevant role).

As regards alanine scanning library, we have found discordant results but it seems that the positions 1st-2nd-3rd-4th-5th of the Hexapeptide are important for the antagonist effect of the hexapeptide. Interestingly, the substitution to beta-alanine in the last position of the Hexapeptide seems to change its activity from antagonist to agonist. This result is confirmed in both native and transfected U87 cells at both concentration (20-200 nM). This candidate agonist is currently under characterization for its ability to trigger EphB1 receptor and downstream signaling; if agonist activity will be confirmed, this peptide will be exploited as hit compound aiming at developing innovative EphB1 receptor selective agonist for the treatment of glioblastoma.

Furthermore, the different levels of EphB1 mRNA and protein seems to correlate the loss of EphB1 receptor expression in glioblastoma cells to some post-transcriptional events involving miRNAs. In future experiments EphB1 3'UTR will be cloned to perform gene reporter assay aimed at unraveling the molecular processes responsible for EphB1 receptor downregulation in glioblastoma cells, elucidating those, we could develop innovative pharmacological approaches to treat this aggressive malignant brain tumor.

Second part

Cardio-vascular diseases, such as peripheral artery disease (PAD) and coronary artery disease (CAD), are the leading causes of death and disability in Western countries. CAD and PAD patients are often not satisfactorily treated by current procedures despite optimal pharmacological or surgical therapy²¹⁷. In this regard, therapeutic angiogenesis, which aims at restoring blood supply through the delivery of growth factors that stimulate the growth of new blood vessels, represents an alternative and attractive strategy to treat CAD and PAD patients. VEGF has already been extensively studied for therapeutic angiogenesis. VEGF induces either normal or aberrant angiogenesis depending on its dose in the microenvironment around each producing cell *in vivo*²⁰². Recently, it has been shown by the host group that VEGF over-expression in skeletal muscle induces microvascular growth by an initial vascular enlargement followed by longitudinal splitting (intussusception), rather than the widely studied process of sprouting⁶⁵.

The understanding of molecular mechanisms that induce the VEGF dose-dependent switch between normal and aberrant angiogenesis is a major target to enable VEGF-induced angiogenesis for therapeutic approaches, in order to determine targets that can expand VEGF therapeutic window and prevent its side effects. Here, we investigated the role of Notch4 in the switch between normal and aberrant angiogenesis induced by VEGF.

The results presented here revealed that the loss of Notch4 did not interfere with normal angiogenesis induced by low and safe levels of VEGF, as quantified by VLD (Figure 2C). On the other hand, no aberrant structures were found in any sample implanted with high levels of VEGF in the absence of Notch4 signalling, whereas the same VEGF dose induced numerous angioma-like structures in WT mice (Figure 4). Therefore Notch4 inhibition completely prevented aberrant angiogenesis by high VEGF and yielded normal capillary networks instead. The results shown here are consistent with previous findings on the Notch4 signalling pathway. In fact, in a transgenic adult mouse model it was shown that conditional expression of a constitutively active form of Notch4 in endothelial cells caused the development of Arterio-Venous Malformations (AVM) in the brain vasculature. However, by switching off the expression of the same constitutively active form of Notch4, the AV shunts regressed and reverted to capillary-like microvessels^{111,112}. Here we extend significantly those results in a therapeutically relevant setting and found that physiological Notch4 signaling is necessary for the development of aberrant angiogenesis

by excessive VEGF doses, but is actually dispensable for normal angiogenesis by moderate VEGF levels.

It is important to recognize that angiogenesis in skeletal muscle can occur through two alternative mechanisms: sprouting, which is mainly initiated by hypoxia during ischemia⁵⁸ and intussusception, or vascular splitting^{218,219}. Since VEGF delivery to skeletal muscle at therapeutically relevant doses induces angiogenesis through the cellular mechanism of intussusception rather than sprouting⁶⁵, it is key to understand the molecular regulation of splitting angiogenesis, which is still poorly understood. Here we show that Notch4 signaling plays an important role in intussusceptive angiogenesis by VEGF. In fact, our results show that new vascular growth by both moderate and high doses of VEGF took place essentially without sprouting (Figure 3 and 4), but rather by an initial circumferential enlargement of pre-existing vessels with the typical sign of intraluminal pillar formation (Figure 3C). The key effect of Notch4 loss could be the limitation of the size of vascular enlargements induced by high VEGF that was observed 4 days after treatment (Figure 5). We previously found that, during intussusceptive angiogenesis the size reached in the initial stage of circumferential enlargement determines the outcome of the process. In fact, the limited size induced by moderate doses of VEGF enables complete transluminal pillar formation and the successful completion of the subsequent step of longitudinal splitting. On the other hand, in the larger-caliber enlargements induced by excessive VEGF doses pillar formation starts, but it cannot be successfully completed due to the excessive vascular diameter to bridge, leading to a failure to split and the continued circumferential growth of affected vessel into abnormally dilated aberrant structures.

These findings are relevant for the design of rational strategies for therapeutic angiogenesis and identify Notch4 as an ideal molecular target to ensure safe and efficient induction of vascular growth through VEGF delivery, since its inhibition selectively targets aberrant angiogenesis without interfering with normal vascularization. Further studies will aim at elucidating how Notch4 signaling can modulate VEGF-induced intussusceptive angiogenesis with the goal to: 1) develop novel strategies for the treatment of peripheral artery disease and 2) control the occurrence of toxic side effects, such as angioma growth, of VEGF gene delivery for therapeutic angiogenesis.

Conclusion

In the last two decades Eph/ephrin molecular system has become more and more relevant and studied, as it is implicated in tumorigenesis, metastasis and angiogenesis.

Glioblastoma is a highly vascularized tumor and it among the most aggressive brain tumors with an exceedingly poor prognosis. Eph/ephrin system is involved in this tumor, in particular EphB1 is downregulated and the loss of its expression is correlated with aggressive cancer phenotype. The modulation of EphB1 expression can control glioblastoma cell aggressiveness, as EphB1 overexpression or activation decreases cancer cell aggressiveness. This receptor could represent an important target to develop novel strategies to treat glioblastoma.

Eph/ephrin system is also involved in angiogenesis. Angiogenesis is a complex, multistep process that requires the fine regulation of different cell types and molecular signals in space and time. Therapeutic angiogenesis aims at restoring blood supply producing normal, stable and functional blood vessels through the delivery of growth factors to ischemic tissues and it represents an attractive strategy for many patients affected by coronary or peripheral artery disease, for whom current medical and surgical therapies are ineffective. Previous studies in the host group show that VEGF expression can induce either normal or aberrant angiogenesis depending on its dose localized in the microenvironment around each producing cell in vivo. They recently identified that stimulating EphrinB2/EphB4 pathway could prevent aberrant angiogenesis by excessive VEGF doses and convert it to normal, whereby EphB4 is a druggable target to modulate the outcome of VEGF gene delivery. Preliminary data by the host group further suggest a similar role for the endothelial-specific Notch4 signaling pathway, whose absence is related to the switch from aberrant to normal angiogenesis induced by high dose of VEGF. Our results show that Notch4 receptor represents an important target to prevent the side effects of VEGF gene delivery, producing normal and functional angiogenesis despite high dose of VEGF.

In conclusion Eph/ephrin system is involved in different pathological conditions and its regulation can be exploit to modulate different signaling pathways to treat tumors and prevent aberrant angiogenesis. In this regard Notch4 was also important to understand the mechanism of angiogenesis.

References

1. Pasquale, E. B. Eph-ephrin bidirectional signaling in physiology and disease. *Cell*. 2008;133, 38–52.
2. Artur Kania and Rüdiger Klein. Mechanisms of ephrin-Eph signalling in development, physiology and disease. *NatRevMol Cell Biol*. 2016 Apr;17(4):240-56.
3. Himanem JP. 2012. Ectodomain structures of Eph receptors. *Semin. Cell Dev. Biol*. 23:35-42
4. Kullander K, Butt SJ, Le Bret JM, Lundfald L, Restrepo CE, Rydström A, et al. 2003. Role of EphA4 and EphrinB3 in local neuronal circuits that control walking. *Science* 299(5614):1889–92.
5. Kullander K, Croll SD, Zimmer M, Pan L, McClain J, Hughes V, et al. 2001. Ephrin-B3 is the midline barrier that prevents corticospinal tract axons from recrossing: allowing for unilateral motor control. *Genes Dev* 15(7):877–88.
6. Himanen JP, Chumley MJ, Lackmann M, Li C, Barton WA, Jeffrey PD, et al. 2004. Repelling class discrimination: ephrin-A5 binds to and activates EphB2 receptor signaling. *NatNeurosci* 7(5):501–9.
7. Davis S, Gale NW, Aldrich TH, Maisonpierre PC, Lhotak V, Pawson T, Goldfarb M, Yancopoulos GD. Ligands for EPH-related receptor tyrosine kinases that require membrane attachment or clustering for activity. *Science*. 1994; 266:816–819.
8. Noren NK, Yang NY, Silldorff M, Mutyala R, Pasquale EB. Ephrin-independent regulation of cell substrate adhesion by the EphB4 receptor. *The Biochemical journal*. 2009; 422:433–442.
9. Marquardt T, Shirasaki R, Ghosh S, Andrews SE, Carter N, Hunter T, Pfaff SL. Coexpressed EphA receptors and ephrin-A ligands mediate opposing actions on growth cone navigation from distinct membrane domains. *Cell*. 2005; 121:127–139.
10. Stein E, Lane AA, Cerretti DP, Schoecklmann HO, Schroff AD, Van Etten RL, Daniel TO. Eph receptors discriminate specific ligand oligomers to determine alternative signaling complexes, attachment, and assembly responses. *Genes Dev*. 1998; 12:667–678.
11. Himanen, J.P. et al. Crystal structure of an Eph receptor–ephrin complex. *Nature* 414, 933–938 (2001).
12. Himanen, J.P. & Nikolov, D.B. Eph signaling: a structural view. *TrendsNeurosc*. 26, 46–51 (2003).
13. Himanen, J.P., Henkemeyer, M. & Nikolov, D.B. Crystal structure of the ligand-binding domain of the receptor tyrosine kinase EphB2. *Nature* 396, 486–491 (1998).
14. Pasquale EB (2005) Eph receptor signalling casts a wide net on cell behaviour. *NatRevMol Cell Biol* 6:462–475.
15. Xu K, Tzvetkova-Robev D, Xu Y, Goldgur Y, Chan YP, Himanen JP, Nikolov DB (2013) Insights into Eph receptor tyrosine kinase activation from crystal structures of the EphA4 ectodomain and its complex with ephrin-A5. *Proc NatlAcad Sci USA* 110:14634–14639.
16. Himanen JP, Yermekbayeva L, Janes PW, Walker JR, Xu K, Atapattu L, Rajashankar KR, Mensinga A, Lackmann M, Nikolov DB, Dhe-Paganon S (2010) Architecture of Eph receptor clusters. *Proc NatlAcad Sci USA* 107:10860–108.
17. Binns KL, Taylor PP, Sicheri F, Pawson T, Holland SJ (2000) Phosphorylation of tyrosine residues in the kinase domain and juxta membrane region regulates the biological and catalytic activities of Eph receptors. *Mol Cell Biol* 20:4791–4805.

18. Pasquale EB (2010) Eph receptors and ephrins in cancer: bidirectional signalling and beyond. *NatRev Cancer* 10:165–180.
19. Lai KO, Chen Y, Po HM, Lok KC, Gong K, Ip NY (2004) Identification of the Jak/Stat proteins as novel downstream targets of EphA4 signaling in muscle: implications in the regulation of acetylcholinesterase expression. *J BiolChem* 279:13383–13392.
20. Vindis C, Cerretti DP, Daniel TO, Huynh-Do U (2003) EphB1 recruits c-Src and p52 Shc to activate MAPK/ERK and promote chemotaxis. *J Cell Biol* 162:661–671.
21. Xu Z, Lai KO, Zhou HM, Lin SC, Ip NY (2003) Ephrin-B1 reverse signaling activates JNK through a novel mechanism that is independent of tyrosine phosphorylation. *J BiolChem* 278:24767–24775.
22. Buchert M, Schneider S, Meskenaite V, Adams MT, Canaani E, Baechi T, Moelling K, Hovens CM (1999) The junction-associated protein AF-6 interacts and clusters with specific Eph receptor tyrosine kinases at specialized sites of cell–cell contact in the brain. *J Cell Biol* 144:361–371.
23. Hock B, Bohme B, Karn T, Yamamoto T, Kaibuchi K, Holtrich U, Holland S, Pawson T, Rubsamen-Waigmann H, Strebhardt K (1998) PDZ-domain-mediated interaction of the Eph-related receptor tyrosine kinase EphB3 and the ras-binding protein AF6 depends on the kinase activity of the receptor. *Proc NatlAcad Sci USA* 95:9779–9784.
24. Torres R, Firestein BL, Dong H, Staudinger J, Olson EN, Haganir RL, Bredt DS, Gale NW, Yancopoulos GD (1998) PDZ proteins bind, cluster, and synaptically colocalize with Eph receptors and their ephrin ligands. *Neuron* 21:1453–1463.
25. Davy A, Gale NW, Murray EW, Klinghoffer RA, Soriano P, Feuerstein C, Robbins SM (1999) Compartmentalized signaling by GPI-anchored ephrin-A5 requires the Fyn tyrosine kinase to regulate cellular adhesion. *Genes Dev* 13:3125–3135.
26. Davy A, Robbins SM (2000) Ephrin-A5 modulates cell adhesion and morphology in an integrin-dependent manner. *EMBO J* 19:5396–5405.
27. Segura I, Essmann CL, Weinges S, Acker-Palmer A (2007) Grb4 and GIT1 transduce ephrinB reverse signals modulating spine morphogenesis and synapse formation. *NatNeurosci* 10:301–310.
28. Palmer A, Zimmer M, Erdmann KS, Eulenburg V, Porthin A, Heumann R, Deutsch U, Klein R (2002) EphrinB phosphorylation and reverse signaling: regulation by Src kinases and PTPBL phosphatase. *Mol Cell* 9:725–737.
29. Tanaka M, Sasaki K, Kamata R, Sakai R (2007) The C-terminus of ephrin-B1 regulates metalloproteinase secretion and invasion of cancer cells. *J Cell Sci* 120:2179–2189.
30. Xu NJ, Henkemeyer M (2009) Ephrin-B3 reverse signaling through Grb4 and cytoskeletal regulators mediates axon pruning. *NatNeurosci* 12:268–276.
31. Nakada M, Drake KL, Nakada S, Niska JA, Berens ME (2006) Ephrin-B3 ligand promotes glioma invasion through activation of Rac1. *Cancer Res* 66:8492–8500.
32. Lee HS, Nishanian TG, Mood K, Bong YS, Daar IO (2008) EphrinB1 controls cell–cell junctions through the Par polarity complex. *Nat Cell Biol* 10:979–986.
33. Bochenek ML, Dickinson S, Astin JW, Adams RH, Nobes CD (2010) Ephrin-B2 regulates endothelial cell morphology and motility independently of Eph-receptor binding. *J Cell Sci* 123:1235–1246.

34. Foo SS, Turner CJ, Adams S, Compagni A, Aubyn D, Kogata N, Lindblom P, Shani M, Zicha D, Adams RH (2006) EphrinB2 controls cell motility and adhesion during blood-vessel-wall assembly. *Cell* 124:161–173.
35. Gucciardo, E., Sugiyama, N., &Lehti, K. (2014). Eph- and ephrin-dependent mechanisms in tumor and stem cell dynamics. *Cellular and Molecular Life Sciences*, 71(19), 3685-3710.
36. Goh LK, Sorkin A. 2013. Endocytosis of receptor tyrosine kinases. *Cold Spring Harb Perspect Biol*.
37. Marston DJ, Dickinson S, Nobes CD. 2003. Rac-dependent trans-endocytosis of ephrin-Bs regulates Eph-ephrin contact repulsion. *Nat Cell Biol* 5: 879–888.
38. Zimmer M, Palmer A, Kohler J, Klein R. 2003. EphB-ephrin-B bi-directional endocytosis terminates adhesion allowing contact mediated repulsion. *Nat Cell Biol* 5: 869– 878.
39. Pitulescu ME, Adams RH. 2010. Eph/ephrin molecules—A hub for signaling and endocytosis. *Genes Dev* 24: 2480– 2492.
40. Walker-Daniels J, Riese DJ 2nd, Kinch MS. 2002. c-Cbl dependent EphA2 protein degradation is induced by ligand binding. *Mol Cancer Res* 1: 79–87.
41. Fasen K, Cerretti DP, Huynh-Do U. 2008. Ligand binding induces Cbl-dependent EphB1 receptor degradation through the lysosomal pathway. *Traffic* 9: 251–266.
42. Risau W. Mechanisms of angiogenesis. *Nature*. 1997;386(6626):671-4.
43. Risau W, and Flamme I. Vasculogenesis. *AnnuRev Cell Dev Biol*. 1995;11(73-91).
44. Fan T-PD, and Kohn EC. The new angiotherapy. Totowa, N.J.: Humana Press; 2002.
45. Semenza GL. Vasculogenesis, angiogenesis, and arteriogenesis: mechanisms of blood vessel formation and remodeling. *J Cell Biochem*. 2007;102(4):840-7.
46. Jin SW, and Patterson C. The opening act: vasculogenesis and the origins of circulation. *Arterioscler Thromb Vasc Biol*. 2009;29(5):623-9.
47. Persson AB, and Buschmann IR. Vascular growth in health and disease. *Front Mol Neurosci*. 2011;4-14.
48. Ribatti D, Vacca A, Nico B, Roncali L, and Dammacco F. Postnatal vasculogenesis. *Mech Dev*. 2001;100(2):157-63.
49. Ziello JE, Jovin IS, and Huang Y. Hypoxia-Inducible Factor (HIF)-1 regulatory pathway and its potential for therapeutic intervention in malignancy and ischemia. *Yale J BiolMed*. 2007;80(2):51-60.
50. Vokes SA, and Krieg PA. *Pan Vascular Medicine*. Springer-Verlag Berlin Heidelberg; 2015:27-51.
51. Gianni-Barrera R, Trani M, Reginato S, and Banfi A. To sprout or to split? VEGF, Notch and vascular morphogenesis. *BiochemSoc Trans*. 2011;39(6):1644-8.
52. Carmeliet P, and Jain RK. Principles and mechanisms of vessel normalization for cancer and other angiogenic diseases. *Nat Rev Drug Discov*. 2011;10(6):417-27.
53. Eklund L, and Saharinen P. Angiopietin signaling in the vasculature. *Exp Cell Res*. 2013;319(9):1271-80.
54. Andrae J, Gallini R, and Betsholtz C. Role of platelet-derived growth factors in physiology and medicine. *Genes Dev*. 2008;22(10):1276-312.

55. Bergers G, and Song S. The role of pericytes in blood-vessel formation and maintenance. *Neuro Oncol.* 2005;7(4):452-64.
56. Benjamin LE, Golijanin D, Itin A, Pode D, and Keshet E. Selective ablation of immature blood vessels in established human tumors follows vascular endothelial growth factor withdrawal. *J Clin Invest.* 1999;103(2):159-65.
57. Davis GE, and Senger DR. Endothelial extracellular matrix: biosynthesis, remodeling, and functions during vascular morphogenesis and neovessel stabilization. *Circ Res.* 2005;97(11):1093-107.
58. Carmeliet P. Mechanisms of angiogenesis and arteriogenesis. *NatMed.* 2000;6(4):389-95.
59. Cai W, and Schaper W. Mechanisms of arteriogenesis. *Acta BiochimBiophys Sin (Shanghai).* 2008;40(8):681-92.
60. Tzima E, Irani-Tehrani M, Kiosses WB, Dejana E, Schultz DA, Engelhardt B, Cao G, DeLisser H, and Schwartz MA. A mechanosensory complex that mediates the endothelial cell response to fluid shear stress. *Nature.* 2005;437(7057):426-31.
61. Schaper W. Collateral circulation: past and present. *Basic Res Cardiol.* 2009;104(1):5-21.
62. Yla-Herttuala S, Rissanen TT, Vajanto I, Hartikainen J (2007) Vascular endothelial growth factors: biology and current status of clinical applications in cardiovascular medicine. *J Am Coll Cardiol* 49(10):1015–1026
63. Gianni-Barrera R, Bartolomeo M, Vollmar B, Djonov V, Banfi A. Split for the cure: VEGF, PDGF-BB and intussusception in therapeutic angiogenesis. *BiochemSoc Trans.* 2014;42:1637-1642.
64. Egginton S, Zhou AL, Brown MD, Hudlická O. Unorthodox angiogenesis in skeletal muscle. *Cardiovasc Res.* 2001;49:634-646.
65. Gianni-Barrera R, Trani M, Fontanellaz C, et al. VEGF over-expression in skeletal muscle induces angiogenesis by intussusception rather than sprouting. *Angiogenesis.* 2013;16:123-136.
66. Blanco R, Gerhardt H. VEGF and Notch in tip and stalk cell selection. *Cold Spring Harb Perspect Med.* 2013;3(1).
67. Egginton S. Invited review: activity-induced angiogenesis. *Pflugers Arch.* 2009;457(5):963–77.
68. Makanya AN, Hlushchuk R, Djonov VG. Intussusceptive angiogenesis and its role in vascular morphogenesis, patterning, and remodeling. *Angiogenesis.* 2009;12(2):113–23.
69. Mor F, Quintana FJ, and Cohen IR. Angiogenesis-inflammation cross-talk: vascular endothelial growth factor is secreted by activated T cells and induces Th1 polarization. *J Immunol.* 2004;172(7):4618-23.
70. Kiriakidis S, Andreakos E, Monaco C, Foxwell B, Feldmann M, and Paleolog E. VEGF expression in human macrophages NF-kappaB dependent: studies using adenoviruses expressing the endogenous NFkappaB inhibitor IkappaB alpha and a kinase-defective form of the IkappaB kinase 2. *Journal of cell science.* 2003;116(Pt 4):665-74.
71. Viac J, Palacio S, Schmitt D, and Claudy A. Expression of vascular endothelial growth factor in normal epidermis, epithelial tumors and cultured keratinocytes. *Arch Dermatol Res.* 1997;289(3):158-63.
72. Imoukhuede PI, and Popel AS. Expression of VEGF receptors on endothelial cells in mouse skeletal muscle. *PLoS One.* 2012;7(9):447-91.

73. Olsson AK, Dimberg A, Kreuger J, and Claesson-Welsh L. VEGF receptor signalling - in control of vascular function. *NatRevMol Cell Biol.* 2006;7(5):359-71.
74. Ogawa S, Oku A, Sawano A, Yamaguchi S, Yazaki Y, and Shibuya M. A novel type of vascular endothelial growth factor, VEGF-E (NZ-7 VEGF), preferentially utilizes KDR/Flk-1 receptor and carries a potent mitotic activity without eparin-binding domain. *J BiolChem.* 1998;273(47):31273-82.
75. Yamazaki Y, Tokunaga Y, Takani K, and Morita T. C-terminal heparin binding peptide of snake venom VEGF specifically blocks VEGF stimulated endothelial cell proliferation. *Pathophysiol Haemost Thromb.* 2005;34(4-5):197-9.
76. Koch S, and Claesson-Welsh L. Signal transduction by vascular endothelial growth factor receptors. *Cold Spring Harb Perspect Med.* 2012;2(7):0065-02.
77. Terman BI, Carrion ME, Kovacs E, Rasmussen BA, Eddy RL, and Shows TB. Identification of a new endothelial cell growth factor receptor tyrosine kinase. *Oncogene.* 1991;6(9):1677-83.
78. Grunewald FS, Prota AE, Giese A, and Ballmer-Hofer K. Structure function analysis of VEGF receptor activation and the role of coreceptors in angiogenic signaling. *Biochim Biophys Acta.* 2010;1804(3):567-80.
79. Ito N, Wernstedt C, Engstrom U, and Claesson-Welsh L. Identification of vascular endothelial growth factor receptor-1 tyrosine phosphorylation sites and binding of SH2 domain-containing molecules. *J Biol Chem.* 1998;273(36):23410-8.
80. Ferrara N, Gerber HP, and LeCouter J. The biology of VEGF and its receptors. *NatMed.* 2003;9(6):669-76.
81. Kendall RL, and Thomas KA. Inhibition of vascular endothelial cell growth factor activity by an endogenously encoded soluble receptor. *Proc Natl Acad Sci U S A.* 1993;90(22):10705-9.
82. Shinkai A, Ito M, Anazawa H, Yamaguchi S, Shitara K, and Shibuya M. Mapping of the sites involved in ligand association and dissociation at the extracellular domain of the kinase insert domain-containing receptor for vascular endothelial growth factor. *J BiolChem.* 1998;273(47):31283-8.
83. Fuh G, Li B, Crowley C, Cunningham B, and Wells JA. Requirements for binding and signaling of the kinase domain receptor for vascular endothelial growth factor. *J BiolChem.* 1998;273(18):11197-204.
84. Dumont DJ, Jussila L, Taipale J, Lymboussaki A, Mustonen T, Pajusola K, Breitman M, and Alitalo K. Cardiovascular failure in mouse embryos deficient in VEGF receptor-3. *Science.* 1998;282(5390):946-9.
85. Takahashi H, and Shibuya M. The vascular endothelial growth factor (VEGF)/VEGF receptor system and its role under physiological and pathological conditions. *Clin Sci (Lond).* 2005;109(3):227-41.
86. Albuquerque RJ, Hayashi T, Cho WG, Kleinman ME, Dridi S, Takeda A, Baffi JZ, Yamada K, Kaneko H, Green MG, et al. Alternatively spliced vascular endothelial growth factor receptor-2 is an essential endogenous inhibitor of lymphatic vessel growth. *NatMed.* 2009;15(9):1023-30.

87. Kawasaki T, Kitsukawa T, Bekku Y, Matsuda Y, Sanbo M, Yagi T, and Fujisawa H. A requirement for neuropilin-1 in embryonic vessel formation. *Development*. 1999;126(21):4895-902.
88. Ferrara N. Role of vascular endothelial growth factor in regulation of physiological angiogenesis. *Am J Physiol Cell Physiol*. 2001;280(6):C1358-66.
89. Pham I, Uchida T, Planes C, Ware LB, Kaner R, Matthay MA, and Clerici C. Hypoxia upregulates VEGF expression in alveolar epithelial cells in vitro and in vivo. *Am J Physiol Lung Cell Mol Physiol*. 2002;283(5):1133-42.
90. Ke Q, and Costa M. Hypoxia-inducible factor-1 (HIF-1). *Mol Pharmacol*. 2006;70(5):1469-80.
91. Akiri G, Nahari D, Finkelstein Y, Le SY, Elroy-Stein O, and Levi BZ. Regulation of vascular endothelial growth factor (VEGF) expression is mediated by internalinitiation of translation and alternative initiation of transcription. *Oncogene*. 1998;17(2):227-36.
92. Ikeda E, Achen MG, Breier G, and Risau W. Hypoxia-induced transcriptional activation and increased mRNA stability of vascular endothelial growth factor in C6 glioma cells. *J Biol Chem*. 1995;270(34):19761-6.
93. Vincenti V, Cassano C, Rocchi M, and Persico G. Assignment of the vascular endothelial growth factor gene to human chromosome 6p21.3. *Circulation*. 1996;93(8):1493-5.
94. Harper SJ, and Bates DO. VEGF-A splicing: the key to anti-angiogenic therapeutics? *NatRev Cancer*. 2008;8(11):880-7.
95. Sun Y, Jin K, Childs JT, Xie L, Mao XO, and Greenberg DA. Increased severity of cerebral ischemic injury in vascular endothelial growth factor-deficient mice. *J Cereb Blood Flow Metab*. 2004;24(10):1146-52.
96. Aase K, von Euler G, Li X, Ponten A, Thoren P, Cao R, Cao Y, Olofsson B, Gebre-Medhin S, Pekny M, et al. Vascular endothelial growth factor-B-deficient mice display an atrial conduction defect. *Circulation*. 2001;104(3):358-64.
97. Stacker SA, Caesar C, Baldwin ME, Thornton GE, Williams RA, Prevo R, Jackson DG, Nishikawa S, Kubo H, and Achen MG. VEGF-D promotes the metastatic spread of tumor cells via the lymphatics. *NatMed*. 2001;7(2):186-91.
98. Carmeliet P, Moons L, Luttun A, Vincenti V, Compernelle V, De Mol M, Wu Y, Bono F, Devy L, Beck H, et al. Synergism between vascular endothelial growth factor and placental growth factor contributes to angiogenesis and plasma extravasation in pathological conditions. *NatMed*. 2001;7(5):575- 83.
99. Artavanis-Tsakonas S, Rand MD, and Lake RJ. Notch signaling: cell fate control and signal integration in development. *Science*. 1999;284(5415):770-6.
100. Yavropoulou MP, and Yovos JG. The role of Notch signaling in bone development and disease. *Hormones (Athens)*. 2014;13(1):24-37.
101. Kume T. Novel insights into the differential functions of Notch ligands in vascular formation. *J Angiogenes Res*. 2009;1-8.
102. Gridley T. Notch signaling in the vasculature. *Curr Top Dev Biol*. 2010;92(277-309).

103. Krebs LT, Xue Y, Norton CR, Shutter JR, Maguire M, Sundberg JP, Gallahan D, Closson V, Kitajewski J, Callahan R, et al. Notch signaling is essential for vascular morphogenesis in mice. *Genes Dev.* 2000;14(11):1343-52.
104. Krebs LT, Shutter JR, Tanigaki K, Honjo T, Stark KL, and Gridley T. Haploinsufficient lethality and formation of arteriovenous malformations in Notch pathway mutants. *Genes Dev.* 2004;18(20):2469-73.
105. Uyttendaele H, Ho J, Rossant J, and Kitajewski J. Vascular patterning defects associated with expression of activated Notch4 in embryonic endothelium. *Proc Natl Acad Sci U S A.* 2001;98(10):5643-8.
106. Kageyama R, and Kobayashi T. Regulation of neural development by the bHLH factor Hes1. *Tanpakushitsu Kakusan Koso.* 2008;53(4 Suppl):318- 23.
107. Blanco R, and Gerhardt H. VEGF and Notch in tip and stalk cell selection. *Cold Spring Harb Perspect Med.* 2013;3(1):006569.
108. Geudens I, and Gerhardt H. Coordinating cell behaviour during blood vessel formation. *Development.* 2011;138(21):4569-83.
109. Benedito R, Roca C, Sorensen I, Adams S, Gossler A, Fruttiger M, and Adams RH. The notch ligands Dll4 and Jagged1 have opposing effects on angiogenesis. *Cell.* 2009;137(6):1124-35.
110. Carlson TR, Yan Y, Wu X, Lam MT, Tang GL, Beverly LJ, Messina LM, Capobianco AJ, Werb Z, and Wang R. Endothelial expression of constitutively active Notch4 elicits reversible arteriovenous malformations in adult mice. *Proc Natl Acad Sci U S A.* 2005;102(28):9884-9.
111. Murphy PA, Kim TN, Huang L, Nielsen CM, Lawton MT, Adams RH, Schaffer CB, and Wang RA. Constitutively active Notch4 receptor elicits brain arteriovenous malformations through enlargement of capillary-like vessels. *Proc Natl Acad Sci U S A.* 2014;111(50):18007-12.
112. Murphy PA, Kim TN, Lu G, Bollen AW, Schaffer CB, and Wang RA. Notch4 normalization reduces blood vessel size in arteriovenous malformations. *Science translational medicine.* 2012;4(117):117-8.
113. M. Kandouz, The Eph/Ephrin family in cancer metastasis: communication at the service of invasion, *Cancer Metastasis Rev.* 31 (2012) 353e373.
114. E. Shiuan, J. Chen, Eph receptor tyrosine kinases in tumor immunity, *Cancer Res.* 76 (2016) 6452-6457.
115. H. Miao, N.W. Gale, H. Guo, J. Qian, A. Petty, J. Kaspar, A.J. Murphy, D.M. Valenzuela, G. Yancopoulos, D. Hambardzumyan, J.D. Lathia, J.N. Rich, J. Lee, B. Wang, EphA2 promotes infiltrative invasion of glioma stem cells in vivo through cross-talk with Akt and regulates stem cell properties, *Oncogene* 34 (2015) 558-567
116. N.-Y. Yang, C. Fernandez, M. Richter, Z. Xiao, F. Valencia, D.A. Tice, E.B. Pasquale, Crosstalk of the EphA2 receptor with a serine/threonine phosphatase suppresses the Akt-mTORC1 pathway in cancer cells, *Cell. Signal* 23 (2011) 201-212.
117. Keane, N., Freeman, C., Swords, R. & Giles, F. J. EPHA3 as a novel therapeutic target in the hematological malignancies. *Expert Rev. Hematol.* 5, 325–340 (2012).

118. Wykosky, J. & Debinski, W. The EphA2 receptor and ephrinA1 ligand in solid tumors: function and therapeutic targeting. *Mol. Cancer Res.* 6, 1795–1806 (2008).
119. Oki, M. et al. Overexpression of the receptor tyrosine kinase EphA4 in human gastric cancers. *World J. Gastroenterol.* 14, 5650–5656 (2008).
120. Oricchio, E. & Wendel, H. G. Mining the cancer genome uncovers therapeutic activity of EphA7 against lymphoma. *Cell Cycle* 11, 1076–1080 (2012).
121. Fox, B. P. & Kandpal, R. P. EphB6 receptor significantly alters invasiveness and other phenotypic characteristics of human breast carcinoma cells. *Oncogene* 28, 1706–1713 (2009).
122. Brantley-Sieders, D. M. et al. Impaired tumor microenvironment in EphA2-deficient mice inhibits tumor angiogenesis and metastatic progression. *FASEB J.* 19, 1884–1886 (2005).
123. Brantley-Sieders, D. M. et al. The receptor tyrosine kinase EphA2 promotes mammary adenocarcinoma tumorigenesis and metastatic progression in mice by amplifying ErbB2 signaling. *J. Clin. Invest.* 118, 64–78 (2008).
124. Wu, Q. et al. Expression of Ephb2 and Ephb4 in breast carcinoma. *Pathol. Oncol. Res.* 10, 26–33 (2004).
125. Zelinski, D. P., Zantek, N. D., Stewart, J. C., Irizarry, A. R. & Kinch, M. S. EphA2 overexpression causes tumorigenesis of mammary epithelial cells. *Cancer Res.* 61, 2301–2306 (2001).
126. Noren, N. K., Lu, M., Freeman, A. L., Koolpe, M. & Pasquale, E. B. Interplay between EphB4 on tumor cells and vascular ephrin-B2 regulates tumor growth. *Proc. Natl Acad. Sci. USA* 101, 5583–5588 (2004).
127. Brantley-Sieders, D. M. et al. Eph/ephrin profiling in human breast cancer reveals significant associations between expression level and clinical outcome. *PLoS ONE* 6, 24426 (2011).
128. Noren, N. K., Foos, G., Hauser, C. A. & Pasquale, E. B. The EphB4 receptor suppresses breast cancer cell tumorigenicity through an Abl-Crk pathway. *Nature Cell Biol.* 8, 815–825 (2006).
129. Xiao, Z. et al. EphB4 promotes or suppresses Ras/MEK/ERK pathway in a context-dependent manner: Implications for EphB4 as a cancer target. *Cancer Biol. Ther.* 13, 630–637 (2012).
130. Jubb, A. M. et al. EphB2 is a prognostic factor in colorectal cancer. *Clin. Cancer Res.* 11, 5181–5187 (2005).
131. Herath, N. I. et al. Complex expression patterns of Eph receptor tyrosine kinases and their ephrin ligands in colorectal carcinogenesis. *Eur. J. Cancer* 48, 753–762 (2012).
132. Astin, J. W. et al. Competition amongst Eph receptors regulates contact inhibition of locomotion and invasiveness in prostate cancer cells. *Nature Cell Biol.* 12, 1194–1204 (2010).
133. Day, B. W. et al. EphA3 maintains tumorigenicity and is a therapeutic target in glioblastoma multiforme. *Cancer Cell* 23, 238–248 (2013).
134. Binda, E. et al. The EphA2 receptor drives self-renewal and tumorigenicity in stem-like tumor-propagating cells from human glioblastomas. *Cancer Cell* 22, 765–780 (2012).
135. J. Peng, Q. Wang, H. Liu, M. Ye, X. Wu, L. Guo, EPHA3 regulates the multidrug resistance of small cell lung cancer via the PI3K/BMX/STAT3 signaling pathway, *Tumour Biol. J. Int. Soc. Oncodevelopmental Biol. Med.* 37 (2016) 11959-11971,

- 136.C. Giaginis, N. Tsoukalas, E. Bournakis, P. Alexandrou, N. Kavantzias, E. Patsouris, S. Theocharis, Ephrin (Eph) receptor A1, A4, A5 and A7 expression in human non-small cell lung carcinoma: associations with clinicopathological parameters, tumor proliferative capacity and patients survival, *BMC Clin. Pathol.* 14 (2014) 8.
- 137.P. Saintigny, S. Peng, L. Zhang, B. Sen, I.I. Wistuba, S.M. Lippman, L. Girard, J.D. Minna, J.V. Heymach, F.M. Johnson, Global evaluation of Eph receptors and ephrins in lung adenocarcinomas identifies EphA4 as an inhibitor of cell migration and invasion, *Mol. Cancer Ther.* 11 (2012) 2021-2032.
138. F.I. Staquicini, M.D. Qian, A. Salameh, A.S. Dobroff, J.K. Edwards, D.F. Cimino, B.J. Moeller, P. Kelly, M.I. Nunez, X. Tang, D.D. Liu, J.J. Lee, W.K. Hong, F. Ferrara, A.R.M. Bradbury, R.R. Lobb, M.J. Edelman, R.L. Sidman, I.I. Wistuba, W. Arap, R. Pasqualini, Receptor tyrosine kinase EphA5 is a functional molecular target in human lung cancer, *J. Biol. Chem.* 290 (2015) 7345-7359.
- 139.G. Efazat, M. Novak, V.O. Kaminsky, L. De Petris, L. Kanter, T. Juntti, P. Bergman, B. Zhivotovsky, R. Lewensohn, P. Hååg, K. Viktorsson, Ephrin B3 interacts with multiple EphA receptors and drives migration and invasion in non-small cell lung cancer, *Oncotarget* 7 (2016).
- 140.C. Zhao, A. Wang, F. Lu, H. Chen, P. Fu, X. Zhao, H. Chen, Overexpression of junctional adhesion molecule-A and EphB2 predicts poor survival in lung adenocarcinoma patients, *Tumour Biol. J. Int. Soc. Oncodevelopmental Biol. Med.* 39 (2017).
- 141.L. Peng, P. Tu, X. Wang, S. Shi, X. Zhou, J. Wang, Loss of EphB6 protein expression in human colorectal cancer correlates with poor prognosis, *J. Mol. Histol.* 45 (2014) 555-563.
- 142.B.O. Wu, W.G. Jiang, D. Zhou, Y.-X. Cui, Knockdown of EPHA1 by CRISPR/CAS9 promotes adhesion and motility of HRT18 colorectal carcinoma cells, *Anti- cancer Res.* 36 (2016) 1211-1219.
- 143.S. Gu, J. Feng, Q. Jin, W. Wang, S. Zhang, Reduced expression of EphA5 is associated with lymph node metastasis, advanced TNM stage, and poor prognosis in colorectal carcinoma, *Histol. Histopathol.* 32 (2017) 491-497.
- 144.Liebl DJ, Morris CJ, Henkemeyer M, Parada LF. mRNA expression of ephrins and Eph receptor tyrosine kinases in the neonatal and adult mouse central nervous system. *J Neurosci Res.* 2003;71(1):7–22.
- 145.Martínez A, Soriano E. Functions of ephrin/Eph interactions in the development of the nervous system: emphasis on the hippocampal system. *Brain Res Rev.* 2005;49(2):211–26.
- 146.Henkemeyer M, Itkis OS, Ngo M, Hickmott PW, Ethell IM. Multiple EphB receptor tyrosine kinases shape dendritic spines in the hippocampus. *J Cell Biol.* 2003;163(6):1313–26.
- 147.Murai KK, Pasquale EB. Eph receptors and ephrins in neuron–astrocyte communication at synapses. *Glia.* 2011;59(11):1567–78.
- 148.Chumley MJ, Catchpole T, Silvany RE, Kernie SG, Henkemeyer M. EphB receptors regulate stem/progenitor cell proliferation, migration, and polarity during hippocampal neurogenesis. *J Neurosci.* 2007;27(49):13481–90.
- 149.Petros T, Shrestha B. C: Specificity and sufficiency of EphB1 in driving the ipsilateral retinal projection. *J Neurosci.* 2009;29(11):3463–74.

150. Calò L, Spillantini M, Nicoletti F, Allen ND. Nurr1 co-localizes with EphB1 receptors in the developing ventral midbrain, and its expression is enhanced by the EphB1 ligand, ephrinB2. *J Neurochem.* 2005;92(2):235–45.
151. Yoon JK, Lau LF. Transcriptional activation of the inducible nuclear receptor gene *nur77* by nerve growth factor and membrane depolarization in PC12 cells. *J BiolChem.* 1993;268(12):9148–55.
152. Xia WS, Peng YN, Tang LH, Jiang LS, Yu LN, Zhou XL, Zhang FJ, Yan M. Spinal ephrinB/EphB signalling contributed to remifentanyl-induced hyperalgesia via NMDA receptor. *Eur J Pain.* 2014;18(9):1231–9.
153. Bandoh S, Tsukada T, Maruyama K, Ohkura N, Yamaguchi K. Gene expression of NOR-1, a neuron-derived orphan receptor, is inducible in neuronal and other cell lineages in culture. *Mol Cell Endocrinol.* 1995;115(2):227–30.
154. Rudolph J, Gerstmann K, Zimmer G, Steinecke A, Doeding A, Bolz J. A dual role of EphB1/ephrin-B3 reverse signaling on migrating striatal and cortical neurons originating in the preoptic area: should I stay or go away? *Fron Cell Neurosci.* 2014;8:185.
155. Wei, W., Wang, H. & Ji, S. Paradoxes of the EphB1 receptor in malignant brain tumors. *Cancer Cell Int.* 17, 21 (2017).
156. Teng L, Nakada M, Furuyama N, Sabit H, Furuta T, Hayashi Y, Takino T, Dong Y, Sato H, Sai Y. Ligand-dependent EphB1 signaling suppresses glioma invasion and correlates with patient survival. *Neuro-Oncology.* 2013;15(12):1710–20.
157. Shao-Qing K, Hao B, Zhi-Hong F, Gonzalo L, Hui Y, Weigang T, Wang ZZ, Guillermo GM. Aberrant DNA methylation and epigenetic inactivation of Eph receptor tyrosine kinases and ephrin ligands in acute lymphoblastic leukemia. *Blood.* 2010;115(12):2412–9.
158. Rodriguez S, Huynh-Do U. Phosphatase and tensin homolog regulates stability and activity of EphB1 receptor. *FASEB J.* 2013;27(2):632–44.
159. Egea J, Klein R. Bidirectional Eph-ephrin signaling during axon guidance. *Trends Cell Biol.* 2007;17(5):230–8.
160. Bhatia S, Baig NA, Timofeeva O, Pasquale EB, Hirsch K, MacDonald TJ, Dritschilo A, Lee YC, Henkemeyer M, Rood B, et al. Knockdown of EphB1 receptor decreases medulloblastoma cell growth and migration and increases cellular radiosensitization. *Oncotarget.* 2015;6(11):8929–46.
161. Huynh-Do, U. et al. Ephrin-B1 transduces signals to activate integrin-mediated migration, attachment and angiogenesis. *J. Cell Sci.* 115, (2002).
162. Sawamiphak S, Seidel S, Essmann CL, Wilkinson GA, Pitulescu ME, Acker T, Acker-Palmer A (2010) Ephrin-B2 regulates VEGFR2 function in developmental and tumour angiogenesis. *Nature* 465: 487 – 491.
163. Wang Y, Nakayama M, Pitulescu ME, Schmidt TS, Bochenek ML, Sakakibara A, Adams S, Davy A, Deutsch U, Luthi U et al (2010) Ephrin-B2 controls VEGF-induced angiogenesis and lymphangiogenesis. *Nature* 465: 483 – 486.
164. Erber R, Eichelsbacher U, Powajbo V, Korn T, Djonov V, Lin J, Hammes HP, Grobholz R, Ullrich A, Vajkoczy P (2006) EphB4 controls blood vascular morphogenesis during postnatal angiogenesis. *EMBO J* 25: 628 – 641

165. Groppa E, Brkic S, Uccelli A, Wirth G, Korpisalo-Pirinen P, Filippova M, Dasen B, Sacchi V, Muraro MG, Trani M, Reginato S, Gianni-Barrera R, Ylä-Herttuala S, Banfi A. EphrinB2/EphB4 signaling regulates non-sprouting angiogenesis by VEGF. *EMBO Rep.* 2018 May;19(5):45054.
166. Ahir BK, Engelhard HH, Lakka SS. Tumor Development and Angiogenesis in Adult Brain Tumor: Glioblastoma. *Mol Neurobiol.* 2020 May;57(5):2461-2478.
167. Carmeliet P, Jain RK (2011) Principles and mechanisms of vessel normalization for cancer and other angiogenic diseases. *Nat Rev Drug Discov* 10(6):417–427.
168. Siemann DW, Chaplin DJ, Horsman MR (2017) Realizing the potential of vascular targeted therapy: the rationale for combining vascular disrupting agents and anti-angiogenic agents to treat cancer. *Cancer Investig* 35(8):519–534.
169. Koolpe, M., Burgess, R., Dail, M. & Pasquale, E. B. EphB receptor-binding peptides identified by phage display enable design of an antagonist with ephrin-like affinity. *J. Biol. Chem.* 280, 17301–17311 (2005).
170. Koolpe, M., Dail, M. & Pasquale, E. B. An Ephrin Mimetic Peptide That Selectively Targets the EphA2 Receptor. *Publ. JBC Pap. Press* (2002).
171. Riedl, S. & Pasquale, E. Targeting the Eph System with Peptides and Peptide Conjugates. *Curr. Drug Targets* (2015).
172. Boyd, A. W., Bartlett, P. F. & Lackmann, M. Therapeutic targeting of EPH receptors and their ligands. *Nat. Rev. Drug Discov.* 13, 39–62 (2014).
173. Lamberto I, Qin H, Noberini R, Premkumar L, Bourgin C, Riedl SJ, et al. 2012. Distinctive binding of three antagonistic peptides to the ephrin-binding pocket of the EphA4 receptor. *Biochem J.* 445:47–56.
174. Wu B, Zhang Z, Noberini R, Barile E, Giulianotti M, Pinilla C, et al. 2013. HTS by NMR of combinatorial libraries: a fragment-based approach to ligand discovery. *ChemBiol.* 20:19–33.
175. Chrencik JE, Brooun A, Recht MI, Kraus ML, Koolpe M, Kolatkar AR, et al. 2006. Structure and thermodynamic characterization of the EphB4/Ephrin-B2 antagonist peptide complex reveals the determinants for receptor specificity. *Structure.* 14:321–30.
176. Chrencik JE, Brooun A, Recht MI, Nicola G, Davis LK, Abagyan R, et al. 2007. Three-dimensional Structure of the EphB2 Receptor in Complex with an Antagonistic Peptide Reveals a Novel Mode of Inhibition. *J Biol Chem.* 282:36505–13.
177. Lamberto I, Lechtenberg BC, Olson E, Mace PD, Dawson PE, Riedl SJ, et al. 2014. Development and Structural Analysis of a Nanomolar Cyclic Peptide Antagonist for the EphA4 Receptor. *ACS ChemBiol.* 9:2787–95.
178. Mitra S, Duggineni S, Koolpe M, Zhu X, Huang Z, Pasquale EB. 2010. Structure-activity relationship analysis of peptides targeting the EphA2 receptor. *Biochemistry.* 49:6687–95.
179. Lamberto I, Lechtenberg BC, Olson E, Mace PD, Dawson PE, Riedl SJ, et al. 2014. Development and Structural Analysis of a Nanomolar Cyclic Peptide Antagonist for the EphA4 Receptor. *ACS ChemBiol.* 9:2787–95.

180. Murai KK, Nguyen LN, Koolpe M, McLennan R, Krull CE, Pasquale EB. 2003. Targeting the EphA4 receptor in the nervous system with biologically active peptides. *Mol Cell Neurosci.* 24:1000–11.
181. Noberini R, Mitra S, Salvucci O, Valencia F, Duggineni S, Prigozhina N, et al. 2011. PEGylation potentiates the effectiveness of an antagonistic peptide that targets the EphB4 receptor with nanomolar affinity. *PLoS ONE.* 6:28611.
182. Noren NK, Pasquale EB. 2007. Paradoxes of the EphB4 receptor in cancer. *Cancer Res.* 67(9):3994–7.
183. Yu, X., Zheng, H., Chan, M. T., & Wu, W. K. (2017). Modulation of chemoresponsiveness to platinum-based agents by microRNAs in cancer. *American Journal of Cancer Research*, 7(9), 1769–1778.
184. Berrout, J., Kyriakopoulou, E., Moparthi, L., Hoge, A. S., Berrout, L., Ivan, C., et al. (2017). TRPA1-FGFR2 binding event is a regulatory oncogenic driver modulated by miRNA-142-3p. *Nature Communication*, 8(1), 947.
185. Lv, C., Li, F., Li, X., Tian, Y., Zhang, Y., Sheng, X., et al. (2017). MiR-31 promotes mammary stem cell expansion and breast tumorigenesis by suppressing Wnt signaling antagonists. *Nature Communications*, 8(1), 1036.
186. Rodriguez, M., Bajo-Santos, C., Hessvik, N. P., Lorenz, S., Fromm, B., Berge, V., et al. (2017). Identification of non-invasive miRNAs biomarkers for prostate cancer by deep sequencing analysis of urinary exosomes. *Molecular Cancer*, 16(1), 156.
187. Lang, F. M., Hossain, A., Gumin, J., Momin, E. N., Shimizu, Y., Ledbetter, D., et al. (2018). Mesenchymal stem cells as natural biofactories for exosomes carrying miR-124a in the treatment of gliomas. *Neuro-Oncology*, 20(3), 380–390.
188. Ciafre, S. A., Galardi, S., Mangiola, A., Ferracin, M., Liu, C. G., Sabatino, G., et al. (2005). Extensive modulation of a set of microRNAs in primary glioblastoma. *Biochemical and Biophysical Research Communications*, 334(4), 1351–1358.
189. Figueroa, J., Phillips, L. M., Shahar, T., Hossain, A., Gumin, J., Kim, H., et al. (2017). Exosomes from glioma-associated mesenchymal stem cells increase the tumorigenicity of glioma stem-like cells via transfer of miR-1587. *Cancer Research*, 77(21), 5808–5819.
190. Yu W, Liang S, Zhang C. Aberrant miRNAs Regulate the Biological Hallmarks of Glioblastoma. *Neuromolecular Med.* 2018 Dec;20(4):452-474.
191. Xiao G, Li X, Li G, Zhang B, Xu C, Qin S, Du N, Wang J, Tang SC, Zhang J, Ren H, Chen K and Sun X. MiR-129 blocks estrogen induction of NOTCH signaling activity in breast cancer stem-like cells. *Oncotarget* 2017; 8: 103261- 103273.
192. Han H, Li W, Shen H, Zhang J, Zhu Y and Li Y. microRNA-129-5p, a c-Myc negative target, affects hepatocellular carcinoma progression by blocking the Warburg effect. *J Mol Cell Biol* 2016.
193. Seike M, Goto A, Okano T, Bowman ED, Schetter AJ, Horikawa I, Mathe EA, Jen J, Yang P, Sugimura H, Gemma A, Kudoh S, Croce CM and Harris CC. MiR-21 is an EGFR-regulated anti-apoptotic factor in lung cancer in never smokers. *Proc Natl Acad Sci U S A* 2009; 106: 12085-12090.

- 194.Xue J, Zhou A, Wu Y, Morris SA, Lin K, Amin S, Verhaak R, Fuller G, Xie K, Heimberger AB, Huang S. miR-182-5p Induced by STAT3 Activation Promotes Glioma Tumorigenesis. *Cancer Res.* 2016 Jul 15;76(14):4293-304.
- 195.Jiang L, Mao P, Song L, Wu J, Huang J, Lin C, Yuan J, Qu L, Cheng SY, Li J. miR-182 as a prognostic marker for glioma progression and patient survival. *Am J Pathol.* 2010 Jul;177(1):29-38.
- 196.Zhang Y, Chao T, Li R, et al: MicroRNA-128 inhibits glioma cells proliferation by targeting transcription factor E2F3a. *J MolMed* 87: 43-51, 2009.
- 197.Godlewski J, Nowicki MO, Bronisz A, et al: Targeting of the Bmi-1 oncogene/stem cell renewal factor by microRNA-128 inhibits glioma proliferation and self-renewal. *Cancer Res* 68: 9125-9130, 2008.
- 198.Lee RJ, Springer ML, Blanco-Bose WE, Shaw R, Ursell PC, Blau HM. VEGF gene delivery to myocardium: deleterious effects of unregulated expression. *Circulation.* 2000;102:898-901.
- 199.Schwarz ER, Speakman MT, Patterson M, et al. Evaluation of the effects of intramyocardial injection of DNA expressing vascular endothelial growth factor (VEGF) in a myocardial infarction model in the rat—angiogenesis and angioma formation. *J AmCollCardiol.* 2000;35: 1323-1330.
- 200.Springer ML, Chen AS, Kraft PE, et al. VEGF gene delivery to muscle: potential role for vasculogenesis in adults. *Mol Cell.* 1998;2:549-558.
- 201.Sundberg C, Nagy JA, Brown LF, et al. Glomeruloid microvascular proliferation follows adenoviral vascular permeability factor/vascular endothelial growth factor-164 gene delivery. *Am J Pathol.* 2001;158: 1145-1160.
- 202.Ozawa CR, Banfi A, Glazer NL, Thurston G, Springer ML, Kraft PE, et al. Microenvironmental VEGF concentration, not total dose, determines a threshold between normal and aberrant angiogenesis. *J Clin Invest.* 2004;113(4):516–27.
- 203.Sacchi V, Mittermayr R, Hartinger J, Martino MM, Lorentz KM, Wolbank S, et al. Long-lasting fibrin matrices ensure stable and functional angiogenesis by highly tunable, sustained delivery of recombinant VEGF164. *Proc NatlAcad Sci USA.* 2014;111(19):6952–7.
- 204.von Degenfeld G, Banfi A, Springer ML, Wagner RA, Jacobi J, Ozawa CR, et al. Microenvironmental VEGF distribution is critical for stable and functional vessel growth in ischemia. *FASEB J.* 2006;20(14):2657–9.
- 205.Blau HM, and Springer ML. Muscle-Mediated Gene Therapy. *New England Journal of Medicine.* 1995;333(23):1554-6.
- 206.Blau HM, and Rossi FM. Tet B or nTet B: advances in tetracycline inducible gene expression. *Proc NatlAcad Sci U S A.* 1999;96(3):797-9.
- 207.Martino MM, Brkic S, Bovo E, et al. Extracellular matrix and growth factor engineering for controlled angiogenesis in regenerative medicine. *Front BioengBiotechnol.* 2015;3:45.
- 208.Bao P, Kodra A, Tomic-Canic M, Golinko MS, Ehrlich HP, Brem H. The role of vascular endothelial growth factor in wound healing. *J Surg Res.* 2009;153:347-358.
- 209.Zisch AH, Schenk U, Schense JC, Sakiyama-Elbert SE, Hubbell JA. Covalently conjugated VEGF—fibrin matrices for endothelialization. *J Control Release.* 2001;72:101-113.

210. Sacchi V, Mittermayr R, Hartinger J, et al. Long-lasting fibrin matrices ensures stable and functional angiogenesis by highly tunable, sustained delivery of recombinant VEGF164. *Proc Natl Acad Sci USA*. 2014;111: 6952-6957.
211. Veliz I, Loo Y, Castillo O. Advances and challenges in the molecular biology and treatment of glioblastoma- is there any hope for the future? *Ann Transl Med*. 2015 Jan;3(1):7.
212. T. Gebäck, M.M. Schulz, P. Koumoutsakos, M. Detmar. TScratch: a novel and simple software tool for automated analysis of monolayer wound healing assays. *Biotechniques*, 46 (2009), pp. 265 -274.
213. Bedini A, Baiula M, Spampinato S. 2008. Transcriptional activation of human mu-opioid receptor gene by insulin-like growth factor-I in neuronal cells is modulated by the transcription factor REST. *J Neurochem*. 105(6):2166-78.
214. Schense JC, Bloch J, Aebischer P, and Hubbell JA. Enzymatic incorporation of bioactive peptides into fibrin matrices enhances neurite extension. *Nat Biotechnol*. 2000;18(4):415-9.
215. Schense JC, and Hubbell JA. Cross-linking exogenous bifunctional peptides into fibrin gels with factor XIIIa. *Bioconjug Chem*. 1999;10(1):75- 81.
216. Gupta R, Tongers J, Losordo DW. Human studies of angiogenic gene therapy. *Circ Res*. 2009 Oct 9;105(8):724-36.
217. Mozaffarian D, Benjamin EJ, Go AS, Arnett DK, Blaha MJ, Cushman M, de Ferranti S, Despres JP, Fullerton HJ, Howard VJ, et al. Heart disease and stroke statistics--2015 update: a report from the American Heart Association. *Circulation*. 2015;131(4):29-322.
218. Gianni-Barrera R, Di Maggio N, Melly L, Burger MG, Mujagic E, Gürke L, Schaefer DJ, Banfi A. Therapeutic vascularization in regenerative medicine. *Stem Cells Transl Med*. 2020 Apr;9(4):433-444. doi: 10.1002/sctm.19-0319. Epub 2020 Jan 10.
219. Uccelli A, Wolff T, Valente P, Di Maggio N, Pellegrino M, Gürke L, Banfi A, Gianni-Barrera R. Vascular endothelial growth factor biology for regenerative angiogenesis. *Swiss Med Wkly*. 2019 Jan 27;149:w20011. doi: 10.4414/smw.2019.20011.
220. James AC, Szot JO, Iyer K, Major JA, Pursglove SE, Chapman G, Dunwoodie SL. Notch4 reveals a novel mechanism regulating Notch signal transduction. *Biochim Biophys Acta*. 2014 Jul;1843(7):1272-84. doi: 10.1016/j.bbamcr.2014.03.015.
221. Ruhrberg C, Gerhardt H, Golding M, Watson R, Ioannidou S, Fujisawa H, Betsholtz C, Shima DT. Spatially restricted patterning cues provided by heparin-binding VEGF-A control blood vessel branching morphogenesis. *Genes Dev*. 2002 Oct 15;16(20):2684-98.
222. Park JE, Keller GA, Ferrara N. The vascular endothelial growth factor (VEGF) isoforms: differential deposition into the subepithelial extracellular matrix and bioactivity of extracellular matrix-bound VEGF. *Mol Biol Cell*. 1993 Dec;4(12):1317-26.